Department
of
APPLIED MATHEMATICS

NONLINEAR EQUATIONS OF ACOUSTICS IN INHOMOGENEOUS, THERMOVISCOUS FLUIDS

by

Edel Reiso

Report No. 89 March 1991

UNIVERSITY OF BERGEN
Bergen, Norway

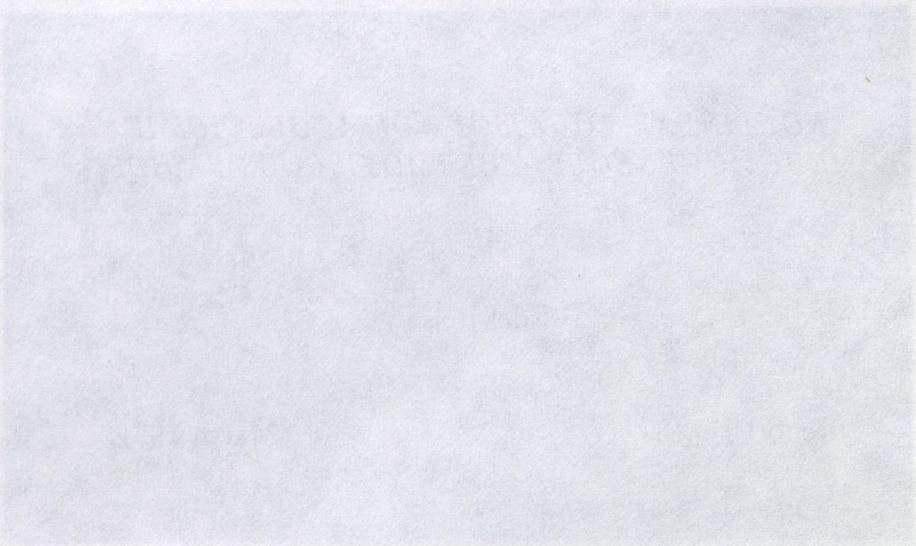

Department of Mathematics
University of Bergen
5007 Bergen

ISSN-0084-778x

NONLINEAR EQUATIONS OF ACOUSTICS IN INHOMOGENEOUS, THERMOVISCOUS FLUIDS

by

Edel Reiso

Report No. 89 March 1991

ABSTRACT

The propagation of finite amplitude sound waves produced by real sources in an inhomogeneous and thermoviscous fluid at rest is considered. A governing equation in the acoustic pressure is derived. It consistently accounts for the effects of diffraction, dissipation, nonlinearity and inhomogeneity, and represents a generalization of the parabolic equation (Khokhlov–Zabolotskaya–Kutznetzov) used for a homogeneous fluid. The equation is expressed in curved coordinates that are determined by the ambient sound speed, which varies with space coordinates. The scale of inhomogeneity must be large compared to a characteristic wavelength. There is no restriction on the direction of the gradients of the ambient acoustic variables. Numerical results are presented and discussed for the linear, the quasi–linear and the fully nonlinear cases. Various sound speed profiles are considered. Models found in the literature, that describe wave propagation in inhomogeneous media, are reviewed.

Acknowledgments

This report includes the main part of my work for the Dr. Scient. degree in applied mathematics. The work was performed at the Department of Mathematics, The University of Bergen, Norway, and at the Department of Mechanical Engineering, The University of Texas at Austin, USA. The financial support has been provided by The Norwegian Research Council for Sciences and Humanities (NAVF) and VISTA/Statoil. A part of the computing resources were provided by The University of Texas System Center for High Performance Computing, by the Department of Mechanical Engineering, The University of Texas at Austin; and by IBM's Bergen Scientific Center, Norway.

I wish to thank my supervisors Professor Jacqueline Naze Tjøtta and Professor Sigve Tjøtta for introducing me to this challenging and interesting problem, for all their help and support, and the useful discussions. I am grateful for the opportunity to join them for two years at the University of Texas at Austin, where they were visiting professors. Also, in Austin they helped me with many practical things, and their hospitality contributed in making the years in the US a good experience.

Dr. Scient. Jarle Berntsen has, together with Dr. Scient. Erlend Vefring, developed the program I have used in the numerical computations. Their help is highly appreciated. I have had many interesting acoustics discussions with Dr. Scient. student Kjell–Eivind Frøysa, and he has also helped me out with tecnical, non–acoustical problems, like graphics.

In Austin, I got to know many nice people working with acoustics, both at the Department of Mechanical Engineering, UT, and at Applied Research Laboratories, and I learned a lot. Especially, I will thank Professor Mark F. Hamilton who made all the practical arrangements for me to be a visiting scholar at UT. He and his wife Karla were always very helpful and friendly.

My present employer, Norsk Hydro, has given me good opportunities to finish the dissertation.

Finally, my thanks to family and friends for their support and encouragement during my studies.

Contents

List of Figures

Chapter 1

INTRODUCTION

In most realistic situations, sound propagation occurs in inhomogeneous media. Inhomogeneity may be caused by an external force (like gravity), or by inhomogeneous boundary conditions (for example on temperature, which would result in a gradient in ambient temperature). Therefore, the ambient sound speed, density, entropy etc. may vary in space and/or time. Depending on the characteristic scales in the problem at hand, these inhomogeneities may be discarded or must be accounted for.

In seismology and underwater acoustics, the range at which a sound wave propagates is so large that the source can be regarded as a point source. The wavelength of a monochromatic wave radiated from the source is the basic characteristic length in these models. The problem formulation is considerably simplified, classical approaches being ray theory and normal mode or parabolic theory.

Closer to the source, the configuration and the finite dimension of the sound source must be included in the model. When characteristic source radius, a, and characteristic wavelength, L, of the on-source boundary condition in pressure can be defined, an important parameter is the ratio a/L, which is related to the effects of diffraction of the sound wave. Nearfield and farfield regions can be identified, with respect to the source location. The acoustic Mach number (defined as the ratio of the velocity on the source and the reference sound speed in the medium) gives an indication whether the pressure perturbation can be regarded as infinitesimal or not, i.e., whether the perturbed hydrodynamic equations can be linearized in the acoustic variables, or nonlinear equations must be used. A parameter related to the effects of inhomogeneity, H, can be introduced. If the ambient variables only vary in space, H can be defined as $H = L/L_H$, where L_H is a characteristic length of inhomogeneity.

We will develop a mathematical model for a finite amplitude sound beam propagating in an inhomogeneous, thermoviscous fluid. The effects of diffraction, absorption, nonlinearity and inhomogeneity will be accounted for. The beam is generated by a (real) source with characteristic radius a, radiating into an unbounded halfspace. We assume the ambient medium to be at rest, although the ambient acoustic

variables may vary in space. The direction of the gradients in the medium is arbitrary, relative to the start direction of the beam. External forces can be included in the model. [We assume that any boundaries are far away from the region where the beam propagates, so as to justify the assumption of a semi–infinite medium.]

Beam propagation in a homogeneous medium is described by the Khoklhov–Zabolotskaya–Kutznetzov (KZK) equation, which consistently accounts for diffraction, absorption and nonlinearity. Here, we do not pretend to derive a general theory for sound wave propagation in an inhomogeneous medium. However, we will investigate what physical situations can be modeled by a suitable modification of the KZK equation. The present derivation is motivated by the approach in Ref. (1).

In Chapter 2, a governing parabolic equation in one acoustic variable is derived, consistently accounting for diffraction, inhomogeneity, nonlinearity and absorption. Assumptions and further simplifications in the model are discussed.

In Chapter 3, a numerical method for solving the parabolic partial differential equation is presented. Possibilities for analytical solution in special cases are discussed.

In Chapter 4, the linear solution is investigated. In Sec. 4.1, numerical results are presented for various values of a/L and various sound speed profiles. In Sec. 4.2, we apply the model to simulate interfaces, i.e., discontinuities in the medium. In Sec. 4.3, further applications of the model are discussed.

In Chapter 5, nonlinear propagation is studied, for various sound speed profiles. Numerical results for the pressure amplitude are presented and discussed, both in the quasilinear and the fully nonlinear models. [In the quasilinear model, a perturbation expansion in the pressure is inserted in the governing nonlinear, parabolic equation, which is solved to each order of the Mach number. In the fully nonlinear model, the governing nonlinear equation is solved directly.]

Chapter 6 is a presentation and discussion of models found in the literature, that describe wave propagation in inhomogeneous media.

Chapter 2

The mathematical model

2.1. Basic equations

The medium is a thermoviscous fluid at rest. Here t denotes the time, $\mathbf{x} = (x, y, z)$ the space variables in cartesian coordinates, $p, \rho, \mathbf{v}$ the total pressure, density, velocity, and s the entropy per unit mass. The absolute temperature is Θ, and $\mathbf{F}$ is the external force per unit volume. The governing equations are[1,2]

1. the equation of continuity

$$\frac{\partial \rho}{\partial t} + \nabla \cdot (\rho \mathbf{v}) = 0, \tag{2.1}$$

2. the equation of motion

$$\rho \left(\frac{\partial \mathbf{v}}{\partial t} + \mathbf{v} \cdot \nabla \mathbf{v} \right) + \nabla p = \mathbf{F} + \mathcal{V}, \tag{2.2}$$

where

$$\mathcal{V} = (\kappa + \frac{4}{3}\mu)\nabla(\nabla \cdot \mathbf{v}) - \mu \nabla \times \nabla \times \mathbf{v} + (\nabla \cdot \mathbf{v})\nabla \left(\kappa - \frac{2}{3}\mu \right) + 2\nabla\mu \cdot \nabla \mathbf{v} + \nabla\mu \times \nabla \times \mathbf{v}, \tag{2.3}$$

and μ, κ are the coefficients of shear and bulk viscosity of the fluid,

3. the equation of state

$$p = p(\rho, s), \tag{2.4}$$

4. the heat exchange equation (consequence of the equation of energy)

$$\rho\Theta \left(\frac{\partial s}{\partial t} + \mathbf{v} \cdot \nabla s \right) = \nabla \cdot (\rho c_v K \nabla \Theta) + Q - \rho c_v q(\Theta - \Theta_0), \tag{2.5}$$

where c_v is the specific heat at constant volume, K the coefficient of thermal conductivity, Θ absolute temperature, and Q the viscous dissipation function,

$$Q = (\kappa - \frac{2}{3}\mu)(\nabla \cdot \mathbf{v})^2 + \frac{\mu}{2} ||\nabla \mathbf{v} + \mathbf{v} \nabla||^2. \tag{2.6}$$

The last term in Eq. (2.5) accounts for radiation and q is a radiation coefficient. The symbol $||\mathbf{A}||^2$ stands here for $\sum_{i,j} A_{ij}^2$, where A_{ij} are the elements of the tensor $\mathbf{A}$.

Combining Eqs. (2.1) and (2.2) we obtain

$$\nabla^2 p - \frac{\partial^2 \rho}{\partial t^2} + \boldsymbol{\nabla}\boldsymbol{\nabla}:(\rho \mathbf{v}\mathbf{v}) = \boldsymbol{\nabla} \cdot \mathbf{F} + \boldsymbol{\nabla} \cdot \mathcal{V}. \tag{2.7}$$

In a linearized theory, $\mathbf{v}$ is related to p alone through the linearised equation of motion. For a monochromatic plane wave motion, this leads to the impedance relation. In other cases, however, the elimination of $\mathbf{v}$ is by no means trivial, if it is to be performed consistently. In Ref. 1, the problem of eliminating $\mathbf{v}$ is solved for the case of a narrow beam which propagates in a homogeneous, thermo-viscous medium at rest. [By "narrow beam" is meant that the ratio of characteristic source radius and characteristic wavelength of the wave radiated from the source is much larger than one.] Equation (2.7) is then shown to lead to a nonlinear parabolic equation for the acoustic pressure (Khokhlov–Zabolotskaya–Kuznetsov, or KZK equation[3,4]), which consistently accounts for the effects of nonlinearity, diffraction, and absorption. Our purpose is to generalize the derivation in Ref. 1 to the case where inhomogeneity is present in the static state of equilibrium. We introduce the perturbed variables

$$p = p_0 + p', \qquad \rho = \rho_0 + \rho', \qquad s = s_0 + s' \tag{2.8}$$

$$\mathbf{v} = \mathbf{0} + \mathbf{v}, \qquad \Theta = \Theta_0 + \Theta', \qquad \mathbf{F} = \mathbf{F}_0 + \mathbf{F}', \tag{2.9}$$

where p_0, etc. are functions of $\mathbf{x}$ that refer to ambient values in a static state of equilibrium. The unperturbed medium must satisfy the governing equations:

$$\boldsymbol{\nabla} p_0 = \mathbf{F}_0, \qquad \boldsymbol{\nabla} \cdot (\rho_0 c_{v0} K_0 \boldsymbol{\nabla} \Theta_0) = 0. \tag{2.10}$$

Equation (2.7) becomes

$$\nabla^2 p' - \frac{\partial^2 \rho'}{\partial t^2} + \boldsymbol{\nabla}\boldsymbol{\nabla}:(\rho \mathbf{v}\mathbf{v}) = \boldsymbol{\nabla} \cdot \mathbf{F}' + \boldsymbol{\nabla} \cdot \mathcal{V}. \tag{2.11}$$

We introduce the following quantities characteristic for the medium:

$\bar{c}$ - Reference sound speed in the medium (for example sound speed at the source location).

T, $L = \bar{c}T$ - Characteristic time and length of the wave (period and wavelength for the case of a monochromatic source in a homogeneous medium).

$\bar{\rho}$ - Reference density in the medium (for example ambient density at the source location).

$\bar{S} = \bar{D}/T\bar{c}^2$ - Characteristic Stokes number of the wave, where $\bar{D}$ is a reference sound diffusivity.

$\epsilon = \bar{u}/\bar{c}$, where $\bar{u}$ is a characteristic normal velocity on the sound source.

$\bar{\alpha}^{-1} = 2\bar{c}^3 T^2 \bar{D}^{-1}$ is then a characteristic absorption length. For the present case of an inhomogeneous medium, we assume that all ambient values of the acoustic variables p_0, ρ_0, etc., have the same scale of inhomogeneity, thereby introducing

L_H - Characteristic length for inhomogeneity, where $|\nabla \rho_0|/\rho_0$, etc. are of order L_H^{-1}.

$H = L/L_H$ - Inhomogeneity number.

At this point we could introduce nondimensional variables. However, we postpone this for simplicity, suffice it being to remember that in the nondimensional equations, terms containing a factor κ, μ or K would be multiplied by S, terms containing a factor $\nabla \rho_0$, ∇c_0, etc., would be multiplied by H and terms containing a factor p', ρ', $\partial p'/\partial t$, $\nabla p'$, etc., would be multiplied by ϵ.

Following the procedure in Ref. 1, we now want to reduce Eq. (2.11) so that it only contains p' and $\mathbf{v}$, correct to order ϵ^2. In the homogeneous case, dissipative effects are accounted for only in their dominant order, i.e., $S = C_1 \epsilon$, where C_1 is a similarity constant (it is of order one in the expansion procedure, although it may take very large or very small numerical values). The question arises whether it is possible to perform a similar derivation without introducing any assumption about the strength of the inhomogeneity. The answer to this question is found in the vorticity equation, obtained by taking the curl of the linearized equation of motion

$$\frac{\partial}{\partial t} \nabla \times \mathbf{v} = -\nabla \frac{1}{\rho_0} \times \nabla p' + \nabla \times \frac{\mathbf{F}'}{\rho_0} + \nabla \times \frac{\mathcal{V}}{\rho_0}, \tag{2.12}$$

correct to order ϵ. In a homogeneous, nondissipative fluid, the right hand side is zero and no vorticity of order ϵ is generated in the fluid. This means that the impedance relation $\partial \mathbf{v}/\partial t = -\rho_0^{-1} \nabla p'$ is satisfied to order ϵ at any point that is not too close to the boundaries (sound sources and other limiting surfaces) where vorticity may be forced through the prescribed boundary conditions. In presence of dissipation and/or inhomogeneity, however, vorticity of order ϵ is generated at any point where there is a fluctuation in acoustic pressure ($\nabla p' \neq 0$), and the impedance relation is not satisfied at order ϵ, unless the Stokes number S and the inhomogeneity parameter H are small. (The terms on the right hand side of Eq. (2.12) are of order ϵH and SH.) Since the use of the impedance relation is crucial in the process of eliminating $\mathbf{v}$ without raising the order of the equations, we are lead into assuming the following ordering of the parameters:

$$S = C_S \epsilon, \qquad H = C_H \epsilon, \tag{2.13}$$

where C_S, C_H are similarity parameters. This implies (i) that when working correct to order ϵ^2, we may in all quadratic terms, and in all terms containing dissipative

coefficients (κ, μ, K) and/or space derivatives of unperturbed quantities, evaluate the acoustic variables by means of linearized, homogeneous and nondissipative relations, and (ii) that the perturbed external force per unit volume, $\mathbf{F}'$, must be of order $\epsilon H = O(\epsilon^2)$, since $\mathbf{F}_0$ is of order $H = O(\epsilon)$, see Eq. (2.10). We use this to eliminate ρ' from Eq. (2.11). It follows from Eq. (2.5) when assuming that radiation can be neglected, that

$$\frac{\partial s'}{\partial t} = \frac{c_{v0} K_0}{\Theta_0} \nabla^2 \Theta' - \mathbf{v} \cdot \boldsymbol{\nabla} s_0, \tag{2.14}$$

correct to order ϵ^2. This shows that $s' = O(\epsilon^2)$. We notice that, correct to order ϵ, all acoustic variables satisfy the wave equation, say

$$\nabla^2 \Theta' - \frac{1}{c_0^2} \frac{\partial^2 \Theta'}{\partial t^2} = O(\epsilon^2). \tag{2.15}$$

Thus, we may replace $\nabla^2 \Theta'$ by $c_0^{-2} \partial^2 \Theta' / \partial t^2$ in Eq. (2.14). Next, we may eliminate $\partial^2 \Theta' / \partial t^2$ by using Maxwell's equations and thermodynamic relations, as in Ref.(1), Appendix A:

$$\frac{\partial^2 \Theta'}{\partial t^2} = \frac{c_0^2 \eta_0 \Theta_0}{\rho_0 c_{p0}} \frac{\partial^2 \rho'}{\partial t^2} + O(\epsilon^2), \tag{2.16}$$

where η_0 is the coefficient of thermal expansion. Equation (2.14) then gives

$$\frac{\partial s'}{\partial t} = \frac{\eta_0 K_0}{\rho_0 \gamma_0} \frac{\partial^2 \rho'}{\partial t^2} - \mathbf{v} \cdot \boldsymbol{\nabla} s_0 \tag{2.17}$$

correct to order ϵ^2. From Eq. (2.4) we also have

$$\frac{\partial p'}{\partial t} = c^2 \frac{\partial \rho'}{\partial t} + \left(\frac{\partial p}{\partial s} \right)_\rho \frac{\partial s'}{\partial t}, \tag{2.18}$$

where $(\gamma - 1)\rho/\eta = (\partial p / \partial s)_\rho$ (see Ref. 1, Appendix A, Eq. (A6) and following). Dividing Eq. (2.18) by c^2, derivating with respect to t and using Eq. (2.17), we finally obtain, correct to order ϵ^2,

$$\frac{\partial^2 \rho'}{\partial t^2} = \frac{\partial}{\partial t} \left[\frac{1}{c^2} \frac{\partial p'}{\partial t} \right] - \frac{1}{c_0^2} \left[K_0 \frac{\gamma_0 - 1}{\gamma_0} \frac{\partial^3 \rho'}{\partial t^3} - \left(\frac{\partial p}{\partial s} \right)_{\rho,0} \frac{\partial \mathbf{v}}{\partial t} \cdot \boldsymbol{\nabla} s_0 \right]. \tag{2.19}$$

To this order of approximation, we may replace $\partial^3 \rho' / \partial t^3$ by $c_0^{-2} \partial^3 p' / \partial t^3$ and $\rho_0 \partial \mathbf{v} / \partial t$ by $-\boldsymbol{\nabla} p'$ in the second term on the right-hand side of Eq. (2.19). In the same way, the first term on the right-hand side can also be expressed in terms of p' alone by noticing that

$$\frac{1}{c^2} = \frac{1}{c_0^2} - \frac{1}{c_0^6} \left(\frac{\partial c^2}{\partial \rho} \right)_{s,0} p', \tag{2.20}$$

correct to order ϵ, since c^2 is a function of ρ, s and $s' = O(\epsilon^2)$. This gives

$$\frac{\partial^2 \rho'}{\partial t^2} = \frac{1}{c_0^2}\frac{\partial^2 p'}{\partial t^2} - \frac{1}{2c_0^6}\left(\frac{\partial c^2}{\partial \rho}\right)_{s,0}\frac{\partial^2 p'^2}{\partial t^2} \tag{2.21}$$
$$-\frac{1}{c_0^2}\left[K_0\frac{\gamma_0 - 1}{\gamma_0 c_0^2}\frac{\partial^3 p'}{\partial t^3} + \frac{1}{\rho_0}\left(\frac{\partial p}{\partial s}\right)_{\rho,0}\nabla p' \cdot \nabla s_0\right].$$

We now turn to the $\nabla \cdot \mathcal{V}$ term in Eq. (2.11). Correct to order ϵ^2, we may neglect the terms containing $\nabla\mu, \nabla\kappa$ in the expression for $\mathcal{V}$, Eq. (2.3), and replace the first term in $\nabla \cdot \mathcal{V}$ by C.13

$$(\kappa_0 + \frac{4}{3}\mu_0)\nabla \cdot (\nabla\nabla \cdot \mathbf{v}) = -(\kappa_0 + \frac{4}{3}\mu_0)\frac{1}{\rho_0 c_0^4}\frac{\partial^3 p'}{\partial t^3} \tag{2.22}$$

(using Eqs. (2.1) and (2.4) to order ϵ, together with Eq. (2.15) for p'). The $\nabla \times \nabla \times \mathbf{v}$ term in Eq. (2.3) is negligible because the vorticity is of order ϵ^2.

Thus the second term on the right-hand side of Eq. (2.11) is

$$\nabla \cdot \mathcal{V} = -\frac{1}{\rho_0 c_0^4}(\kappa_0 + \frac{4}{3}\mu_0)\frac{\partial^3 p'}{\partial t^3}, \tag{2.23}$$

correct to order ϵ^2. Bringing Eqs. (2.21) and (2.23) into Eq.(2.11), we obtain

$$\nabla^2 p' - \frac{1}{c_0^2}\frac{\partial^2 p'}{\partial t^2} + \frac{1}{\rho_0 c_0^2}\left(\frac{\partial p}{\partial s}\right)_{\rho,0}\nabla s_0 \cdot \nabla p' - \nabla \cdot \mathbf{F}' + \frac{D_0}{c_0^4}\frac{\partial^3 p'}{\partial t^3} \tag{2.24}$$
$$+ \frac{1}{2c_0^6}\left(\frac{\partial c^2}{\partial \rho}\right)_{s,0}\frac{\partial^2 p'^2}{\partial t^2} + \rho_0 \nabla\nabla{:}\mathbf{vv} = 0,$$

correct to order ϵ^2. Here, D_0 denotes the ambient value of the sound diffusivity,

$$D_0 = \frac{\frac{4}{3}\mu_0 + \kappa_0}{\bar{\rho}} + \frac{\gamma - 1}{\gamma}K_0, \tag{2.25}$$

and $\gamma = c_p/c_v$, where c_p is the specific heat at constant pressure.

The first two terms in this reduced equation are the d'Alembertian of the linearized wave equation (with $c_0(\mathbf{x})$). The next two terms are due to inhomogeneity in the static state of equilibrium, and to fluctuations in external forces. The term of inhomogeneity may be transformed by differentiating the unperturbed equation of state Eq. (2.4) and by using Eq. (2.10),

$$\left(\frac{\partial p}{\partial s}\right)_{\rho,0}\nabla s_0 = \nabla p_0 - c_0^2 \nabla \rho_0 = \mathbf{F}_0 - c_0^2 \nabla \rho_0. \tag{2.26}$$

The term of inhomogeneity is of order $H\epsilon = O(\epsilon^2)$, and it represents the effects of external forces and of variations in density [variations in density may result from the presence of external forces, gravity, for example, and from prescribed boundary conditions (temperature gradients, for example)]. The fifth term accounts for dissipative effects. The last two terms account for nonlinear effects. The first one comes from nonlinearity in the equation of state, since $(\partial c^2/\partial\rho)_{s,0} = (\partial^2 p/\partial\rho^2)_{s,0}$. The second nonlinear term, which accounts for convection, still contains $\mathbf{v}$.

We define the following nondimensional variables,

$$\tilde{t} = \frac{t}{T}, \qquad \tilde{\mathbf{x}} = \frac{\mathbf{x}}{\bar{c}T}, \qquad \tilde{\mathbf{x}}_1 = \frac{\mathbf{x}}{L_H} = H\tilde{\mathbf{x}}, \tag{2.27}$$

nondimensional unperturbed quantities,

$$\tilde{p}_0 = \frac{p_0}{\bar{\rho}\bar{c}^2}, \qquad \tilde{\rho}_0 = \frac{\rho_0}{\bar{\rho}}, \qquad \tilde{c}_0 = \frac{c_0}{\bar{c}}, \tag{2.28}$$

and nondimensional perturbations,

$$\tilde{p}' = \frac{p'}{\bar{\rho}\bar{c}\bar{u}} = \frac{1}{\epsilon}\frac{p'}{\bar{\rho}\bar{c}^2}, \qquad \tilde{\mathbf{v}} = \frac{\mathbf{v}}{\bar{u}} = \frac{1}{\epsilon}\frac{\mathbf{v}}{\bar{c}}. \tag{2.29}$$

All unperturbed variables are functions of $\tilde{\mathbf{x}}$ only through the stretched variable $\tilde{\mathbf{x}}_1$, so that, for example,

$$\tilde{p}_0 = \tilde{p}_0(\tilde{\mathbf{x}}_1), \qquad \nabla p_0 = \frac{\bar{\rho}\bar{c}}{T}\tilde{\nabla}\tilde{p}_0 = H\frac{\bar{\rho}\bar{c}}{T}\tilde{\nabla}_1\tilde{p}_0, \tag{2.30}$$

where $\tilde{\nabla}$ and $\tilde{\nabla}_1$ denote the gradient with respect to $\tilde{\mathbf{x}}$ and $\tilde{\mathbf{x}}_1$, respectively. It follows from Eq. (2.10) that $\mathbf{F}_0 = H(\bar{\rho}\bar{c}/T)\tilde{\mathbf{F}}_0$. Combining Eqs. (2.24) and (2.26) leads to

$$\begin{aligned}\tilde{\nabla}^2\tilde{p}' - \frac{1}{\tilde{c}_0^2}\frac{\partial^2\tilde{p}'}{\partial\tilde{t}^2} + \frac{H}{\tilde{\rho}_0\tilde{c}_0^2}(\tilde{\mathbf{F}}_0 - \tilde{c}_0^2\tilde{\nabla}_1\tilde{\rho}_0)\cdot\tilde{\nabla}\tilde{p}' - H\tilde{\nabla}\cdot\tilde{\mathbf{F}}' + S\frac{\tilde{D}_0}{\tilde{c}_0^4}\frac{\partial^3\tilde{p}'}{\partial\tilde{t}^3} \\ + \epsilon\frac{1}{2\tilde{c}_0^6}\left(\frac{\partial\tilde{c}^2}{\partial\tilde{\rho}}\right)_{s,0}\frac{\partial^2\tilde{p}'^2}{\partial\tilde{t}^2} + \epsilon\tilde{\rho}_0\tilde{\nabla}\tilde{\nabla}:\tilde{\mathbf{v}}\tilde{\mathbf{v}} = 0,\end{aligned} \tag{2.31}$$

where $\mathbf{F}' = (H\epsilon\bar{\rho}\bar{c}/T)\tilde{\mathbf{F}}'$. (In the following, this equation will be used without writing the "tildes" over the dependent and independent variables, for simplicity.)

In order to illustrate the difficulties that are met when solving Eq. (2.31) without introducing simplifying approximations, let us consider the special case of a nondissipative, inhomogeneous fluid with no external forces. Let the source be monochromatic, with angular frequency ω. The linear part of Eq. (2.31) is the Helmholtz equation with varying wavenumber, for $q = p'/\rho_0^{1/2}$, where p' is the complex pressure amplitude (we assume $\mathbf{F}_0\cdot\nabla p' = 0$):

$$\nabla^2 q + K^2(\mathbf{x})q = 0, \tag{2.32}$$

where

$$K^2(\mathbf{x}) = \frac{1}{2}\left[\frac{\nabla^2\rho_0}{\rho_0} - \frac{3}{2}(\frac{\nabla\rho_0}{\rho_0})^2\right] + \frac{\omega^2}{c_0^2}. \tag{2.33}$$

It is not easy to find an analytical solution of Eq. (2.32), with boundary conditions in pressure or normal velocity given on a (source) surface. Standard integral transforms (like Fourier transform in transverse variable) cannot be applied: If c_0 varies, the problem may not be separable since the equation has varying coefficients. In the Fourier transform coordinate space, Eq. (2.32) becomes an integro–differential equation, and the transformed problem is as difficult as the original one. Another example: For $K = K(\mathbf{x}_\perp)$, one could try a Laplace transform with respect to the longitudinal variable z. However, this approach calls for information about both p' and $\partial p'/\partial n$ at the source surface, and both cannot be specified simultaneously.

A fundamental solution of the equation satisfies:

$$(\nabla^2 + K^2(\mathbf{x}))g(\mathbf{x}|\mathbf{x}_0) = \delta(\mathbf{x} - \mathbf{x}_0). \tag{2.34}$$

[Equation (2.34) is to be understood in the sense of distributions[6].] The free wave fundamental solution g can be interpreted as the pressure radiated from a point source in an unbounded medium. For K = constant, $g = \exp(ikR)/R$, where $R = |\mathbf{x}-\mathbf{x}_0|$. No general solution is known if K varies. However, in certain cases, analytical solutions for g can be obtained. For instance: $K^2(\mathbf{x}_\perp)$ linear gives g in terms of Airy–functions; $K^2(\mathbf{x}_\perp)$ quadratic gives g as parabolic cylinder functions; $K^2(\mathbf{x}_\perp)$ exponential gives Bessel functions[7]. These problems are all separable.

In theoretical models in underwater acoustics (as noted in for instance Refs. (51, 52 54, 59, 60)), the free wave fundamental solution, g, is often said to be the Green's function for the problem, for general source configurations. In that case, an arbitrary source is assumed to be a superposition of point sources, each radiating the wave $g(\mathbf{x}|\mathbf{x}_i)$ with amplitude $Q(\mathbf{x}_i)$. [Usually, a line source or a volume source is considered.] However, the Green's function G depends on the geometry of the source (and satisfies Eq. (2.34) for $g = G$). At the source, either G or $\partial(\rho_0^{1/2}G)/\partial n$ must be zero (in the case of constant K: $\partial G/\partial n$ must be zero), corresponding to membrane or piston type boundary conditions in the acoustic pressure. This is not satisfied by the free wave, which is singular at the source surface, by construction. The pressure $p' = \rho_0^{1/2}q$ is found from the Kirchhoff–Helmholtz integral:

$$q(\mathbf{x}) = -\frac{1}{4\pi}\int_{\partial\Omega}\left(q\frac{\partial G}{\partial n} - \frac{\partial q}{\partial n}G\right)\, dS. \tag{2.35}$$

If G is replaced by g, i.e., the fundamental solution corresponding to the appropriate varying $K(\mathbf{x})$, Eq. (2.35) becomes an integral equation for q. Depending on whether p' or $\partial p'\partial n$ is specified at the source (i.e., $\rho_0^{1/2}q$ or $\partial(\rho_0^{1/2}q)/\partial n$), a Fredholm integral equation of first or second type will result from Eq. (2.35)[6,8].

Even in the linear case, it is difficult and time consuming to solve numerically the generalized wave equation Eq. (2.31). Therefore, we try to introduce approximations to simplify the problem. In order to eliminate v from Eq. (2.31) without increasing the order of the equation, we must introduce a new characteristic length and a new assumption. Our approach is guided by the knowledge that for the case of a homogeneous medium, the KZK equation is obtained by introducing a suitable scaling of transverse and longitudinal variations of the sound pressure, so that the d'Alembertian operator can be approximated by a parabolic operator. Second order longitudinal differentiations are discarded while second order transverse differentiations are kept in the equation. Thus diffraction effects are accounted for, although, the solution will not be valid close to the source. Both analytically and numerically, it is easier and less time consuming to solve the KZK equation than the full nonlinear wave equation. We will in the following investigate whether the KZK equation can be generalized to include inhomogeneity.

Let us specify that the perturbation is generated by a sound source located in the plane $z = 0$, and that either the on-source pressure or the on-source velocity is $f(\mathbf{x}_\perp, 0, t)$, where $\mathbf{x}_\perp = (x, y)$. We introduce:

a - Characteristic length for the variation of f, (a can be a characteristic dimension of the sound source, for instance).

$N = \bar{c}T/a$ - Diffraction number, (wavelength to source radius ratio, of order "$(ka)^{-1}$" when the source is monochromatic with wavenumber k).

When the medium is homogeneous, the acoustic axis of the sound beam is along the z axis, and it is reasonable to choose a as the characteristic length for the variation of the acoustic variables in $\mathbf{x}_\perp$ direction (transverse to the beam), with an a priori different scale for the variation in z direction (along the beam axis). In the inhomogeneous case, however, the axis of the beam may be bent. We therefore introduce orthogonal curvilinear coordinates $(\boldsymbol{\psi}, \phi) = (\varphi, \psi, \phi)$, which depend on $\mathbf{x}_\perp, z, N, H$, and are such that the curve $\varphi = \psi = 0$ corresponds to the axis of the beam. Retarded times $\tau_\pm = t \mp \phi$ are also introduced. We assume that

$$|\nabla\phi|, |\nabla\boldsymbol{\psi}| = O(1), \qquad |\nabla^2\phi|, |\nabla^2\boldsymbol{\psi}| = O(H). \tag{2.36}$$

$\boldsymbol{\psi}$ denotes a vector with components (φ, ψ) transverse to the beam axis. The second assumption implies that the wave front is weakly curved, the radius of curvature being of the order of the characteristic length $\bar{r}$ for slow variation in the acoustic variables. By analogy with the procedure in Ref. 1, to obtain a uniformly valid solution we introduce different scales. The acoustic variables are considered as functions of $\boldsymbol{\psi}$ and ϕ through the variables $\boldsymbol{\psi}_{1/2} = N\boldsymbol{\psi} = (N\varphi, N\psi)$ and $\phi_1 = H\phi$, in addition to $\tau_\pm$, say

$$p'(x, y, z, t) = p'(\boldsymbol{\psi}_{1/2}, \phi_1, \tau_+, \tau_-) = p'(N\boldsymbol{\psi}, \epsilon\phi, t - \phi, t + \phi). \tag{2.37}$$

This implies

$$\frac{\partial}{\partial t} = \frac{\partial}{\partial \tau_+} + \frac{\partial}{\partial \tau_-}, \tag{2.38}$$

$$\nabla = \nabla\phi \left[-\frac{\partial}{\partial \tau_+} + \frac{\partial}{\partial \tau_-} + H\frac{\partial}{\partial \phi_1} \right] + N\nabla\psi \cdot \frac{\partial}{\partial \psi_{1/2}}. \tag{2.39}$$

The acoustic variables may also depend on even slower variables, $\psi_1 = N^2\psi$, $\phi_2 = H^2\phi$, etc., so that extra terms as $N^2\nabla\psi \cdot \partial/\partial\psi_1 + H^2\nabla\phi\partial/\partial\phi_2 + \cdots$ should be added in Eq. (2.39). However, variations over these slower scales do not contribute to our order of approximation, and they will therefore not be written. We also have

$$\begin{aligned}\nabla^2 = {} & \nabla^2\phi \left[-\frac{\partial}{\partial \tau_+} + \frac{\partial}{\partial \tau_-} + H\frac{\partial}{\partial \phi_1} \right] + N\nabla^2\psi \cdot \frac{\partial}{\partial \psi_{1/2}} \\ & + |\nabla\phi|^2 \left[-\frac{\partial}{\partial \tau_+} + \frac{\partial}{\partial \tau_-} + H\frac{\partial}{\partial \phi} \right]^2 + N^2(\nabla\psi \cdot \nabla\psi) : \frac{\partial^2}{\partial \psi_{1/2}\partial \psi_{1/2}}. \end{aligned} \tag{2.40}$$

Here the last term stands for

$$N^2 \left[|\nabla\varphi|^2 \frac{\partial^2}{\partial \varphi_{1/2}} + |\nabla\psi|^2 \frac{\partial^2}{\partial \psi_{1/2}} + 2\nabla\varphi \cdot \nabla\psi \frac{\partial^2}{\partial \varphi_{1/2}\partial \psi_{1/2}} \right] \tag{2.41}$$

and $(\varphi_{1/2}, \psi_{1/2})$ are the components of $\psi_{1/2}$ in the plane orthogonal to $\nabla\phi$. The terms of order one represent fast variations (characteristic length one wavelength for a monochromatic perturbation), while the other terms represent slower variations caused by nonlinearity, diffraction, absorption and inhomogeneity. Further, we decompose the velocity $\mathbf{v}$ into a longitudinal velocity w and a transverse velocity $\mathbf{v}_\perp$, $\mathbf{v} = \mathbf{v}_\perp + w\mathbf{e}_\phi$, where $\mathbf{e}_\phi = \nabla\phi/|\nabla\phi|$ is the tangent vector to the beam axis, and we seek solutions in the form of asymptotic expansions

$$p' = \epsilon p^{(1)} + \epsilon^2 p^{(2)} + \ldots, \quad w = \epsilon w^{(1)} + \epsilon^2 w^{(2)} + \ldots, \quad \mathbf{v}_\perp = N\mathbf{v}_\perp{}^{(1)} + N^2\mathbf{v}_\perp{}^{(2)} + \ldots \quad . \tag{2.42}$$

This scaling of $\mathbf{v}_\perp$ to N and of w to ϵ is dictated by the transverse component of the vorticity equation Eq. (2.12)

$$\nabla\phi \times \left(-\frac{\partial}{\partial \tau_+} + \frac{\partial}{\partial \tau_-} + \epsilon\frac{\partial}{\partial \phi_1} \right) \mathbf{v}_\perp + N \left(\nabla\psi \cdot \frac{\partial w}{\partial \psi_{1/2}} \right) \times \frac{\nabla\phi}{|\nabla\phi|} = O(\epsilon^2). \tag{2.43}$$

Sofar, we have not precised what is the order of N. Bringing Eqs. (2.42) in the transverse component of the equation of motion, Eq. (2.2), we have

$$\rho_0 (N\frac{\partial \mathbf{v}_\perp{}^{(1)}}{\partial t} + N^2\frac{\partial \mathbf{v}_\perp{}^{(2)}}{\partial t} + N^3\frac{\partial \mathbf{v}_\perp{}^{(3)}}{\partial t} + \cdots) = O(\epsilon N) + O(\epsilon^2) + \cdots \quad . \tag{2.44}$$

Since $N \ll 1$, we must have $\mathbf{v}_\perp{}^{(1)} = 0$. One possibility is to choose $\mathbf{v}_\perp{}^{(2)} \neq 0$ and $N = O(\epsilon)$, but then Eq. (2.31) contains no differentiation with respect to the transverse variables, to the dominating order. This means that diffraction effects are not represented in Eq. (2.31) if $N = O(\epsilon)$. We must therefore choose $\mathbf{v}_\perp{}^{(2)} = 0$ and $N^2 = O(\epsilon)$. We note that this scaling is consistent with Eq. (2.43).

Thus, we have the following ordering of parameters:

$$S = C_S\epsilon, \qquad H = C_H\epsilon, \qquad N = C_N\epsilon^{1/2}, \tag{2.45}$$

where C_N is a new similarity constant. The ordering is the same as in Ref. (1), but we are now operating in curvilinear coordinates and the beam axis is a curve with tangent vector $\nabla\phi$. The procedure is the distinguished limit approach of Ref. (5). To order ϵ, Eq. (2.31) gives now

$$\left(|\nabla\phi|^2 - \frac{1}{c_0^2}\right)\left(\frac{\partial^2 p^{(1)}}{\partial\tau_+{}^2} + \frac{\partial^2 p^{(1)}}{\partial\tau_-{}^2}\right) - 2\left(|\nabla\phi|^2 + \frac{1}{c_0^2}\right)\frac{\partial^2 p^{(1)}}{\partial\tau_+\partial\tau_-} = 0. \tag{2.46}$$

If we want the sound field to be a superposition of progressive and regressive waves on the fast scale, i.e., $p^{(1)} = f(\psi_{1/2}, \phi_1, \tau_+) + g(\psi_{1/2}, \phi_1, \tau_-)$, we must demand

$$|\nabla\phi|^2 - \frac{1}{c_0^2} = 0. \tag{2.47}$$

This is the eikonal equation, known from ray theory as the equation that determines the characteristic surfaces of a wave equation. If Eq. (2.47) can not be satisfied, it is impossible to describe $p^{(1)}$ as a simple wave in the limit $N \to 0$. Thus, in the inhomogeneous case, the wavefronts that appear on the fast scale in the curvilinear coordinates are analogous to the wavefronts in ray theory. Equation (2.46) reduces to

$$\frac{\partial^2 p^{(1)}}{\partial\tau_+\partial\tau_-} = 0, \tag{2.48}$$

with solution $p^{(1)}(\psi_{1/2}, \phi_1, \tau_+)$ when we assume that the beam propagates in the halfspace $z > 0$ and that no perturbation is present at any point in the medium before the passage of the wavefront. Writing Eqs. (2.1) and (2.2) correct to order ϵ,

$$\frac{\partial p^{(1)}}{\partial\tau_-} + \rho_0 c_0 \frac{\partial w^{(1)}}{\partial\tau_-} = 0, \qquad \frac{\partial p^{(1)}}{\partial\tau_+} - \rho_0 c_0 \frac{\partial w^{(1)}}{\partial\tau_+} = 0, \tag{2.49}$$

and using the same argument as above, we obtain

$$w^{(1)} = \frac{1}{\rho_0 c_0} p^{(1)}(\psi_{1/2}, \phi_1, \tau_+). \tag{2.50}$$

This impedance relation in the curvilinear coordinates permits to eliminate $w^{(1)}$ when we change variables in Eq. (2.31), using Eqs. (2.38), (2.39) and (2.40). We obtain

$$\frac{4}{c_0^2}\frac{\partial^2 p^{(2)}}{\partial\tau_+\partial\tau_-} = -C_H\left[\frac{2}{c_0^2}\frac{\partial}{\partial\phi_1} - \frac{1}{c_0^3}\frac{\partial c_0}{\partial\phi_1} + \frac{1}{\rho_0 c_0^2}\left(\frac{1}{c_0^2}\frac{\partial p_0}{\partial\phi_1} - \frac{\partial\rho_0}{\partial\phi_1}\right)\right]\frac{\partial p^{(1)}}{\partial\tau_+} - C_H\mathcal{F}'$$
$$+ C_N^2(\nabla\psi\cdot\nabla\psi):\frac{\partial^2}{\partial\psi_{1/2}\partial\psi_{1/2}}p^{(1)} + C_S\frac{D_0}{c_0^4}\frac{\partial^3 p^{(1)}}{\partial{\tau_+}^3} + \frac{\beta_0}{\rho_0 c_0^4}\frac{\partial^2(p^{(1)})^2}{\partial{\tau_+}^2}, \tag{2.51}$$

where $\beta_0 = 1 + B/2A$ is the parameter of nonlinearity of the medium, with $B/A = (\rho_0 c_0^2)^{-1}(\partial^2 p/\partial\rho^2)_{s,0}$. The following relations, consequences of Eqs. (2.4), (2.13), (2.39) and (2.47) have also been used:

$$\nabla\phi\cdot\nabla = \epsilon|\nabla\phi|^2\frac{\partial}{\partial\phi_1} = \frac{\epsilon}{c_0^2}\frac{\partial}{\partial\phi_1}, \qquad \nabla^2\phi = -\frac{\epsilon}{c_0^3}\frac{\partial c_0}{\partial\phi_1} \tag{2.52}$$

$$\frac{1}{\rho_0 c_0^2}\left(\frac{\partial p}{\partial s}\right)_{\rho,0}\nabla s_0\cdot\nabla\phi = \frac{1}{\rho_0 c_0^2}\nabla\phi\cdot[\nabla p_0 - c_0^2\nabla\rho_0] = \frac{H}{\rho_0 c_0^2}\left[\frac{1}{c_0^2}\frac{\partial p_0}{\partial\phi_1} - \frac{\partial\rho_0}{\partial\phi_1}\right]. \tag{2.53}$$

Direct integration of Eq. (2.51) with respect to τ_- gives for $p^{(2)}$ an expression which grows with τ_- because the right-hand side is independent of τ_-. In order to avoid this secularity, we demand that the right-hand side be identically equal to zero. Thus, $p^{(2)}$ is the superposition of a progressive and a regressive wave on the fast scale, and $p^{(1)}$ satisfies the equation

$$C_H\left[\frac{2}{c_0^2}\frac{\partial}{\partial\phi_1} - \frac{1}{c_0^3}\frac{\partial c_0}{\partial\phi_1} + \frac{1}{\rho_0 c_0^2}\left(\frac{1}{c_0^2}\frac{\partial p_0}{\partial\phi_1} - \frac{\partial\rho_0}{\partial\phi_1}\right)\right]\frac{\partial p^{(1)}}{\partial\tau_+} + C_H\mathcal{F}'$$
$$- C_N^2(\nabla\psi\cdot\nabla\psi):\frac{\partial^2}{\partial\psi_{1/2}\partial\psi_{1/2}}p^{(1)} - C_S\frac{D_0}{c_0^4}\frac{\partial^3 p^{(1)}}{\partial{\tau_+}^3} - \frac{\beta_0}{\rho_0 c_0^4}\frac{\partial^2(p^{(1)})^2}{\partial{\tau_+}^2} = 0. \tag{2.54}$$

Eq. (2.54) is a parabolic equation for $p^{(1)}(\psi_{1/2},\phi_1,\tau_+)$. The coefficients, however, are unknown functions of $(\psi_{1/2},\phi_1)$ as long as we have not solved the eikonal equation Eq. (2.47). The functions in this equation may also depend on other variables (for instance $\psi_1 = N^2\psi$, $\phi_2 = H^2\phi$, as mentioned earlier). These slower variables, however, play the role of parameters at the order of approximation where Eq. (2.54) is valid, since derivatives are taken only with respect to τ_+, $\psi_{1/2}$ and ϕ_1.

Because of the linear impedance relation Eq. (2.50), Eq. (2.54) is equivalent to the following equation in dimensional variables:

$$\left[\frac{1}{c_0^2}\frac{\partial^2}{\partial t^2} - \nabla^2\right](p-p_0) - \frac{1}{\rho_0 c_0^2}(\nabla p_0 - c_0^2\nabla\rho_0)\cdot\nabla(p-p_0) + \nabla\cdot\mathcal{F}' \tag{2.55}$$
$$-\frac{D_0}{c_0^4}\frac{\partial^3}{\partial t^3}(p-p_0) - \frac{\beta_0}{\rho_0 c_0^4}\frac{\partial^2}{\partial t^2}(p-p_0)^2 + O(\epsilon^2(p-p_0)) = 0.$$

In the parabolic approximation, membrane and piston boundary conditions are equivalent (i.e., pressure amplitude or normal velocity specified at the source), since the impedance relation is satisfied in curved coordinates (Eq. (2.50)).

2.2. Eikonal equation

To determine the orthogonal, curvilinear coordinate system $(\psi_{1/2}, \phi_1)$, we must solve the eikonal equation Eq. (2.47) to an order which is consistent with the approximations used in the previous section. Among others, we have assumed that the unperturbed sound speed c_0 depends on the physical variables $\mathbf{x}$ only through the stretched variables $\mathbf{x}_1 = H\mathbf{x}$, i.e., $c_0(\mathbf{x}) = c_0^*(\mathbf{x}_1) = c_0^*(H\mathbf{x})$. If the transformation $\mathbf{x} = (x, y, z) \longrightarrow (\psi, \phi) = (\varphi, \psi, \phi)$ is not singular, c_0 is also a function of (ψ, ϕ) which satisfies

$$\nabla c_0 = H\nabla_1 c_0^* = \nabla\psi \cdot \frac{\partial c_0}{\partial \psi} + \nabla\phi \frac{\partial c_0}{\partial \phi}. \tag{2.56}$$

Since $\nabla\psi$, $\nabla\phi$ are assumed of order one, c_0 can depend on (ψ, ϕ) only through $\phi_1 = H\phi$ and slower variables (for example $\psi_1 = N^2\psi$),

$$c_0^*(\mathbf{x}_1) = c_0^{**}(\psi_1, \phi_1, \ldots) = c_0^{**}(N^2\psi, H\phi, \ldots). \tag{2.57}$$

This means that c_0^{**} cannot depend on $\psi_{1/2} = N\psi$. This consequence of the scaling $N = O(\epsilon^{1/2})$, $H = O(\epsilon)$, is crucial in solving the eikonal equation to an order that is consistent with the parabolic approximation.

Since Eq. (2.54) does not account for transverse and longitudinal variations that are slower than those described by $\psi_{1/2}$ and ϕ_1, respectively, we must solve Eq. (2.47) as if c_0^{**} was only a function of ϕ_1. Regarding c_0^{**} as a function of $\psi_{1/2}$ would mean keeping contributions of the same order as terms that have been neglected when deriving Eq. (2.54). Noticing that $\partial\phi_1/\partial\mathbf{x}_1 = \partial\phi/\partial\mathbf{x}$, we may interprete Eq. (2.47) as an eikonal equation for the slow variable ϕ_1 in the stretched coordinates $\mathbf{x}_1$:

$$\left|\frac{\partial\phi_1}{\partial\mathbf{x}_1}\right| = \frac{1}{c_0^*(\mathbf{x}_1)} = \frac{1}{c_0^{**}(\phi_1)}. \tag{2.58}$$

Since ψ_1 and the other slower variables are parameters in this content, we will use the notation $c_0^{**}(\phi_1)$ in the rest of this section.

The ray-tracing equations corresponding to Eq. (2.58)

$$\frac{d\mathbf{x}_1}{d\phi_1} = c_0^{**2}\mathbf{s}, \qquad \frac{d\mathbf{s}}{d\phi_1} = -\frac{\mathbf{s}}{c_0^{**}}\frac{dc_0^{**}}{d\phi_1} \tag{2.59}$$

where $\mathbf{s}$ is the slowness vector, are readily solved:

$$\frac{d^2\mathbf{x}_1}{d\phi_1^2} = \frac{d}{d\phi_1}(c_0^{**2}\mathbf{s}) = 2c_0\frac{dc_0^{**}}{d\phi_1}\mathbf{s} - \frac{1}{c_0^{**}}\frac{d\mathbf{x}_1}{d\phi_1}\frac{dc_0^{**}}{d\phi_1} = c_0^{**}\mathbf{s}\frac{dc_0^{**}}{d\phi_1} = \frac{1}{c_0^{**}}\frac{dc_0^{**}}{d\phi_1}\frac{d\mathbf{x}_1}{d\phi_1}, \tag{2.60}$$

$$c_0^{**}\left[\frac{1}{c_0^{**}}\frac{d^2\mathbf{x}_1}{d\phi_1^2}-\frac{1}{c_0^{**2}}\frac{dc_0^{**}}{d\phi_1}\frac{d\mathbf{x}_1}{d\phi_1}\right]=c_0^{**}\frac{d}{d\phi_1}\left[\frac{1}{c_0^{**}}\frac{d\mathbf{x}_1}{d\phi_1}\right]=0. \tag{2.61}$$

Therefore:

$$\frac{d\mathbf{x}_1}{d\phi_1}=c_0^{**}\cdot\mathbf{T}_0, \tag{2.62}$$

and

$$\mathbf{x}_1=\mathbf{T}_0\int_0^{\phi_1}c_0^{**}(\phi_1)\,d\phi_1+\mathbf{x}_1^{(0)},\qquad \mathbf{s}=\frac{\partial\phi_1}{\partial\mathbf{x}_1}=\frac{\mathbf{T}_0}{c_0^{**}}, \tag{2.63}$$

where $\mathbf{T}_0$ and $\mathbf{x}_1^{(0)}$ are constant vectors, $|\mathbf{T}_0|=1$.

Eq. (2.63) implies that if the sound source is located in the plane $z=0$, this plane should be a wavefront, say $\phi_1=0$. Accordingly, we choose $\mathbf{T}_0=\mathbf{e}_z$ and $\mathbf{x}_1^{(0)}=(\mathbf{x}_{\perp 1},0)=(H\mathbf{x}_\perp,0)$. The ray passing through the point $(\mathbf{x}_{\perp 1},0)$ in the plane of the source is parallel to the z axis, and the surfaces $\varphi=$ constant, $\psi=$ constant are thus planes parallel to the z axis, for instance $x=$ constant and $y=$ constant. Therefore: $\boldsymbol{\psi}_1=\mathbf{x}_{\perp 1}$, or $\varphi_1=x_1$ and $\psi_1=y_1$.

Projecting Eq. (2.63) on the z axis gives

$$z_1=\int_0^{\phi_1}c_0^{**}(\phi_1)\,d\phi_1 \tag{2.64}$$

which is inverted to

$$\phi_1=\int_0^{z_1}\frac{dz_1}{c_0^{*}(\mathbf{x}_1)} \tag{2.65}$$

where $\mathbf{x}_{\perp 1}$ is kept constant under the integration. Changing back to the variable $\mathbf{x}$, the transform $(\mathbf{x}_\perp,z)\longrightarrow(\boldsymbol{\psi},\phi)$ is defined by

$$\boldsymbol{\psi}=\mathbf{x}_\perp=(x,y),\quad \phi(\mathbf{x})=\int_0^z\frac{dz}{c_0(\mathbf{x})},\quad z=\int_0^{\phi}c_0(\mathbf{x}_\perp,\phi)\,d\phi, \tag{2.66}$$

where $\mathbf{x}_\perp$ is kept constant under the integration.

Thus, consistently solving the eikonal equation leads to rays which in the stretched coordinates $(N\mathbf{x}_\perp,H\phi)$ are straight lines. In the physical space, however, the rays are bent, since $\phi=$ constant does not imply $z=$ constant, unless c_0 is a function of z only. For a medium with a given inhomogeneity structure specified in physical coordinates, beams propagating in the same direction, but with different diffraction number N $(=(ka)^{-1}$ for the homogeneous, monochromatic case) will not be equally affected by the sound speed gradient.

In classical ray theory, the eikonal equation is stated in physical coordinates. Ray tracing is related to a point source and diffraction is discarded, so that characteristic lengths other than the wavelength of the signal (in the monochromatic case), do not naturally occur. The eikonal equation is integrated exactly, without restrictions on variations in sound speed or radius of curvature of the wavefront, relative to a

wavelength. This implies that, eventually, rays will cross, i.e., caustics will appear. At caustics, the wavefronts vary on a scale shorter than a wavelength – thus these variations are not detected properly. The pressure amplitude along a ray is given by the transport equation, which does not include diffraction effects. The transport equation breaks down at caustics, where asymptotic matching methods[47] can be applied to obtain the acoustic pressure.

The reason for the breakdown of ray theory in caustics regions is that variations in the field transverse to each separate ray are neglected, in order to uncouple the equations for the ray paths and the amplitude. Along each ray, the pressure field is described as a simple wave, to all orders considered. When the ray paths cross, the simple waves are no longer defined. Therefore, caustics result from the approximations in ray theory. In our model, the equations for the ray paths (Eq. (2.47)) and the amplitude (Eq. (2.54)) are also uncoupled. The coordinate transform Eq. (2.66) is regular whenever c_0, c_0^{-1} is integrable. However, we calculate approximate ray paths and do not discard the transverse variations in the field. On the short scale, the pressure perturbation behaves as a simple wave, but on the long scale, diffraction is accounted for over a scale that preserves the effects of inhomogeneity, nonlinearity and dissipation. Due to these consistent approximations, caustics cannot appear in our model.

Equation (2.54) can be interpreted as a nonlinear, "global" transport equation for a beam consisting of a bundle of "rays" described by Eq. (2.66). To our order of approximation, these "rays" are parallel curves in space.

2.3. Simplifications of the equation

So far, we have shown that the nondimensional pressure $p^{(1)}$ is consistently described by Eq. (2.54) in terms of the nondimensional stretched variables $(\psi_{1/2}, \phi_1, \tau_+)$. Here the nondimensional, unperturbed quantities appearing in the coefficients are to be considered (to dominating order) as functions of ϕ_1 alone, as justified in the discussion of the eikonal equation. (These quantities should be denoted c_0^{**}, p_0^{**}, etc., but we omit ** for simplicity.) In general, this equation must be solved numerically, subject to a boundary condition prescribed at the source. If the source is in the plane $z = 0$, the boundary condition is of the form $p^{(1)}(\psi_{1/2}, 0, \tau_+) = f(\psi_{1/2}, t)$, since $\phi_1 = 0$ and $\tau_+ = t$ at $z = 0$. The acoustic pressure at $(\mathbf{x}, t) = (\mathbf{x}_\perp, z, t)$ is obtained from $p^{(1)}(N\mathbf{x}_\perp, H\phi(\mathbf{x}), t - \phi(\mathbf{x}))$, where ϕ is given by Eq. (2.66). We write $\mathbf{x}_\perp$, $\mathbf{x}_{\perp 1/2}$, $\nabla_{\perp 1/2}$ for ψ, $\psi_{1/2}$, $\partial/\partial\psi_{1/2}$. In this section we will present alternative forms for Eq. (2.54) and the coordinate transform Eq. (2.66), that facilitate analytical and numerical work.

The inhomogeneity term may be simplified by introducing a new unknown func-

tion $P^{(1)}$,

$$P^{(1)}(\mathbf{x}_{\perp 1/2}, \phi_1, \tau_+) = (\rho_0 c_0)^{-1/2} \cdot \exp\left[\int_0^{\phi_1} \frac{1}{2\rho_0 c_0^2} \frac{\partial p_0}{\partial \phi_1}\, d\phi_1\right] p^{(1)}$$
$$= (\rho_0 c_0)^{-1/2} \cdot \mathcal{K}_0^{-1} p^{(1)}(\mathbf{x}_{\perp 1/2}, \phi_1, \tau_+). \tag{2.67}$$

Since $(\partial p_0/\partial \phi) = c_0 \mathbf{e}_z \cdot \mathbf{F}_0$, see Eq. (2.10), $\mathcal{K}_0$ is equal to one whenever the external force is transverse to the beam axis (or zero).

Since to dominating order $(\rho_0 c_0)^{1/2} \cdot \mathcal{K}$ is independent of $\mathbf{x}_{\perp 1/2}$, Eq. (2.54) is transformed into

$$- C_H \frac{2}{c_0^2} \frac{\partial^2 P^{(1)}}{\partial \phi_1 \partial \tau_+} - C_H \mathcal{F}''$$
$$+ C_N^2 \nabla_{\perp 1/2} P^{(1)} + \frac{\beta_0 (\rho_0 c_0)^{1/2} \mathcal{K}_0}{\rho_0 c_0^4} \frac{\partial^2 P^{(1)2}}{\partial {\tau_+}^2} + C_S \frac{D_0}{c_0^4} \frac{\partial^3 P^{(1)}}{\partial {\tau_+}^3} = 0, \tag{2.68}$$

where

$$\mathcal{F}'' = (\rho_0 c_0)^{-1/2} \mathcal{K}_0^{-1} \mathcal{F}'. \tag{2.69}$$

For a homogeneous reference medium with the ambient nondimensional quantities $\rho_0, c_0 = 1$, $\phi_1 = z_1$, where z_1 is scaled to a characteristic length for slow variation along the beam axis. In this case, Eq. (2.68) reduces to the KZK equation. For an inhomogeneous medium, there are two important differences: (i) The coefficients in the parabolic equation are not constant, they are functions of the varying ambient density, ρ_0, and soundspeed, c_0 ($\rho_0 = \rho_0(c_0)$). (ii) The functional relation between ϕ_1 and z_1 depends on the sound speed profile.

The factor $1/c_0^2$ in front of the first term in Eq. (2.68) can be removed without modifying the remaining terms by introducing a new longitudinal variable

$$\sigma = \int_0^{z_1} c_0(z_1)\, dz_1, \tag{2.70}$$

and by noticing that

$$\frac{\partial}{\partial \sigma} = \frac{1}{c_0} \frac{\partial}{\partial z_1} = \frac{1}{c_0^2} \frac{\partial}{\partial \phi_1}. \tag{2.71}$$

This leads to a new equation for $P^{(1)}(\mathbf{x}_{\perp 1/2}, \sigma, \tau_+)$:

$$2C_H \frac{\partial^2 P^{(1)}}{\partial \sigma \partial \tau_+} - C_N^2 \nabla_{\perp 1/2}^2 P^{(1)} - \mathcal{P}_{abs} \frac{\partial^3 P^{(1)}}{\partial {\tau_+}^3} - \mathcal{P}_{nonl} \frac{\partial^2 {P^{(1)}}^2}{\partial {\tau_+}^2} + C_H \mathcal{F}'' = 0, \tag{2.72}$$

where

$$\mathcal{P}_{abs} = C_S \frac{D_0}{c_0^4}, \qquad \mathcal{P}_{nonl} = \frac{\beta_0 (\rho_0 c_0)^{1/2} \mathcal{K}_0}{\rho_0 c_0^4} \tag{2.73}$$

depend on σ and ψ_1 through ρ_0, c_0, etc.. Equation (2.72) becomes a linear parabolic equation with constant coefficients when nonlinearity and dissipation are discarded.

Introducing dimensional variables, the curved coordinates defined in an inhomogeneous medium can be related to corresponding coordinates in a homogeneous medium.

$$\begin{aligned}
&\underline{\text{Inhomogeneous}} && \longleftrightarrow && \underline{\text{Homogeneous}} \\
&\phi = \frac{1}{T}\int_0^z \frac{dz}{c_0} && \longleftrightarrow && \frac{z}{L} \\
&t - \phi = \frac{1}{T}(t - \int_0^z \frac{dz}{c_0}) && \longleftrightarrow && \frac{1}{T}(t - \frac{z}{c_0}) \\
&\phi_1 = \frac{L}{L_H}\frac{1}{T}\int_0^z \frac{dz}{c_0} = \bar{c}\int_0^{z/L_H} \frac{1}{c_0}\, d\frac{z}{L_H} && \longleftrightarrow && \frac{z}{L_H} \\
&\psi_{1/2} = N\psi = \frac{L}{a}\frac{\mathbf{x}_\perp}{L} = \frac{\mathbf{x}_\perp}{a} && \longleftrightarrow && \frac{\mathbf{x}_\perp}{a} \\
&\sigma = \int_0^{z/L_H} \frac{c_0}{\bar{c}}\, d\frac{z}{L_H} = \frac{1}{\bar{c}L_H}\int_0^z c_0\, dz && \longleftrightarrow && \frac{z}{L_H}
\end{aligned}$$

For the homogeneous, monochromatic case, the Rayleigh distance, R, may be introduced as characteristic length for slow variations along the beam axis. It is defined as $R = ka^2/2$, where k is the wavenumber of the source function. In the homogeneous case, L_H is infinitely large. When the KZK equation is derived, R takes the role L_H has in the present derivation. For the inhomogeneous, monochromatic case, no constant analogue to R can be defined, since c_0 is not a constant. L_H is defined through $|\nabla c_0/c_0| = O(L_H^{-1})$ and depends on what functional expression is used for the sound speed profile; thus there is a certain degree of freedom in specifying L_H. By choosing the similarity coefficients as $C_H = 2C_N^2$, we get a definition of L_H which reduces to the Rayleigh distance in the homogeneous, monochromatic case. Thus, $L_H = a^2/(2T\bar{c}_0)$, where $\bar{c}_0$ is the sound speed in the homogeneous reference medium. The motivation for this choice is that the effects of inhomogeneity can be described within the terminology for a beam propagating in a homogeneous medium.

By this choice of similarity coefficients new interpretations of ϕ and σ appear. For the monochromatic case:

$$\begin{aligned}
\sigma &= \frac{1}{\bar{c}L_H}\int_0^{z/L_H} c_0\, dz = \int_0^z \frac{2c_0\, dz}{\omega a^2} = \int_0^z \frac{2\, dz}{k(z)a^2}, \\
\phi &= \frac{1}{T}\int_0^z \frac{dz}{c_0} = \int_0^z \frac{\omega\, dz}{c_0} = \int_0^z k(z)\, dz,
\end{aligned} \tag{2.74}$$

where $k(z)$ is a variable wavenumber and c_0 is dimensional soundspeed. Thus, σ is scaled to the local "Rayleigh distance" $k(z)a^2/2$, while ϕ is scaled to the local

"wavelength" $(k(z))^{-1}$. Equation (2.72) becomes:

$$4\frac{\partial^2 P^{(1)}}{\partial\sigma\partial\tau_+} - \nabla_{\perp 1/2}^2 P^{(1)} - 4\mathcal{P}^*_{abs}\frac{\partial^3 P^{(1)}}{\partial{\tau_+}^3} - 2\mathcal{P}^*_{nonl}\frac{\partial^2 (P^{(1)})^2}{\partial{\tau_+}^2} + 2\mathcal{F}'' = 0, \tag{2.75}$$

where

$$\mathcal{P}^*_{abs} = \bar{\alpha}L_H\frac{D_0}{c_0^4}, \qquad \mathcal{P}^*_{nonl} = \frac{L_H}{l_d}\frac{(\rho_0 c_0)^{1/2}\mathcal{K}_0}{\rho_0 c_0^4}. \tag{2.76}$$

Here $L_H = a^2/2\bar{c}T$ and $l_d^{-1} = \beta_0\epsilon/(\bar{c}T)$ is the shock formation distance for a sinusoidal wave with frequency $\omega = T^{-1}$. The dimensional form of Eq. (2.75) is:

$$\frac{2}{\bar{c}}\frac{\partial^2\bar{p}^{(1)}}{\partial\sigma_0\partial\tau_0} - {\nabla_\perp}^2\bar{p}^{(1)} - \frac{D_0}{c_0^4}\frac{\partial^3\bar{p}^{(1)}}{\partial\tau_0^3} - \frac{\beta_0}{\rho_0 c_0^4}\frac{\partial^2(\bar{p}^{(1)})^2}{\partial\tau_0^2} - \nabla\cdot\mathbf{F}' = 0, \tag{2.77}$$

where $\sigma_0 = L_H\sigma$, $\tau_0 = \tau_+ T$, $\bar{p}^{(1)} = P^{(1)}\bar{\rho}\bar{c}\bar{u}(\rho_0 c_0)^{1/2}$, and all quantities in Eq. (2.77) are dimensional.

2.4. The limit process $N \to 0$.

The importance of the ordering of the diffraction number N will now be discussed. Assume that the source is monochromatic. What happens in the limit $N \to 0$, (i.e., $ka \to \infty$)? In the derivation of Eqs. (2.54, 2.75), the inhomogeneity length is related to the Rayleigh distance corresponding to given values a and k by specifying the similarity coefficients as $C_H = 2C_N^2$. The similarity parameters can be small numerically, and $H = O(\epsilon)$ and $N = O(\epsilon^{1/2})$ still be satisfied, i.e., the effects of diffraction are still accounted for when N decreases. However, it can be useful to go back to the derivation to discuss other possible orderings of the parameters.

In the homogeneous case ($H = 0$), the limit $ka \to \infty$ provides a plane wave propagating in the positive z-direction, i.e., diffraction is removed from the model. It is consistent to let $N \to 0$ in the parabolic equation, since $H = 0$ and the characteristic length for slow longitudinal variations thus is connected only to diffraction (in absence of dissipation). In the inhomogeneous case $H \neq 0$. Is it consistent with our simplified solution of the eikonal equation to let $N \to 0$, assuming $H = O(\epsilon)$?

A first step towards the limit $N \to 0$ is to assume $N = O(\epsilon)$. In that case, $\mathbf{v}_\perp = O(\epsilon^2)$ and $\nabla \times \mathbf{v}$ can be neglected, according to Eq. (2.43). In order to have uncoupled progressive and regressive waves on the short scale, the eikonal equation Eq. (2.47) must be satisfied, hence Eqs. (2.48, 2.50) are satisfied. This scaling of transverse coordinate implies that transverse derivatives disappear in Eq. (2.54), and the condition to avoid secularities in p' on the short scale is

$$C_H\left[\frac{2}{c_0^2}\frac{\partial}{\partial\phi_1} - \frac{1}{c_0^3}\frac{\partial c_0}{\partial\phi_1} + \frac{1}{\rho_0 c_0^2}\left(\frac{1}{c_0^2}\frac{\partial p_0}{\partial\phi_1} - \frac{\partial\rho_0}{\partial\phi_1}\right)\right]\frac{\partial p^{(1)}}{\partial\tau_+} + C_H\mathcal{F}'$$
$$- C_S\frac{D_0}{c_0^4}\frac{\partial^3 p^{(1)}}{\partial{\tau_+}^3} - \frac{\beta_0}{\rho_0 c_0^4}\frac{\partial^2(p^{(1)})^2}{\partial{\tau_+}^2} = 0. \tag{2.78}$$

The similarity coefficients can be determined by for instance relating the reference absorption length and shock formation distance to the inhomogeneity length L_H. For a source in the plane $z = 0$, the boundary conditions are:

$$p^{(1)}|_{z=0} = f(t). \tag{2.79}$$

However, when $N = O(\epsilon)$, the eikonal equation can no longer be solved approximately as in Eq. (2.66). Transverse and longitudinal variables (ϕ_1, ψ_1) now vary over the same scale, therefore:

$$|\frac{\partial \phi}{\partial \mathbf{x}}| = |\frac{\partial \phi_1}{\partial \mathbf{x}_1}| = \frac{1}{c_0^*(\mathbf{x}_1)} = \frac{1}{c_0^{**}(\psi_1, \phi_1)}. \tag{2.80}$$

Equation (2.80) must be solved exactly on the slow space scale, subject to boundary conditions suitable for a plane source at $z = 0$:

$$\phi_1(\mathbf{x}_\perp, z = 0) = 0, \qquad \nabla\phi_1|_{z=0} = \frac{\mathbf{e}_z}{c_0(\mathbf{x}_{\perp 1}, z = 0)}. \tag{2.81}$$

Hence, by the scaling $N = O(\epsilon)$, exact rays are calculated, and the solution for ϕ_1 will become singular at caustics.

The introduction of $P^{(1)}$ as defined in Eq. (2.67) simplifies the first term in Eq. (2.78) without further approximations:

$$-C_H \frac{2}{c_0^2} \frac{\partial^2 P^{(1)}}{\partial \phi_1 \partial \tau_+} - C_H \mathcal{F}'' + \frac{\beta_0 (\rho_0 c_0)^{1/2} \mathcal{K}_0}{\rho_0 c_0^4} \frac{\partial^2 P^{(1)2}}{\partial {\tau_+}^2} + C_S \frac{D_0}{c_0^4} \frac{\partial^3 P^{(1)}}{\partial {\tau_+}^3} = 0. \tag{2.82}$$

By the definition

$$\sigma = \int_0^{\phi_1} c_0^2 d\phi_1, \tag{2.83}$$

the factor c_0^2 in the first term in Eq. (2.82) is removed. Equation (2.82) is a generalized Burgers equation, expressed in curved coordinates, with varying coefficients and cotributions from an external force. Even though diffraction is neglected, $P^{(1)}$ depends on (x, y, z) through $\rho_0(\mathbf{x}_1)$, $c_0(\mathbf{x}_1)$ and the coordinates ϕ_1, τ_+.

To conclude: The specific ordering of diffraction by $N = O(\epsilon^{1/2})$ (i.e., parabolic approximation) and inhomogeneity by $H = O(\epsilon)$ is essential for (1) consistently accounting for diffraction when approximating the nonlinear, generalized wave equation, Eq. (2.31), and (2) avoiding the caustics problem connected to the solution of the eikonal equation.

In order to picture the *ka*-region (bounded from below and above) where (i) the parabolic approximation of Eq. (2.31) and (ii) the approximate solution of the eikonal equation, Eq. (2.66) are valid, one should: (1) Compare the solution of Eq. (2.75) with the solution of Eq. (2.32) (the Helmholtz equation with varying coefficients), with boundary conditions specified on a real source and investigate how sensitive our model is to variations of *ka*. (2) Compare with the solution of Burgers equation in curved coordinates, Eq. (2.82). However, in absence of suitable reference solutions, we will here omit both comparisons (1) and (2).

Chapter 3

Numerical calculations

Equation (2.75), with linearized, monochromatic, real boundary conditions

$$P^{(1)}(\tau_+, \sigma, \mathbf{x}_{\perp 1/2})|_{z=0} = f(\mathbf{x}_{\perp 1/2}) \sin t, \tag{3.1}$$

is solved numerically by a finite difference method (cf. Refs. (9–17)). Also, in the linear case, an analytical solution is obtained. The source is a membrane or piston source in a baffle, hence f is approximately zero in the source plane beyond a characteristic source radius, i.e., for $|\mathbf{x}_{\perp 1/2}| > 1$. $P^{(1)}$ is either nondimensional pressure amplitude or nondimensional longitudinal velocity – these variables are equivalent in the parabolic approximation, as are the membrane and piston boundary conditions. In all the following computations, the perturbation in external force, $\mathcal{F}''$ and the longitudinal component of the unperturbed external force, $c_0^{-1}\partial p_0/\partial \phi_1$ are both chosen to be 0, to isolate the effects of ∇c_0.

To simplify calculations in the farfield of the source, the grid in $(\sigma, \mathbf{x}_{\perp 1/2})$ coordinates for numerical calculations is adjusted within our approximation, to be more dense near the source than further away, as was done in Refs. (10, 12). Accordingly, new transformed coordinates are defined:

$$\tau_p = \tau_+ + A(\mathbf{x}_{1/2}, \mathbf{x}_1, \ldots), \qquad \mathbf{u} = \mathbf{u}(\mathbf{x}_{1/2}, \mathbf{x}_1, \ldots). \tag{3.2}$$

Since c_0 is to be considered as independent of $\mathbf{x}_{\perp 1/2}$ and the source is in the plane $z = 0$, the result is:

$$A = -\frac{|\mathbf{x}_{\perp 1/2}|^2}{\sigma + 1}, \qquad \mathbf{u} = \frac{\mathbf{x}_{\perp 1/2}}{\sigma + 1}. \tag{3.3}$$

Hence Eq. (2.75) is transformed into:

$$4\frac{\partial^2 U}{\partial \sigma \partial \tau_p} - \frac{1}{(\sigma+1)^2}\nabla_{\perp \mathbf{u}}^2 U - \frac{2}{\sigma+1}\mathcal{P}^*_{nonl}\frac{\partial^2 U^2}{\partial {\tau_p}^2} - 4\mathcal{P}^*_{abs}\frac{\partial^3 U}{\partial {\tau_p}^3} + 2\mathcal{F}'' = 0, \tag{3.4}$$

where

$$U(\tau_p, \sigma, \mathbf{u}) = (\sigma + 1)P^{(1)}(\tau_+, \sigma, \mathbf{x}_{\perp 1/2}). \tag{3.5}$$

The boundary condition Eq. (3.1) now reads:

$$U(\tau_p, \sigma, \mathbf{u})|_{z=0} = f(\mathbf{x}_{\perp 1/2}) \sin(t + |\mathbf{x}_{\perp 1/2}|^2) \tag{3.6}$$
$$= f(\mathbf{x}_{\perp 1/2})(\sin t \cos |\mathbf{x}_{\perp 1/2}|^2 + \cos t \sin |\mathbf{x}_{\perp 1/2}|^2).$$

Eq. (3.4) can be solved in frequency domain, assuming a Fourier series[9] for the real pressure perturbation U with respect to τ_p:

$$U = \sum_{n=1}^{\infty} (a_n \sin n\tau_p + b_n \cos n\tau_p) \tag{3.7}$$
$$= Re\left[\sum_{n=1}^{\infty} (ig_n \exp[i(n\tau_p + \Delta_n)])\right]$$
$$a_n = g_n \cos \Delta_n, \qquad b_n = g_n \sin \Delta_n,$$
$$\Delta_n = \arctan(b_n/a_n), \qquad g_n = (a_n^2 + b_n^2)^{1/2}. \tag{3.8}$$

Inserted in Eq. (3.4) and Eq. (3.6), Eq. (3.7) provides an infinite set of equations for the Fourier coefficients[13,14,15,16] $a_n(\sigma, \mathbf{u})$ and $b_n(\sigma, \mathbf{u})$:

$$\frac{\partial a_n}{\partial \sigma} = -\mathcal{P}^*_{abs} n^2 a_n + \frac{1}{4n(1+\sigma)^2} \nabla^2_{\perp \mathbf{u}} b_n$$
$$+ \frac{\mathcal{P}^*_{nonl}}{2(1+\sigma)} \left[\frac{1}{2}\sum_{i=1}^{n-1} (a_{n-i}a_i - b_{n-i}b_i) - \sum_{i=n+1}^{\infty} (b_i b_{i-n} + a_i a_{i-n})\right],$$
$$\frac{\partial b_n}{\partial \sigma} = -\mathcal{P}^*_{abs} n^2 b_n - \frac{1}{4n(1+\sigma)^2} \nabla^2_{\perp \mathbf{u}} a_n$$
$$+ \frac{\mathcal{P}^*_{nonl}}{2(1+\sigma)} \left[\sum_{i=1}^{n-1} (b_{n-i}a_i) + \sum_{i=n+1}^{\infty} (a_i b_{i-n} - b_i a_{i-n})\right], \tag{3.9}$$
$$n = 1, 2, \ldots,$$

with boundary conditions

$$a_1|_{z=0} = f(\mathbf{x}_{\perp 1/2}) \cos |\mathbf{x}_{\perp 1/2}|^2, \qquad b_1|_{z=0} = f(\mathbf{x}_{\perp 1/2}) \sin |\mathbf{x}_{\perp 1/2}|^2, \tag{3.10}$$
$$a_n|_{z=0} = b_n|_{z=0} = 0, \qquad n = 2, 3, \ldots,$$

or

$$g_1|_{z=0} = f(\mathbf{x}_{\perp 1/2}), \qquad \Delta_1|_{z=0} = 0, \tag{3.11}$$
$$g_n|_{z=0} = \Delta_n|_{z=0} = 0, \qquad n = 2, 3, \ldots.$$

In the fully nonlinear model, Eqs. (3.9) are truncated at a finite $n = n_{max}$. In the quasilinear model, Eqs. (3.9) are truncated at $n = 2$ and in the nonlinear terms, the sums starting at $i = n + 1$ are discarded. Hence, the calculated fundamental is identical to the solution of the linear equation. [For a monochromatic source in a homogeneous medium: In the quasilinear model the pressure cannot be calculated

up to ranges near the shock formation distance, while in the fully nonlinear model, the pressure can be calculated beyond the shock formation distance. The number of harmonics kept in the calculations, n_{max}, is essential for the accuracy of the solution for the individual harmonics.[14,15,16,17] Two examples of boundary conditions are considered:

$$\text{Gaussian source}: \quad f(\mathbf{x}_{\perp 1/2}) = \exp\left(-|\mathbf{x}_{\perp 1/2}|^2\right). \tag{3.12}$$

$$\text{Uniform source}: \quad f(\mathbf{x}_{\perp 1/2}) = 1,\ |\mathbf{x}_{\perp 1/2}| \leq 1,\ f(\mathbf{x}_{\perp 1/2}) = 0,\ |\mathbf{x}_{\perp 1/2}| > 1. \tag{3.13}$$

The truncated system Eq. (3.9) with boundary conditions Eq. (3.10) is solved numerically by a finite difference method in three dimensions, the ADI method (Alternating Direction Implicit)[13,14,15,16] with second order accuracy. The source can be asymmetric, although only axisymmetric sources are considered here. The transverse Laplace operator is approximated by a central difference operator. For uniform sources, some initial implicit steps are taken in the σ-direction, to damp the Gibbs oscillations due to the discontinuity in the boundary condition at the source. The program continues with a second order trapeze method. The nonlinear terms are treated by an explicit method.

In the $(\sigma, \mathbf{u})$ coordinates, the mesh where the solution is computed, is rectangular in directions both transverse and parallel to the σ-axis. We choose $-7.0 \leq |\mathbf{u}| \leq 7.0$, both for linear, quasilinear and fully nonlinear computations. The boundary conditions at $|\mathbf{u}| = U_{max}$ are artificially set to $a_n, b_n = 0$, $n = 1, 2, \ldots$. This gives bad approximation in the solution near the u-boundary, but other choices of boundary conditions did not improve the result[14,16]. [The relative error is large, but it has little influence on the total solution. By using a large enough window in $\mathbf{u}$, we get acceptable results for a_n, b_n in the main region of interest, i.e., not too close to the boundary of the window[14].] The number of transverse grid points is 301 or 201, depending on the smoothness of $f(\mathbf{x}_{\perp 1/2})$. [This choice of maximum $|\mathbf{u}|$ and number of grid points gives a reasonable resolution within an acceptable computation time. If the number of transverse grid points in the axisymmetric program is X_{max}, the same resolution in the 3–D case demands $(2X_{max} - 1)^2$ grid points. Hence the 3–D program is much more time consuming.] Transformed into Cartesian coordinates, the rectangular mesh in σ and one transverse variable becomes irregular and curved in the plane spanned by ∇c_0 and $\mathbf{e}_z$, depending on the varying sound speed, see Fig. 3.1. To get beampatterns and propagation curves, the computed values of a_n and b_n must be interpolated to provide values on a rectangular grid in Cartesian coordinates. One possibility could be to carry out this interpolation of the a_n's and b_n's as soon as they are computed by the finite difference program, for specified σ values. However, since we omit this procedure, the results of the numerical computations are best visualized by contour plots of the amplitude in planes spanned by the z–axis and one transverse axis.

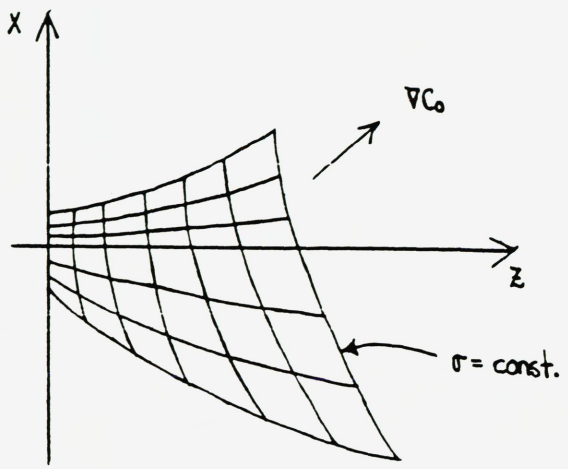

FIG. 3.1. Curved coordinate mesh used in the numerical calculations.

In the linear, nondissipative, monochromatic case, Eq. (2.75) can be solved analytically by Fourier transform with respect to the transverse variables. Assume

$$P^{(1)} = e^{i\tau} V(\sigma, \mathbf{x}_{\perp 1/2}), \qquad V(0, \mathbf{x}_{\perp 1/2}) = f(\mathbf{x}_{\perp 1/2}). \tag{3.14}$$

The solution for the complex amplitude V is then

$$V(\sigma, \mathbf{x}_{\perp 1/2}) = \frac{1}{i\pi\sigma} \int\int_{\infty}^{\infty} f(\mathbf{x}'_{\perp 1/2}) \exp\left(i \frac{|\mathbf{x}'_{\perp 1/2} - \mathbf{x}_{\perp 1/2}|^2}{\sigma} \right) d\mathbf{x}'_{\perp 1/2}. \tag{3.15}$$

In the "farfield" of the source, that is, for $\sigma \gg 1$, this becomes

$$V(\sigma, \mathbf{x}_{\perp 1/2}) = \frac{2}{i\sigma} \exp\left(i \frac{|\mathbf{x}_{\perp 1/2}|^2}{\sigma} \right) \hat{f}\left(\frac{2\mathbf{x}_{\perp 1/2}}{\sigma} \right), \tag{3.16}$$

where $\hat{f}$ is the Fourier transform of f with respect to transverse variables, defined as:

$$\hat{f}(\mathbf{k}) = \frac{1}{2\pi} \int_{-\infty}^{+\infty} f(\mathbf{x}_\perp) \exp\left(-i\mathbf{k} \cdot \mathbf{x}_\perp\right) d\mathbf{x}_\perp. \tag{3.17}$$

In the special case of a circular, uniform source:

$$V(\sigma, \mathbf{x}_{\perp 1/2}) = \frac{2}{i\sigma} \exp\left(i \frac{|\mathbf{x}_{\perp 1/2}|^2}{\sigma} \right) \frac{J_1\left(\frac{2\mathbf{x}_{\perp 1/2}}{\sigma}\right)}{\frac{2\mathbf{x}_{\perp 1/2}}{\sigma}}, \tag{3.18}$$

where J_1 is the Bessel function of first type of order 1. Since $\sigma = \sigma(z_1, \mathbf{x}_{\perp 1})$, the $(z_1, \mathbf{x}_{\perp 1/2})$ range where the farfield approximation in σ is valid, depends on the sound speed profile.

The total phase of $P^{(1)}$ in the "farfield" is:

$$\Phi = \tau_+ + \left(\frac{|\mathbf{x}_{\perp 1/2}|^2}{\sigma} - \frac{\pi}{2}\right) + arg\left[\hat{f}\left(\frac{2\mathbf{x}_{\perp 1/2}}{\sigma}\right)\right]. \tag{3.19}$$

The first term is the rapid phase corresponding to progressive simple waves, the second term represents spherical spreading and the third term comes from the Fourier transform of the pressure distribution on the source. Depending on whether σ = constant is larger or smaller than the corresponding z, i.e., whether c_0 increases or decreases, the spherical spreading in the inhomogeneous medium occurs closer to or further away from the source, than in the homogeneous medium.

In the linear, monochromatic case, the dissipation term can be simplified. $\mathcal{P}^*_{abs}$ = $\mathcal{P}^*_{abs}(\sigma, \mathbf{x}_{\perp 1})$ in Eq. (2.75), since c_0, etc., are independent of $\mathbf{x}_{\perp 1/2}$, cf. Sect. 2.2. Due to the ordering of the transverse scale, it is consistent with the derivation of Eq. (2.75) to consider $\mathbf{x}_{\perp 1}$ as a parameter in $\mathcal{P}^*_{abs}$, and we define

$$V(\sigma, \mathbf{x}_{\perp 1/2}) = v(\sigma, \mathbf{x}_{\perp 1/2}) \cdot h(\sigma, \mathbf{x}_{\perp 1}), \tag{3.20}$$

with

$$h(\sigma, \mathbf{x}_{\perp 1}) = h(z_1, N\mathbf{x}_{\perp 1/2}) = \exp\left(-\int_0^\sigma \frac{\bar{\alpha}\bar{L}_H D_0}{c_0^4} d\sigma'\right), \tag{3.21}$$

$$= \exp\left(-\int_0^{z_1} \frac{\bar{\alpha}\bar{L}_H D_0}{c_0^3} dz_1'\right). \tag{3.22}$$

$v(\sigma, \mathbf{x}_{\perp 1/2})$ satisfies the linear, nondissipative version of Eq. (2.75). Boundary condition is given in Eq. (3.14) and the solution is Eq. (3.15), with V replaced by v. For several discrete frequency components, each component could be treated as shown above. For a thermo-viscous fluid, the effective absorption coefficient $\mathcal{P}_{abs}$ increases as the square of the frequency.

The soundspeed profiles are for simplicity chosen so that in regions where c_0 varies, $|\nabla c_0|$ is strictly positive, since the intention is to illustrate qualitatively the implications of inhomogeneity in our model. However, profiles having maxima and/or minima can easily be included (thus there should be a possibility to model approximations to wave guides, for instance). The only limit on the choice of profile is that the transform and its inverse (Eqs. (2.66) combined with Eq. (2.70)) can be calculated explicitely, to save computer time. Since $c_0 > 0$, σ increases with z_1 and the transform $(\sigma, \mathbf{x}_{\perp 1/2}) \rightarrow (z_1, \mathbf{x}_{\perp 1/2})$ is well defined. However, it is also possible to use discrete functions for the sound speed, for instance experimental values known on a grid. Then the coordinate transform can be calculated by numerical integration, and a table of transform values must be stored.

For simplicity, an adiabatic relation was chosen between ρ_0 and c_0: $c_0 = (\Upsilon/\rho_0)^{1/2}$, with Υ the bulk modulus for air. The validity of this approximation is not discussed

further. Inserting $\rho_0 = \Upsilon/c_0^2$ in Eq. (2.67) for the nondimensional pressure amplitude $p^{(1)}$, we see that the amplitude scaling factor $(\rho_0 c_0)^{1/2}$ is maximized in regions in space of smallest c_0. Equation (2.73) with $\rho_0 = \Upsilon/c_0^2$ shows that the varying nonlinearity coefficient in Eq. (2.75), $\mathcal{P}_{nonl}$, is largest in regions in space of smallest c_0. Hence the choice of function $\rho_0 = \rho_0(c_0)$ will have influence on the conclusions in Chapters 4 and 5, concerning the effects of inhomogeneous medium on variations of linear and nonlinear pressure amplitude.

Chapter 4

Applications

4.1. Numerical results for the linear case

Numerical examples are presented for the linear case with an axisymmetric source located in the plane $z = 0$. In all the following computations, we assume $\mathbf{e}_z \cdot \mathbf{F}_0 = 0$ and $\mathcal{F}' = 0$. In the nondissipative case, the geometry of the problem in the transformed coordinate system is also axisymmetric, and identical to the homogeneous problem. Therefore analytical/asymptotic results and programs for the axisymmetric, homogeneous case can be used. [See Chap. 3.] The effects of inhomogeneity appear through the coordinate transform and the varying amplitude scaling factor $(\rho_0 c_0)^{1/2}$. By accounting for dissipation through the factor $h(\sigma, \mathbf{x}_{\perp 1})$, results from the homogeneous, nondissipative case can also be applied to the dissipative case. The normalized pressure amplitude is shown in the plane spanned by the z–axis and the sound speed gradient. [This plane is in the following specified as the xz-plane.] The pressure (or normal velocity) distribution on the source is either Gaussian (Eq. (3.12)) or uniform (Eq. (3.13)).

4.1.1. Sound speed profiles.

Four different sound speed profiles are considered, all of the form $c_0 = \bar{c} f(U)$:

$$\text{Profile 1} : \quad c_0 = \bar{c}U, \tag{4.1}$$

$$\text{Profile 11} : \quad c_0 = \bar{c}U^{-1}, \tag{4.2}$$

$$\text{Profile 2} : \quad c_0 = \bar{c}U^{-1/2}, \tag{4.3}$$

$$\text{Profile 22} : \quad c_0 = \bar{c}U^{1/2}, \tag{4.4}$$

where

$$U = \begin{cases} 1 + A_1 z + A_2 x, & x \geq \bar{x}_c \\ 1 + A_1 z + A_2 \bar{x}_c, & x < \bar{x}_c. \end{cases} \tag{4.5}$$

Thus, ∇c_0 is along the constant vector $\mathbf{A} = (A_2, 0, A_1)$ in the half–space $x > \bar{x}_c$ and along $\mathbf{e}_z$ in the half–space $x < \bar{x}_c$. We must choose $\bar{x}_c$ finite in order to avoid

unphysical situations where c_0 would become zero or infinite. Let θ be the angle between ∇c_0 and $\mathbf{e}_z$ when $x > \bar{x}_c$. In terms of the dimensionless coordinates we have

$$U = \begin{cases} 1 + AL_H(\cos\theta z_1 + 2\epsilon^{1/2}\sin\theta x_{1/2}), & x_{1/2} \geq x_c, \\ 1 + AL_H(\cos\theta z_1 + 2\epsilon^{1/2}\sin\theta x_c), & x_{1/2} < x_c. \end{cases} \tag{4.6}$$

The reference inhomogeneity length L_H is defined as the Rayleigh distance corresponding to the value of k and a at the source. [Recall that in an inhomogeneous medium, the "effective wavenumber" $k = \omega/c_0$ varies, since c_0 varies. Hence the "effective Rayleigh distance" in the medium also varies.] Since $\nabla c_0/\bar{c} = f'\nabla U = \mathbf{A}f'$, $(|\mathbf{A}|f')^{-1}$ is the effective inhomogeneity length.

The above definition of inhomogeneity length is suitable as long as the values of k and a (at the source) both are fixed, and we only wish to study the effects of various soundspeed profiles. However, if we wish to study the effects of varying k and/or a for a source in a medium with a given inhomogeneity, the inhomogeneity length could be defined as the Rayleigh distance corresponding to fixed reference values of k and a: $L_H = \bar{k}\bar{a}^2/2$. This is a question of redefining the similarity parameters C_N, C_H in Eq. (2.72).

When k or a increases, the Rayleigh distance, $R = ka^2/2$ increases. Thus, the soundspeed profile, expressed in nondimensional coordinates will appear stronger in the longitudinal direction, (since the fixed inhomogeneity length L_H decreases compared to R), and weaker in the transverse direction, (since the beam becomes more directive). The variation of the direction of ∇c_0 is independent of whether k or a are varied. However, $|\partial c_0/\partial(z/R)|$ increases more when a increases than when k increases by the same amount.

4.1.2. Interpretation of the coordinate transform

The bending process of a beam propagating in an inhomogeneous medium is schematized in Fig. 4.1, for the nondissipative case. The factor $(\rho_0 c_0)^{1/2}$ introduced in Eq. (2.67), is a decreasing function of c_0, by the choice of functional relation between ρ_0 and c_0 (for instance adiabatic, cf. Chapt. 3). The planes σ = constant are curved surfaces in the stretched $(z_1, \mathbf{x}_{\perp 1/2})$ coordinates, as well as in physical coordinates. The value of the scaled, normalized pressure perturbation $P^{(1)}$, cf. Eqs. (2.67, 2.68), along the surface σ = constant is the same as the value of $p^{(1)}$ along the plane z = constant in the corresponding homogeneous case. $\sigma(z,x) = \Sigma \Rightarrow z = Z_1(x)$, and:

$$\frac{dz}{dx} = -\frac{A}{B}\left(1 - \frac{f(1+Ax)}{f(1+Ax+Bz)}\right). \tag{4.7}$$

with $c_0 = f(1+Ax+Bz)$. Equation (4.7) can be discussed for different combinations of the signs of f', A, B. In regions where c_0 increases, σ grows faster than z. Including

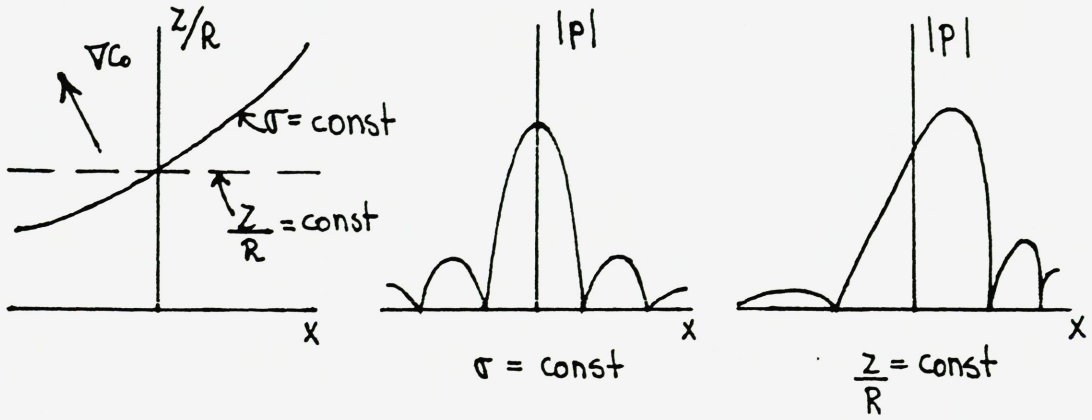

FIG. 4.1. The transform $\sigma = \sigma(z_1)$.

the variation of the factor $(\rho_0 c_0)^{1/2}$, ∇c_0 implies that in physical coordinates, the sound field is compressed towards the source. In regions where c_0 decreases, the opposite happens, so that the field is "stretched" outwards.

An investigation of the curves $x/\sigma_0 = \text{constant} = C$ ($\sigma_0 = L_H \sigma$), i.e., $z = Z_2(x)$, provides information about how the directivity of the sound beam is affected by inhomogeneity:

$$\frac{dz}{dx} = \left[1 - C\frac{\partial \sigma_0}{\partial x}\right] \frac{1}{Cc_0}, \tag{4.8}$$

$$= \frac{1 - C\frac{A}{B}[f(1 + Ax + Bz) - f(1 + Ax)]}{Cf(1 + Ax + Bz)}, \qquad \frac{\partial \sigma_0}{\partial x} = \int_0^z \frac{\partial c_0}{\partial x}\, dz'.$$

Transverse inhomogeneity implies: If $(\partial c_0/\partial x) < 0$, an angle between the curve $x/\sigma_0 = C$ and the z-axis in the xz-plane represents a smaller similar angle in the $x\sigma_0$-plane. The beam is thus bent in the direction of decreasing c_0. If $(\partial c_0/\partial x) > 0$, an angle between the curve $x/\sigma_0 = C$ and the z-axis represents a larger angle in the $x\sigma_0$-plane than in the xz-plane, and the beam is also now bent towards the direction of decreasing c_0. Thus the beam will avoid the regions in space where c_0 increases. See Fig. 4.2.

4.1.3. Nondissipative case. Fixed *ka*.

Numerical results are presented for ka fixed and various sound speed profiles. Series of beampatterns and contour plots of the amplitude normalized to the on-source peak amplitude are shown. Here, a is an unspecified source radius. (In all contour plots in this section, the difference between the pressure amplitude values corresponding to two neighbouring contour lines is 2 dB.)

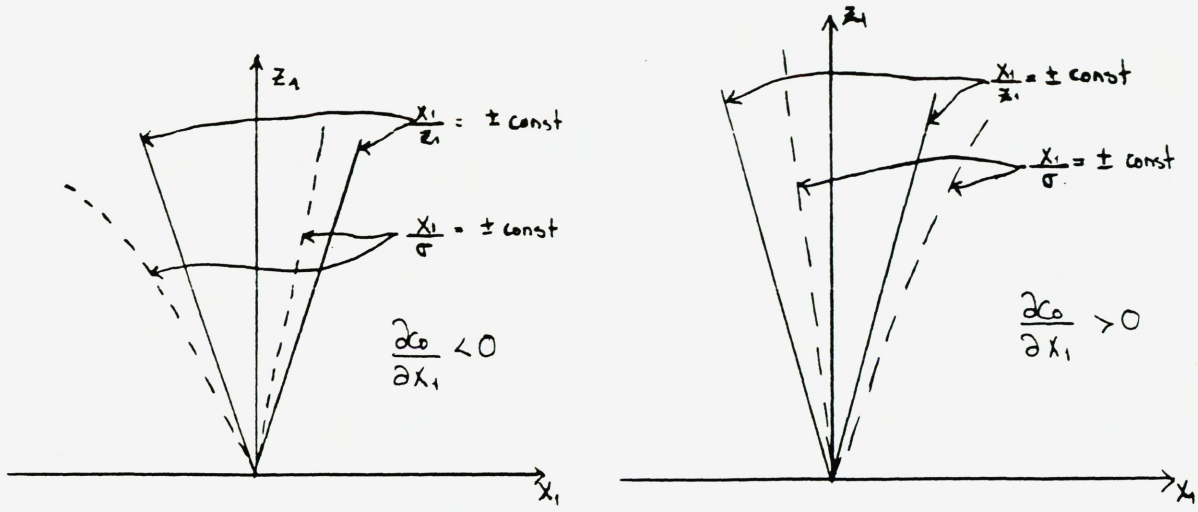

FIG. 4.2. Bending of the lines x/z = constant due to inhomogeneity.

Figure 4.3 shows three series of beam patterns obtained from the farfield asymptotic expression (assuming $\sigma >> 1$) for a uniform piston source in the linear case, at $z/R = 2.0, 5.0, 8.0, 11.0$, for $-50 \leq x/a \leq 50$. [In these computations, $L_H = R$ with $ka = 20$.] The homogeneous case is shown in Fig. 4.3(a). In Fig. 4.3(b) and (c), c_0 is Profile 1 and 2, respectively, with $AL_H = 0.5$, $\theta = 70°$ and $x_c = 0.0$. A comparison of (a), (b) and (c) in the region $x_{1/2} < x_c$ (cf. Eq. (4.6)) illustrates the isolated effect of a longitudinal ∇c_0 on the geometrical spreading of the beam. For c_0 decreasing with U, the sound pressure amplitude is less damped than in the homogeneous case. The contrary applies when c_0 is an increasing function of U. For $x_{1/2} > x_c$, the stretching/compression of the beam combines with bending of the main and side lobes relative to the z-axis. The lobes are bent in the direction of decreasing c_0 in (c) and avoid the region of increasing c_0 in (b), as expected.

Figure 4.4 shows how the beam direction is bent due to inhomogeneity. Here c_0 = Profile 2, $AL_H = 0.5$, $\theta = 75°$, $x_c = -2.0$; i.e., c_0 is a decreasing function of U, cf. Eqs. (4.1–4.6). [In these and the rest of the computations in this section, $L_H = R$ with $ka = 10$.] The on-source amplitude distribution is Gaussian in Fig. 4.4(a) and uniform in Fig. 4.4(b). The beam attempts to propagate in the direction where c_0 decreases the most, this is also the case for the side lobes in (b). For $x_{1/2} \leq x_c$, there is only stretching of the amplitude picture due to a decreasing c_0 with no transverse variation. To a certain extent, the beam thus behaves in accordance with Fermat's principle for a ray emitted from a point source.

Figures 4.5 and 4.6 show the sound pressure amplitude for four different media and various θ. [$x_c = -4.0$. $AL_H = 0.1$ in Fig. 4.5 and 1.0 in Fig. 4.6.] The homogeneous case is shown in Fig. 4.7. It is noted that in regions of increasing c_0, the amplitude

is lower than in the homogeneous case. The effective inhomogeneity length $(Af')^{-1}$ varies in these four series of plots. Depending on $|\nabla c_0|$, the presence of a transverse gradient has a different effect. The effects of a transverse gradient are dominated by the effects of a longitudinal gradient when $0 < \theta \leq 45°$ for all the four profiles. In Fig. 4.5(a), for c_0 = Profile 1, the effects of a transverse gradient are particular weak compared to the three other cases, even for $\theta = 90°$. The reason is that spherical spreading soon becomes the dominating effect, due to the rapid increase of c_0. In Figs. 4.5(b) and 4.6(b), where c_0 decreases when $x_{1/2} > x_c$, we observe that for increasing θ, the beam is more bent in the positive transverse direction. In Figs. 4.5(a) and 4.6(a) c_0 increases for $x_{1/2} > x_c$, so the amplitude avoids the positive transverse direction, and this tendency is more pronounced for larger θ. Accordingly, depending on c_0, the longitudinal component of ∇c_0 dominates, except for values of θ close to 90°. [Fig. 4.6(b) shows an extreme increase in pressure amplitude in the farfield, due to a too rapid decrease in c_0: the spherical spreading of the field is not noticed yet. Further away from the source the field will be more damped.]

Figures 4.5 and 4.6, together with Fig. 4.8 motivate the question: can continuous soundspeed profiles be used to model interfaces, e.g., discontinuities in c_0? The "interface" is here described as a discontinuity of transverse component of ∇c_0 at $x = x_c$. The jump in ∇c_0 over the "interface" is adjusted when A and f are varied in the expression for c_0. Figures 4.5(b) and 4.8 (c_0 = Profile 2) and 4.6(b) (c_0 = Profile 11) can each be interpreted as showing reflection/transmission of a monochromatic beam propagating parallel to an interface approximated by continuously varying media, especially for $\theta = 90°$. The calculated amplitude (i.e., the modulus of the complex amplitude V as given in Eq. (3.15)), can in each case be decomposed into incident, reflected and transmitted beam amplitudes. [The phase variation of the beam is not considered here. On the short scale, the phase variation occurs through the retarded time $\tau_+ = t - \phi$, and for $\sigma >> 1$, the term $\mathbf{x}_{\perp 1/2}/\sigma$ in the phase represents spherical spreading, cf. Eq. (3.19). Since τ_+ and σ vary in space, there is phase difference between the incident, reflected and transmitted parts of the beam. Although, by construction, the phase is continuous. ϕ will be studied closer in Sec. 4.2.] Figure 4.8 shows that for a uniform piston source, also the sidelobes are affected by this "weak interface": The main- and side lobes behave like beams incident at an interface below which the soundspeed increases; transmitted and reflected fields can be identified. Figures 4.5(a), 4.6(a) can be interpreted as illustrating beams propagating through an interface, into a medium with a higher c_0. The reflected and transmitted amplitudes tend to avoid regions of larger c_0.

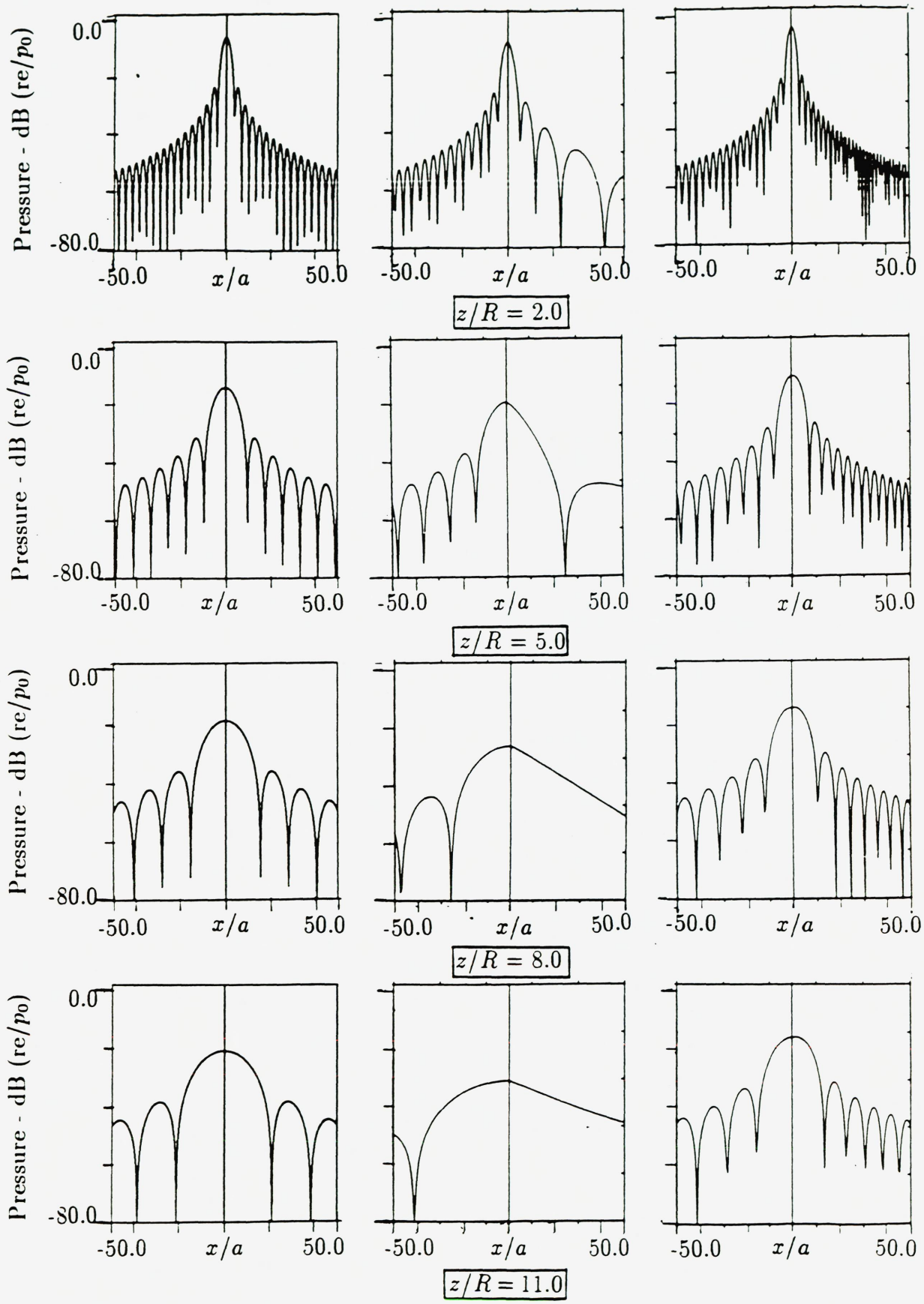

FIG. 4.3. Beampatterns. Uniform piston source, $ka = 20$. (a) Homogeneous medium. (b) c_0 = Profile 1. (c) c_0 = Profile 2. $AL_H = 0.5$, $\theta = 70°$, $x_c = 0.0$, no absorption in all cases. $z/R = 2.0, 5.0, 8.0, 11.0$.

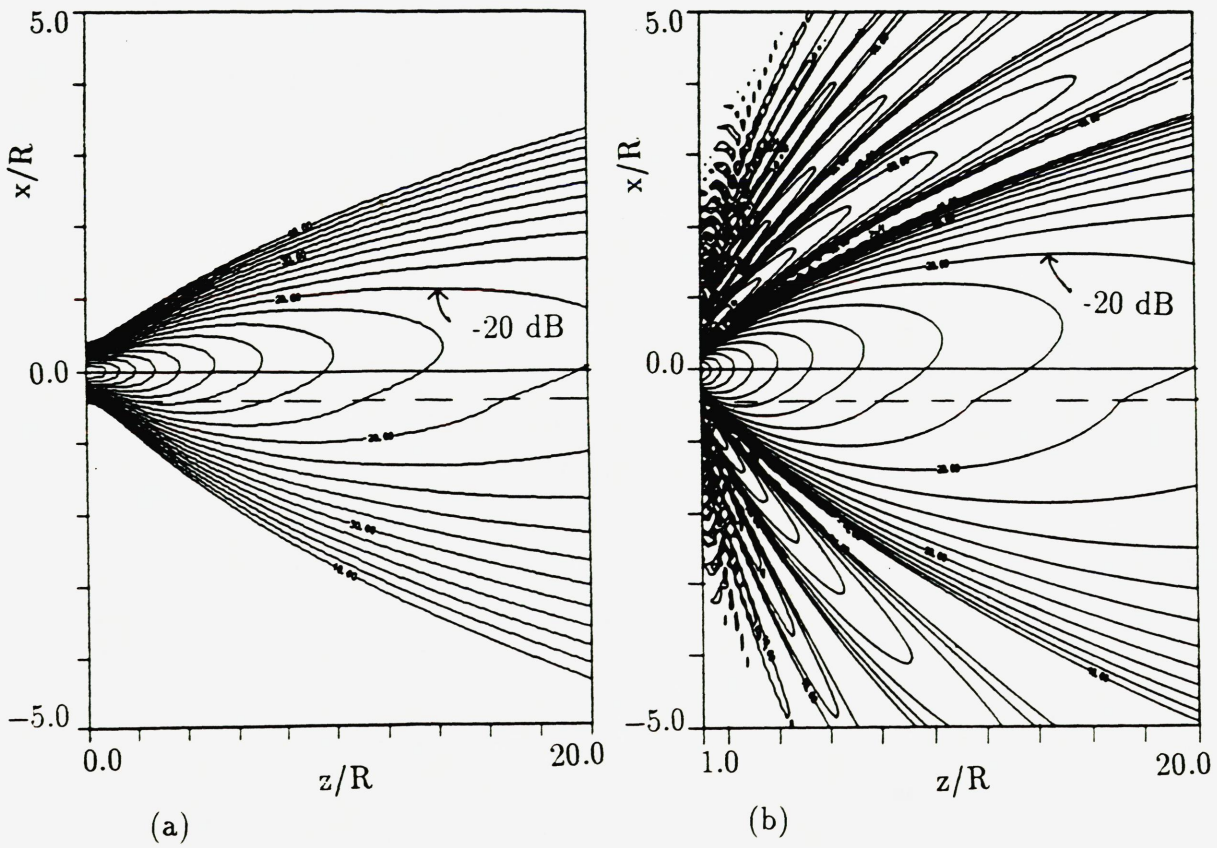

FIG. 4.4. Sound pressure amplitude. c_0 = Profile 2, $\theta = 75°$, $AL_H = 0.5$, $x_c = -2.0$, $ka = 10$, no absorption. (a) Gaussian source. (b) Uniform source. $\Delta dB = 2$.

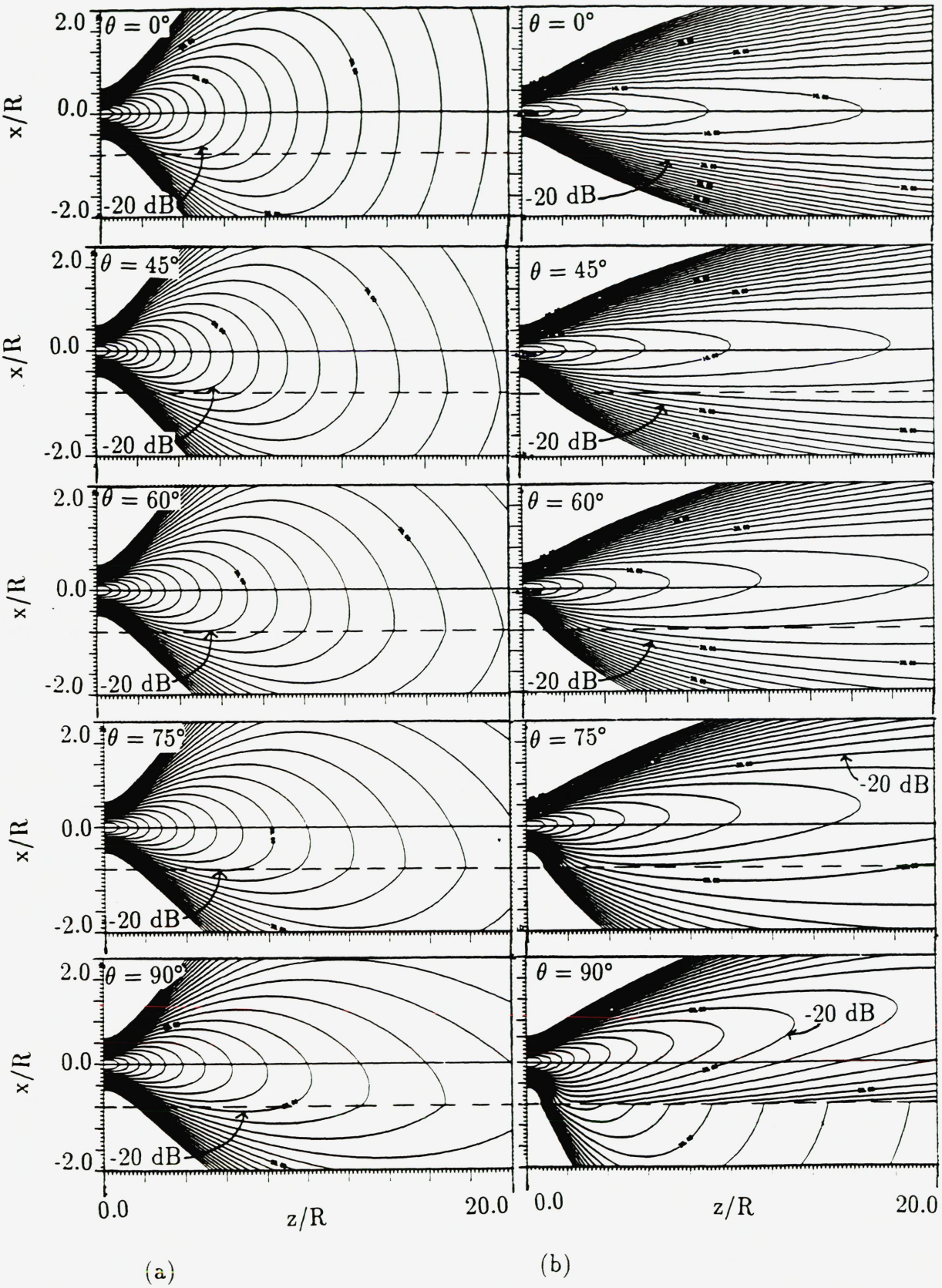

FIG. 4.5. Sound pressure amplitudes for various θ and sound speed profiles. Gaussian source, $x_c = -4.0$, $ka = 10$, no absorption. $\theta = 0°, 45°, 60°, 75°, 90°$, $AL_H = 0.1$. (a) c_0 = Profile 1. (b) c_0 = Profile 2. $\Delta dB = 2$.

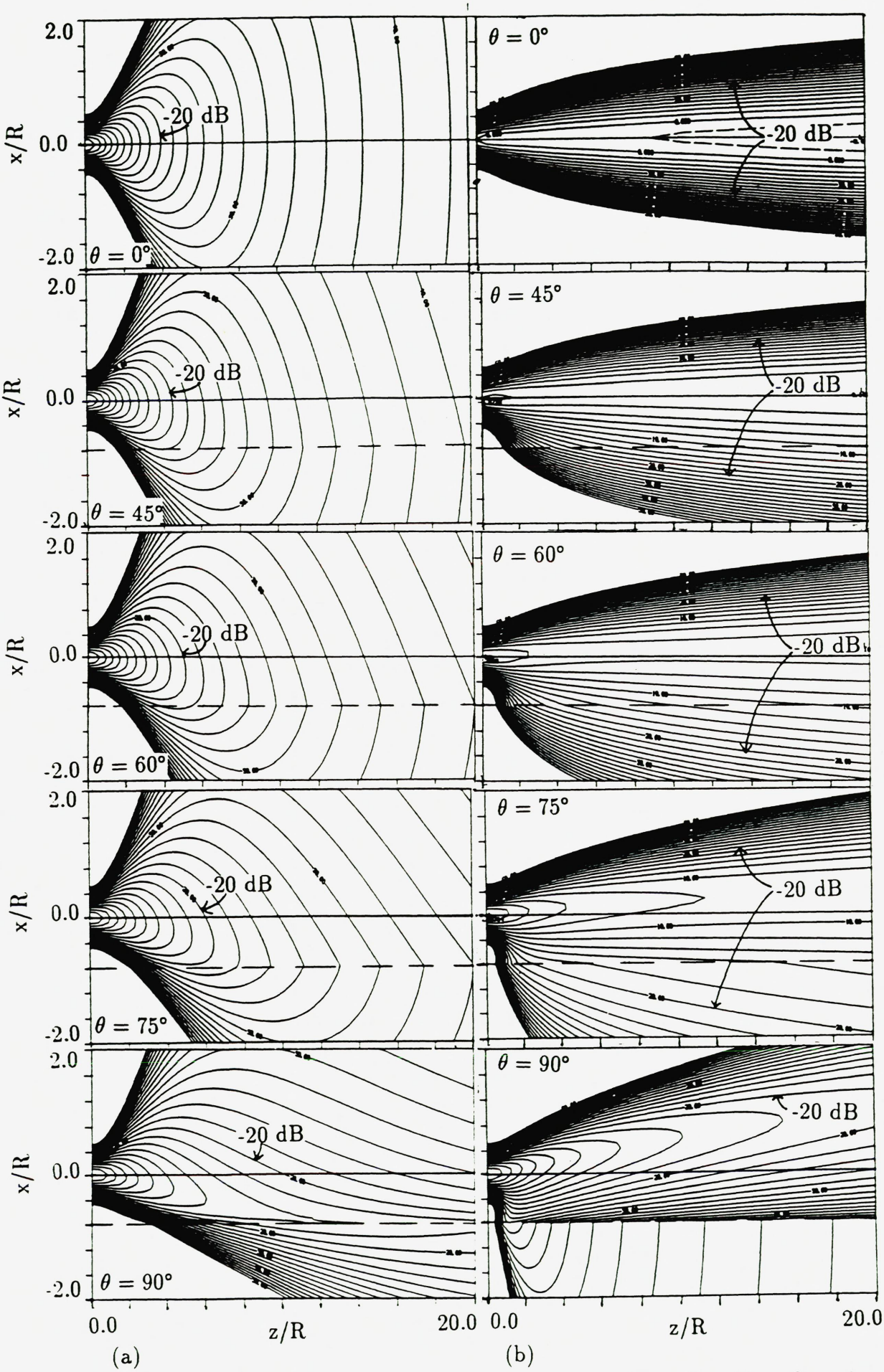

FIG. 4.6. Sound pressure amplitudes for various θ and sound speed profiles. Gaussian source, $x_c = -4.0$, $ka = 10$, no absorption. $\theta = 0°, 45°, 60°, 75°, 90°$, $AL_H = 1.0$. (a) c_0 = Profile 22. (b) c_0 = Profile 11. $\Delta dB = 2$.

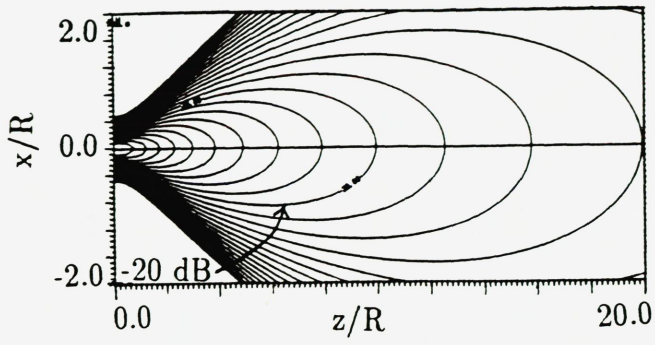

FIG. 4.7. Sound pressure amplitude, $\nabla c_0 = 0$, $ka = 10$. Gaussian source, no absorption. $\Delta dB = 2$.

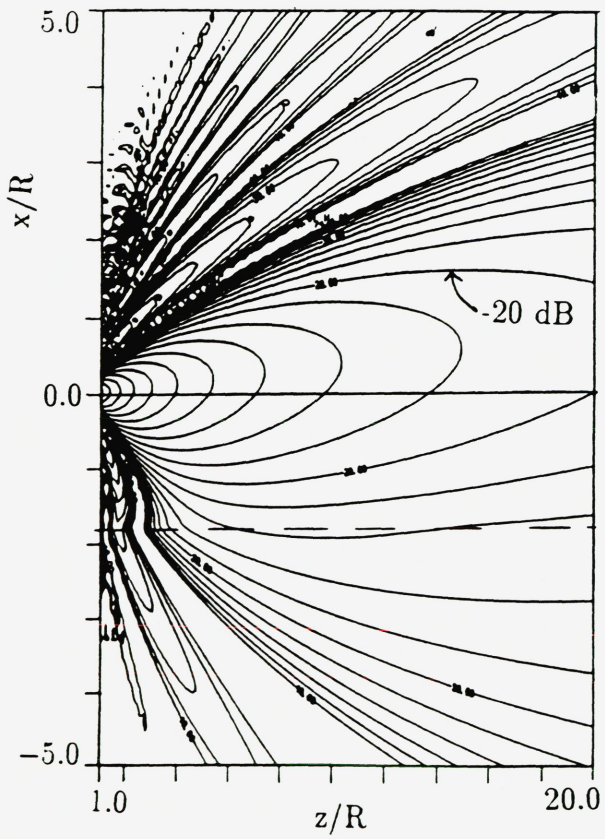

FIG. 4.8. Sound pressure amplitude, uniform source, $ka = 10$, no absorption. $c_0 =$ Profile 2, $\theta = 75°$, $AL_H = 0.5$, $x_c = -9.0$. $\Delta dB = 2$.

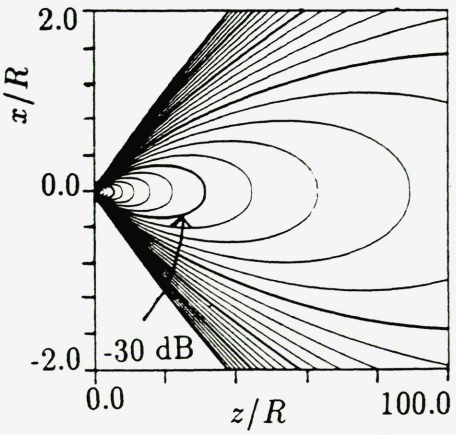

FIG. 4.9. Sound pressure amplitude radiated from Gaussian source, homogeneous, nondissipative case, $ka = 100$.

4.1.4. Nondissipative case. Varying ka.

In the following numerical examples, c_0 = Profile 2 and $|\nabla c_0|$ is of the same order of magnitude as in the previous numerical examples. [Here, $AL_H = 1.0$, where L_H is the Rayleigh distance corresponding to $ka = 10$.] We study the effects of varying k, a in a fixed medium and consider: (i) constant a and varying k; (ii) constant k and varying a; (iii) fixed ka, varying k and a; in all cases $\theta = 90°$, $80°$ or $75°$. Values of ka are in the range 25-200. The normalized amplitude is shown in contour plots for $-2.0 \leq x/R \leq 2.0$ and $0.0 \leq z/R \leq 100.0$, where R is the Rayleigh distance defined with respect to $ka = 100$, $a = \bar{a}$. [$\bar{a}$ is the "unit source radius" used in the previous calculations with $ka = 10$.] $x_c = -4.0$, except for $ka = 200$ and $a = 2\bar{a}$, where $x_c = 0.0$. The homogeneous case with $c_0 = \bar{c}$ is shown in Fig.4.9 (where $\Delta dB = 3$, the level difference between neighbouring contour lines).

In Fig. 4.10, a is fixed (for convenience in later comparisons defined explicitly as $\bar{a}$), while k varies: $ka = 25, 50, 100, 200$. ($\Delta dB = 3$, except for $ka = 200$, $\theta = 75°, 80°$ where $\Delta dB = 6$). The situation with only a transverse component of ∇c_0, i.e., $\theta = 90°$ is fundamentally different from the situation with a longitudinal component present: For all the values of ka, the effect of a transverse inhomogeneity can be noticed. For increasing k the beam becomes more directive, and the amplitude is less influenced by the transverse gradient; the incident, the reflected and the transmitted part of the amplitude all approach the "continuous interface" at $x_{1/2} = x_c$. The short characteristic length L is a decreasing function of k, thus more units of L fit into one fixed source radius; and into the fixed transverse inhomogeneity length. Therefore, over one unit of L transversely, the beam feels a weaker variation of c_0 and ρ_0.

When ∇c_0 has an appreciable longitudinal component, i.e., $\theta = 80°$ or $75°$, the beam is less influenced by the transverse gradient if k is large. For $\theta = 80°$, effects

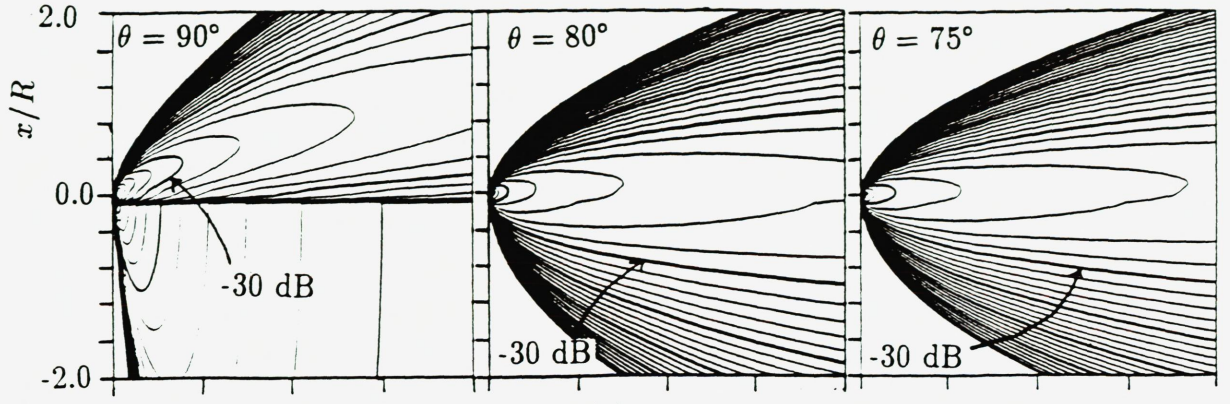

(a) $ka = 25$

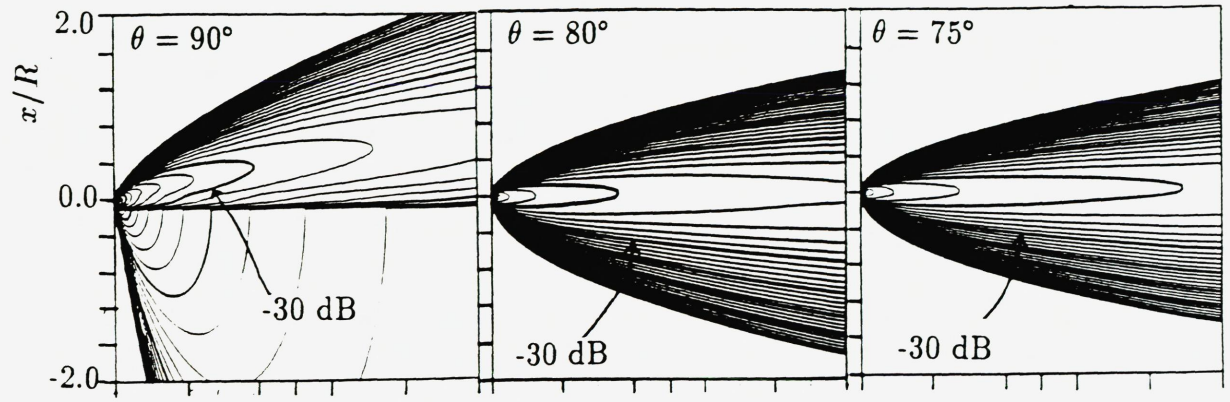

(b) $ka = 50$

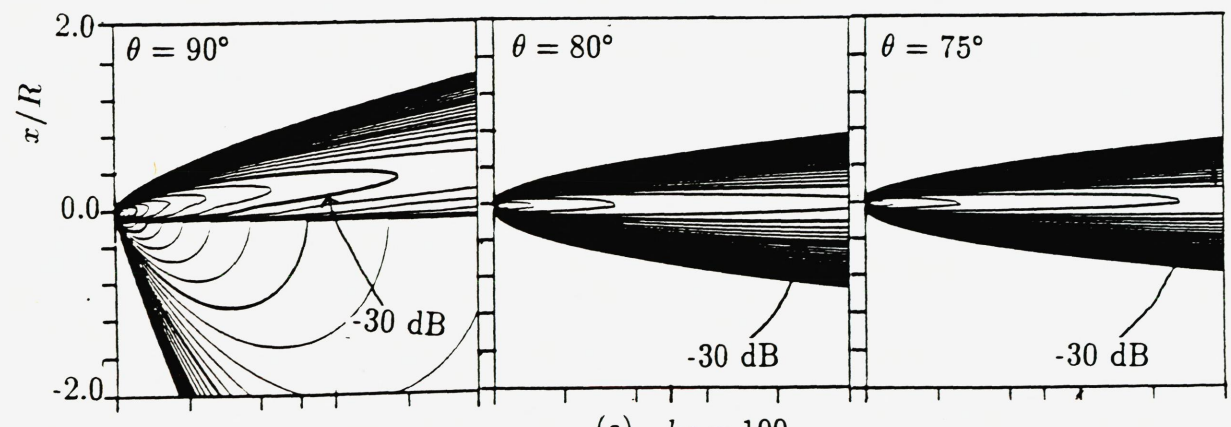

(c) $ka = 100$

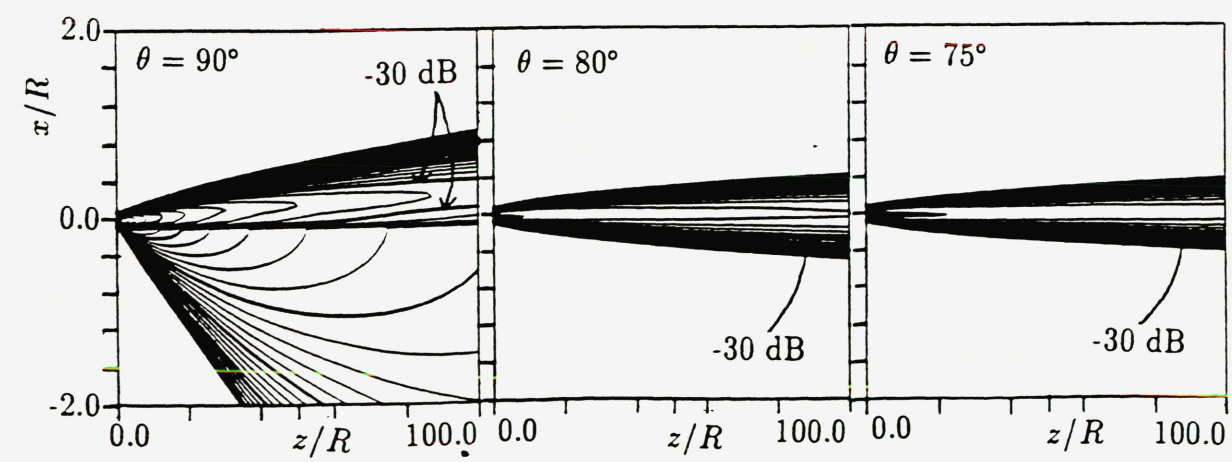

(d) $ka = 200$

FIG. 4.10. Various ka: fixed a and various k. Sound pressure amplitude radiated from Gaussian source. c_0 = Profile 2, $\theta = 90°, 80°, 75°$. (a) $ka = 25$. (b) $ka = 50$. (c) $ka = 100$. (d) $ka = 200$.

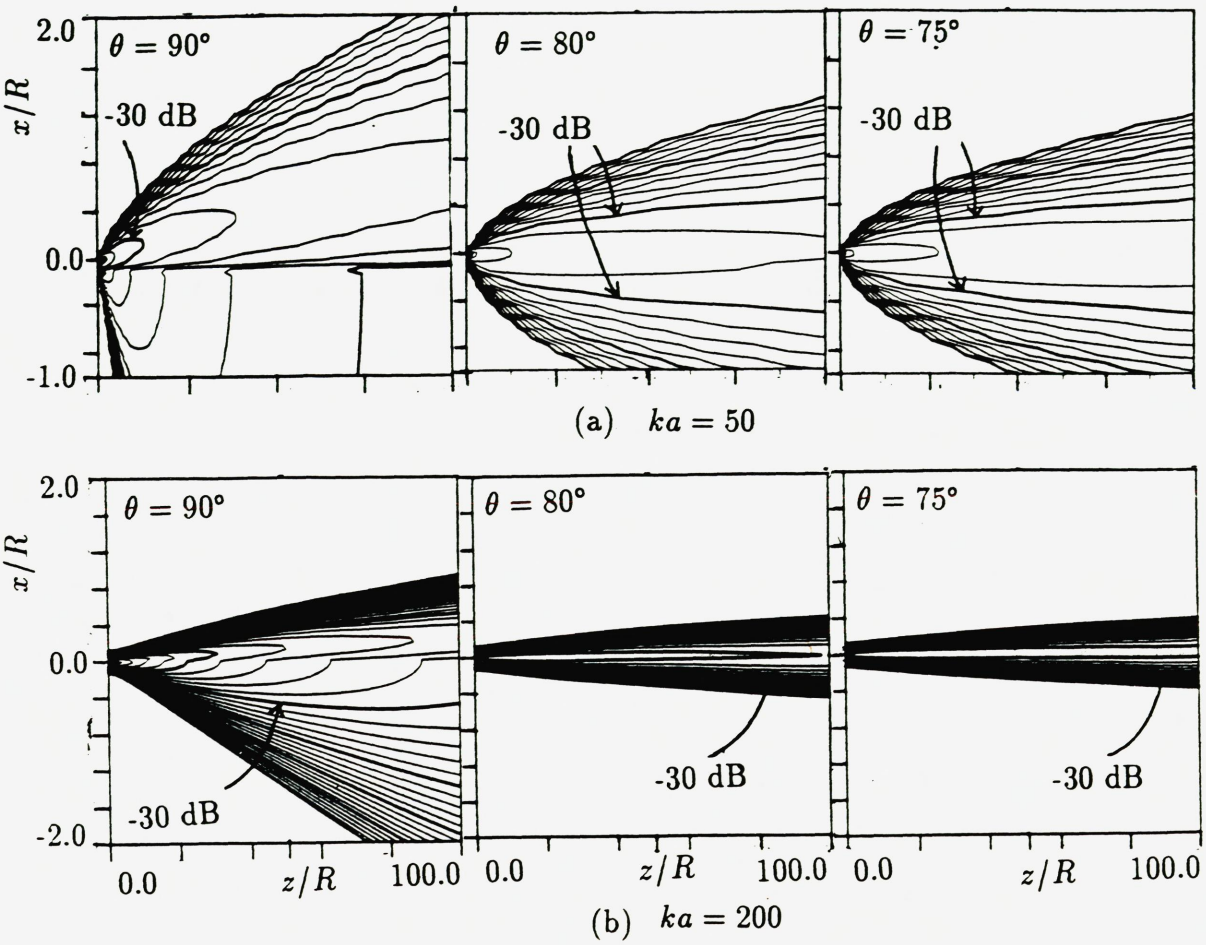

FIG. 4.11. Various ka: fixed k and various a. Sound pressure amplitude radiated from Gaussian source. c_0 = Profile 2, $\theta = 90°, 80°, 75°$. (a) $ka = 50$. (b) $ka = 200$.

of transverse inhomogeneity are observed for $ka = 25$ and 50, while for $\theta = 75°$, they are only noticeable for $ka = 25$. Since the Rayleigh distance increases with k, the longitudinal inhomogeneity plays a relatively more important role when k is large. In the limit $ka \to \infty$, one may expect that the effects of a transverse ∇c_0 will disappear, while the effects of a longitudinal ∇c_0 will remain, according to this model. [However, cf. the discussion in Sec. 2.4.]

In Fig. 4.11, $ka = 50$ and 200 with k fixed, so $a = 0.5\bar{a}$ or $a = 2\bar{a}$. ($\Delta dB = 6$, except for $ka = 200$, $\theta = 90°$ where $\Delta dB = 3$). Here also, it is seen that the transverse component of ∇c_0 has less influence on the directivity when ka is large. As a is increased, the transverse inhomogeneity is stronger relative to the source radius. However, the beam also becomes more directive and thus less sensitive to transverse fluctuations in the medium; the geometrical spreading occurs further away

from the source. For $\theta = 80°$ and 75°, the longitudinal inhomogeneity becomes correspondingly stronger as a increases.

For given values of ka, the effect of varying either k or a can be investigated by comparing Fig. 4.10 with Fig. 4.11, for $ka = 50$ and $ka = 200$ respectively, for $\theta = 90°$, 80° or 75°. (In the comparison, we must recall that $x_c = 0.0$ for $ka = 200$ in Fig. 4.11 and $x_c = -4.0$ in the other calculations.) The beam is bent by the same amount for a given θ and a given ka, in accordance with the analysis above. However, note that (almost) coinciding contour lines do not correspond to a same sound pressure. This is due to the fact that the Rayleigh distance varies differently, following k or a are varied, with ka fixed. The amplitude is more damped when k is increased, (a fixed), than when a increases, (k fixed). The directivity is the same, however.

To conclude: For $\theta = 90°$, the bending of the beam relative to its start direction only depends on the value of ka, (independent of whether k or a are varied). The effect of a transverse gradient is less pronounced, for larger ka. For $\theta < 90°$, the effects of longitudinal inhomogeneity are relatively stronger than the effects of transverse inhomogeneity. How much a longitudinal component of ∇c_0 dominates the transverse component depends on the magnitude of $(Af')^{-1}$ relative to the actual Rayleigh distance and the value of ka. The longitudinal inhomogeneity appears stronger if a is increased than if k is increased. For a given medium, the important factor for bending is how directive the beam is: The lower ka, the more the directivity is affected by a transverse gradient. A longitudinal gradient has more influence on the amplitude when ka is larger.

4.1.5. Dissipative case. Fixed ka.

Dissipation is here accounted for as described in Chap. 3, through an integrating factor $h(\sigma, \mathbf{x}_{\perp 1})$, cf. Eqs. (3.20, 3.22, 3.15). For the special case of a thermoviscous fluid, h is an increasing function of c_0. Therefore, the dissipative damping is weakest in directions where c_0 is largest. Consequently, the beam tends to bend in an opposite direction, compared to the nondissipative case. For other absorption laws, the effect of dissipation may be different, depending on the relation between h and c_0. [In these calculations, a thermo-viscous fluid is considered.]

Figures 4.12 and 4.13 ($\theta = 75°$, $\bar{\alpha} L_H = 0.1$, $x_c = -4.0$, ΔdB = 2) show that the beam propagates in a direction which is a compromize between least increase in c_0 and least damping due to dissipation. Thus, a generalized Fermat's principle is satisfied in the linear case.

In Fig. 4.12, the source is uniform and c_0 = Profile 2 ($AL_H = 0.5$). The main and side lobes are bent in the direction where c_0 increases the most. The discontinuity in transverse ∇c_0 (i.e., "interface") is more pronounced than for the nondissipative case. Even for a dissipation length of $10 L_H$, this effect dominates the nondissipative

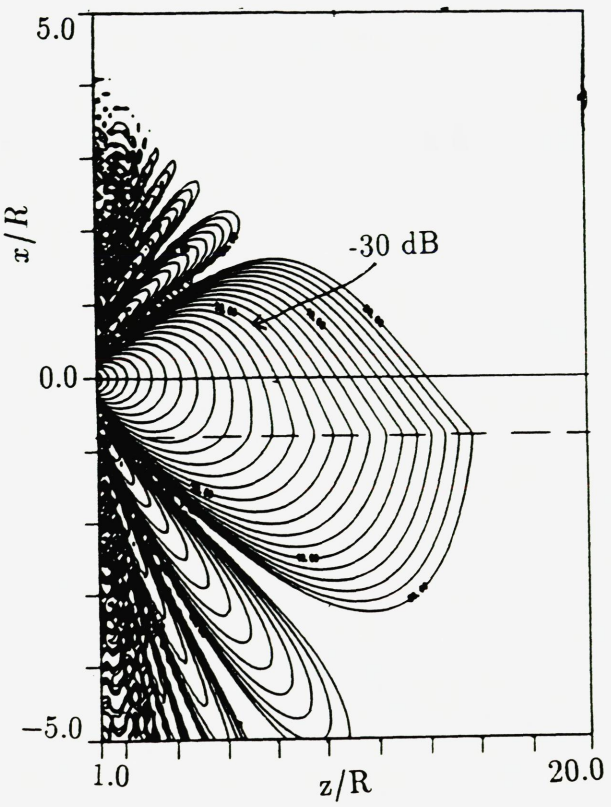

FIG. 4.12. Sound pressure amplitude, uniform source, $ka = 10$, $\bar{\alpha}L_H = 0.1$. $c_0 =$ Profile 2, $x_c = -4.0$, $\theta = 75°$, $AL_H = 0.5$. $\Delta dB = 2$.

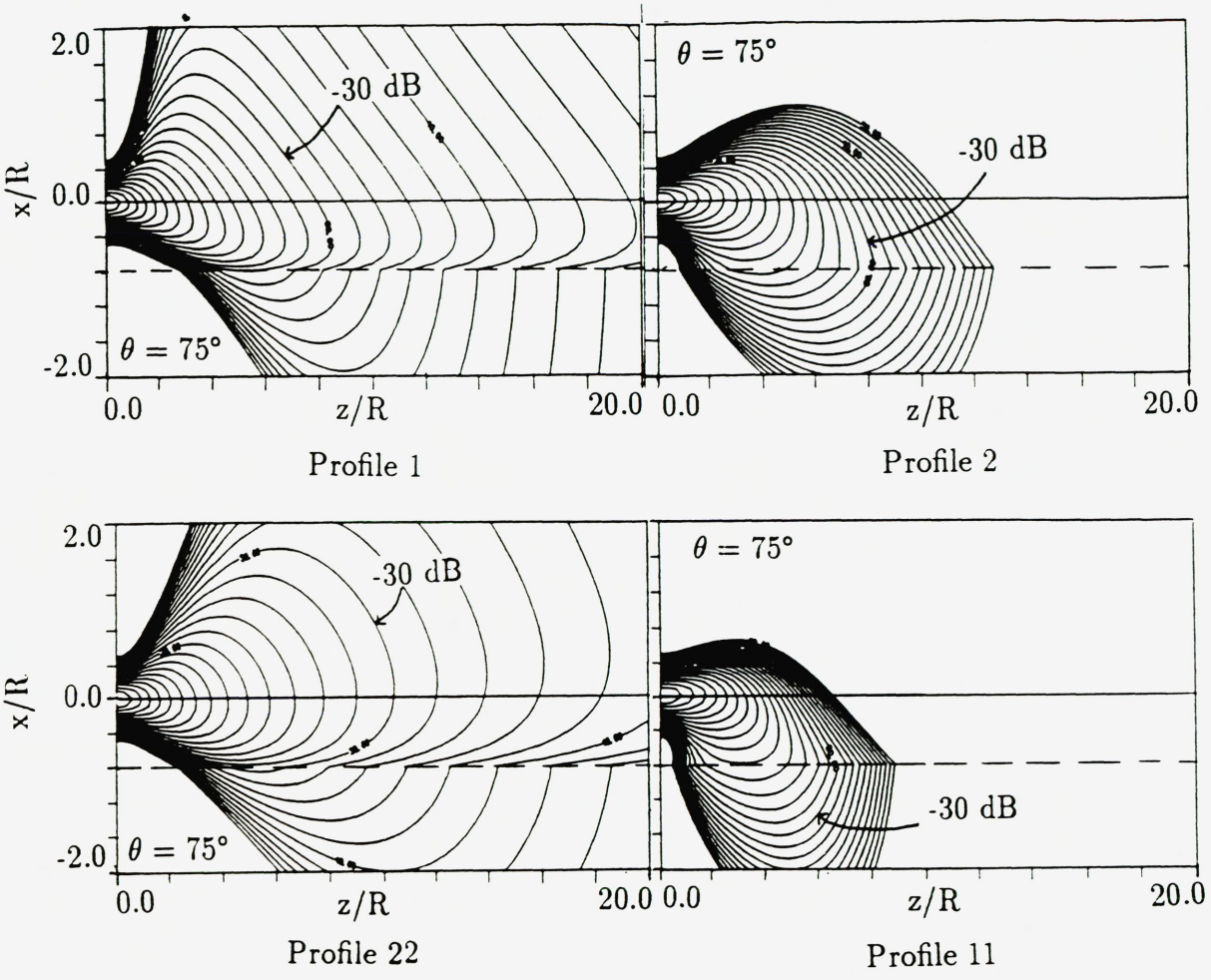

FIG. 4.13. Sound pressure amplitude, Gaussian source, $ka = 10$, $\bar{\alpha}L_H = 0.1$, for various soundspeed profiles. $x_c = -4.0$, $\theta = 75°$, $AL_H = 1.0$. $\Delta dB = 2$.

deformation in Fig. 4.4(b).

In Fig. 4.13, computations of the beam amplitude, for the soundspeed profiles 1,11, 2, 22 ($AL_H = 1.0$) are presented, for a Gaussian source. (The value of AL_H is different from some of the values in Figs. 4.5 and 4.6. Still, the two examples can be compared, since we only want to investigate the qualitative tendencies due to absorption.) A comparison between the dissipative and the nondissipative cases again illustrates the bending of the beams in opposite direction when dissipation is included.

4.2. Simulation of a fluid–fluid interface.

In the present model, $\nabla c_0/c_0$, $\nabla \rho_0/\rho_0$,... are assumed bounded. We will now apply the model to a problem where it a priori is not valid: beam propagation through an interface between two homogeneous media. Let c_0 have constant but different values in two separate regions. We will consider both a linear variation of c_0 in a layer between two parallel planes, (i.e., continuous c_0), and a discontinuity in c_0.

At an interface between two nondissipative fluids, the boundary conditions are: continuity in pressure and normal velocity. For dissipative fluids: continuity of the normal stress and the velocity components through the interface. In the parabolic approximation one does not distinguish between pressure and longitudinal velocity. Therefore, transverse velocity is not accounted for to the leading order ($\mathbf{v}_\perp = O(\epsilon^{3/2})$), and the condition on the normal velocity is "lost".

The linear interface problem with the incident field radiated from a real, monochromatic source can be modeled by the Helmholtz equation. The sound pressure is a superposition of incident, reflected and transmitted beams; where each can be interpreted as a weighted sum of plane waves (through Fourier integrals). Interesting features may occur on the scale of a wavelength in the vicinity of an interface between two homogeneous media (for instance beam displacement[26,27]). Some of these features cannot be described within the parabolic approximation.

In the parabolic approximation for weakly inhomogeneous media, a main direction of propagation for the beam is postulated through $\tau_+ = \tau - \phi$, i.e., the field behaves like a simple wave on the short scale L (diffraction is accounted for on a longer scale). This direction changes (although weakly), since ϕ depends on c_0, and is determined by $\nabla\phi$:

$$\nabla\phi = \frac{1}{c_0}\mathbf{e}_z - \int_0^{z/L} \frac{1}{c_0^2}\nabla_\perp c_0 \, d(\frac{z}{L}). \tag{4.9}$$

It may be interesting to investigate the variations of ϕ through an interface. The presence of gradients in the ambient acoustic variables may imply that the direction of maximum directivity does not necessarily coincide with the direction of propagation

of the "simple wave part" of the beam appearing through the short scale variable $\tau_+ = t - \phi$.

In our model, the interface appears as a discontinuity in c_0, and we solve for the amplitude of the total field, without the decomposition in incident, reflected and transmitted fields. The curved coordinate transform is defined, since c_0 is integrable. We arrived at Eq. (2.68) by defining the relation Eq. (2.67) , assuming $\nabla_{\perp 1/2}(\rho_0 c_0)^{1/2} = O(\epsilon^{1/2})$. However, when c_0 is discontinuous, ρ_0 will also be discontinuous (since $c_0 = c_0(\rho_0)$), and our derivation becomes inconsistent. By construction, the redefined, normalized pressure $P^{(1)}$ (or normalized longitudinal velocity) is continuous through the "interface". However, since the scaling factor $(\rho_0 c_0)^{1/2}$ is discontinuous, the pressure $p^{(1)}$ and the longitudinal velocity $w^{(1)}$ are discontinuous; therefore the velocity component normal to the interface will also be discontinuous. Hence the boundary conditions at the interface are not satisfied. In addition, in our parabolic model we describe the sound pressure as a progressive wave in curvilinear coordinates. It is then inconsistent to introduce boundaries in the medium through discontinuity of sound-speed. Thus the application of our model for sound propagation in inhomogeneous media has limitations.

Let us consider the following two situations. Case 1: The homogeneous regions 1 and 3 where c_0 is equal to constant c_1 or c_2 respectively, are connected by a region 2, with thickness Δ, where c_0 varies linearly from c_1 to c_2: $c_0 = 1 + B(z_1 - z^{1,*})$, ($z^{1,*}$ will be defined below). The regions are separated by parallel planes that intersect the z-axis at $z_1 = z_1^{(1)}$ and $z_1 = z_1^{(2)}$, respectively. Case 2: Region 2 is removed, so that c_0 is discontinuous. In both cases the incident beam propagates in the z-direction, making an angle θ with the planes, angle of incidence is $\Theta_i = \pi/2 - \theta$, as in Fig. 4.14. [$\Delta$ is defined as $(z_1^{(2)} - z_1^{(1)}) \sin\theta$.] For case 1 :

$$\begin{aligned}
&\sigma = z_1, \qquad z_1 \le z^{1,*}, \\
&\sigma = z^{1,*} + K(z_1 - z^{1,*}) + \frac{B}{2}(z_1^2 - (z^{1,*})^2), \qquad z^{1,*} < z_1 < z^{2,*}, \\
&\sigma = z^{1,*} + K(z^{2,*} - z^{1,*}) + \frac{B}{2}((z^{2,*})^2 - (z^{1,*})^2) + \frac{c_2}{c_1}(z_1 - z^{2,*}), \qquad z_1 \ge z^{2,*},
\end{aligned} \tag{4.10}$$

$$\begin{aligned}
&\phi^{(1)} = \frac{z_1}{\epsilon}, \qquad \phi^{(2)} = \frac{z^{1,*}}{\epsilon} + \frac{1}{\epsilon B}\log|1 + B(z_1 - z^{1,*})|, \\
&\phi^{(3)} = \frac{z^{1,*}}{\epsilon} + \frac{1}{\epsilon B}\log|1 + B(z^{2,*} - z^{1,*})| + \frac{c_1}{c_2}\frac{(z_1 - z^{2,*})}{\epsilon},
\end{aligned} \tag{4.11}$$

where

$$\begin{aligned}
&z^{1,*} = \frac{2\epsilon^{1/2} x_{1/2}}{\tan\theta} + z_1^{(1)}, \qquad z^{2,*} = \frac{2\epsilon^{1/2} x_{1/2}}{\tan\theta} + z_1^{(2)}, \\
&B = \frac{c_2 - c_1}{c_1(z^{2,*} - z^{1,*})}, \qquad K = 1 - Bz^{1,*}.
\end{aligned} \tag{4.12}$$

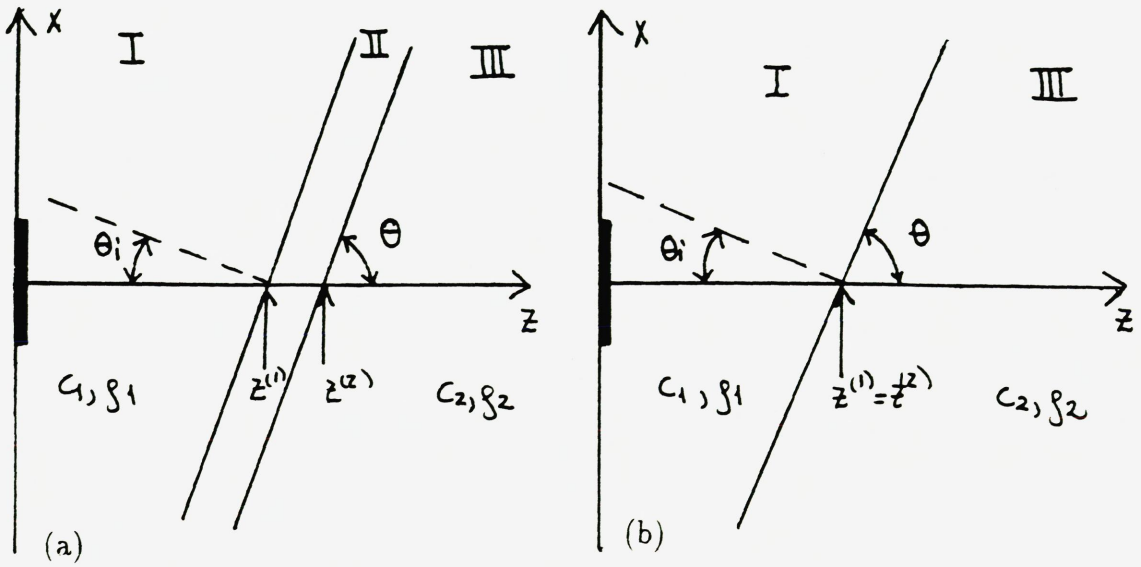

FIG. 4.14. Geometry of a fluid-fluid interface. (a) Case 1. (b) Case 2.

Similarly, for case 2, where $z^{1,*} = z^{2,*}$:

$$\sigma = z_1, \quad z_1 \leq z^{1,*} \qquad \sigma = z^{1,*} + \frac{c_2}{c_1}(z_1 - z^{1,*}), \quad z_1 > z^{1,*}, \tag{4.13}$$

$$\phi^{(1)} = \frac{z_1}{\epsilon}, \qquad \phi^{(3)} = \frac{z^{1,*}}{\epsilon} + \frac{c_1}{c_2}\frac{(z_1 - z^{1,*})}{\epsilon}. \tag{4.14}$$

We see that σ_{case1} approaches σ_{case2}, and ϕ_{case1} approaches ϕ_{case2} continuously as region 2 disappears. In both cases, σ and ϕ are functions of $\mathbf{x}_{\perp 1}$ through $z^{1,*}$ and $z^{2,*}$. σ, ϕ = constants are curved surfaces in region 2, and planes in regions 1 and 3. However, the following numerical calculations will illustrate that this limit process cannot be performed consistently within the assumptions of the weak inhomogeneity.

The direction of $\nabla\phi$ in the different regions for cases 1 and 2 satisfies:

$$\tan(\Theta_t - \Theta_i) = \left(\frac{c_2}{c_1} - 1\right)\frac{1}{\tan\theta} \quad \Rightarrow \quad \tan\Theta_t[1 - (\frac{c_2}{c_1} - 1)\tan^2\Theta_i] = \frac{c_2}{c_1}\tan\Theta_i, \tag{4.15}$$

where Θ_t and Θ_i are angles of transmission and incidence for the "simple wave" defined through τ_+ = constant, relative to the interface, see Fig. 4.15. Eq. (4.15) can be related to Snell's law. For Θ_i and Θ_t "small", e.g. $\tan\Theta_i \simeq \sin\Theta_i$ and $|\tan\Theta_i| \ll |c_2/c_1 - 1|^{-1/2}$, Eq. (4.15) becomes:

$$\sin\Theta_t = \frac{c_2}{c_1}\sin\Theta_i. \tag{4.16}$$

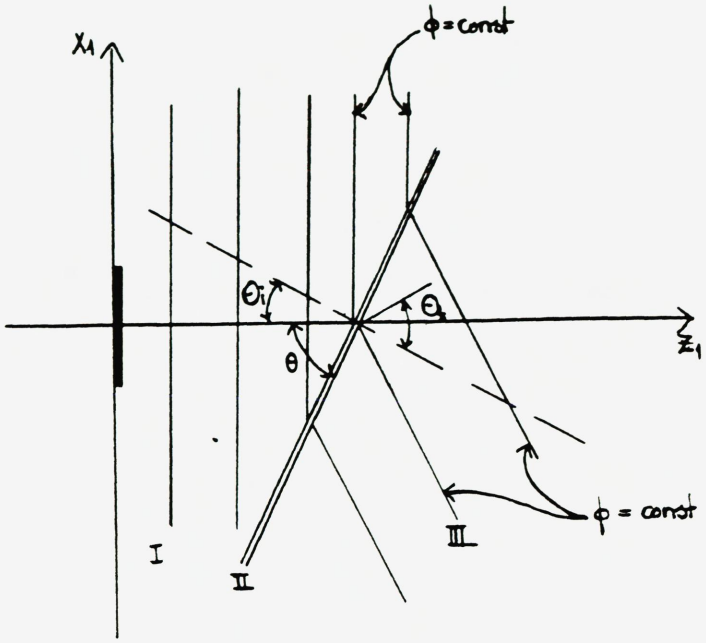

FIG. 4.15. The surfaces ϕ = constant in fluid-fluid interface simulation.

For $|\nabla c_0/\bar{c}|$ to be of $O(L/L_H)$, the following must be satisfied: (i) In the z-direction, $|(c_2 - c_1)/c_1(z_1^{(2)} - z_1^{(1)})| = O(1)$. (ii) In the transverse direction, $|(\Delta c_0/c_1(z_1^{(2)} - z_1^{(1)})|\cdot 2\epsilon^{1/2}\tan\Theta_i \ll 1$. If $|\Delta c_0/(c_1\Delta z_1)| = O(1)$, (ii) implies $\tan\Theta_i \ll (2\epsilon^{1/2})^{-1}$, which is a weak restriction since $\epsilon \ll 1$. However, as casel $\rightarrow$ case 2, $|\Delta c_0/(c_1\Delta z_1)| \rightarrow \infty$. For (ii) to be satisfied, $\epsilon^{1/2}\tan\Theta_i \rightarrow 0$, which means that either $ka \rightarrow \infty$ with Θ_i fixed (i.e., simple wave), or $\Theta_i \rightarrow 0$ with ka fixed (i.e., normal incidence). Although, since $|\nabla c_0/\bar{c}| \rightarrow \infty$ in z-direction, the limit process case 1 $\rightarrow$ case 2 is not consistent.

The parabolic equation with Gaussian amplitude distribution on the (monochromatic) source was solved for cases 1 and 2 respectively to illustrate the limitations in the simulation of interfaces. The pressure amplitude and (in some examples) ϕ are presented as contour plots in the coordinate frame $0 \leq z/R \leq 20.0$, $-10.0 \leq x/R \leq 10.0$ (ΔdB=2). The reference inhomogeneity length $L_H = R$ is the Rayleigh distance for $ka = 10$ (with a unit reference source radius a unspecified). The acoustic axis in region 3 is defined as the curve consisting of points of maximum amplitude in planes parallel to the (continuous or discontinuous) interface. [This is the definition used in Ref. (27).] The incident acoustic axis is in our case defined to be the z-axis.

In Fig. 4.16, the cases 1 and 2 are compared for constant $ka = 10$ and $\theta = 60°$, $65°$. $c_2/c_1 = 2.0$ (i.e., $\theta_c = 30°$), $z_1^{(1)} = 4.0$ and $z_1^{(2)} = 5.0$. [Hence in this figure, the thickness Δ varies as θ varies.] We see that: (1) The direction of the acoustic axis

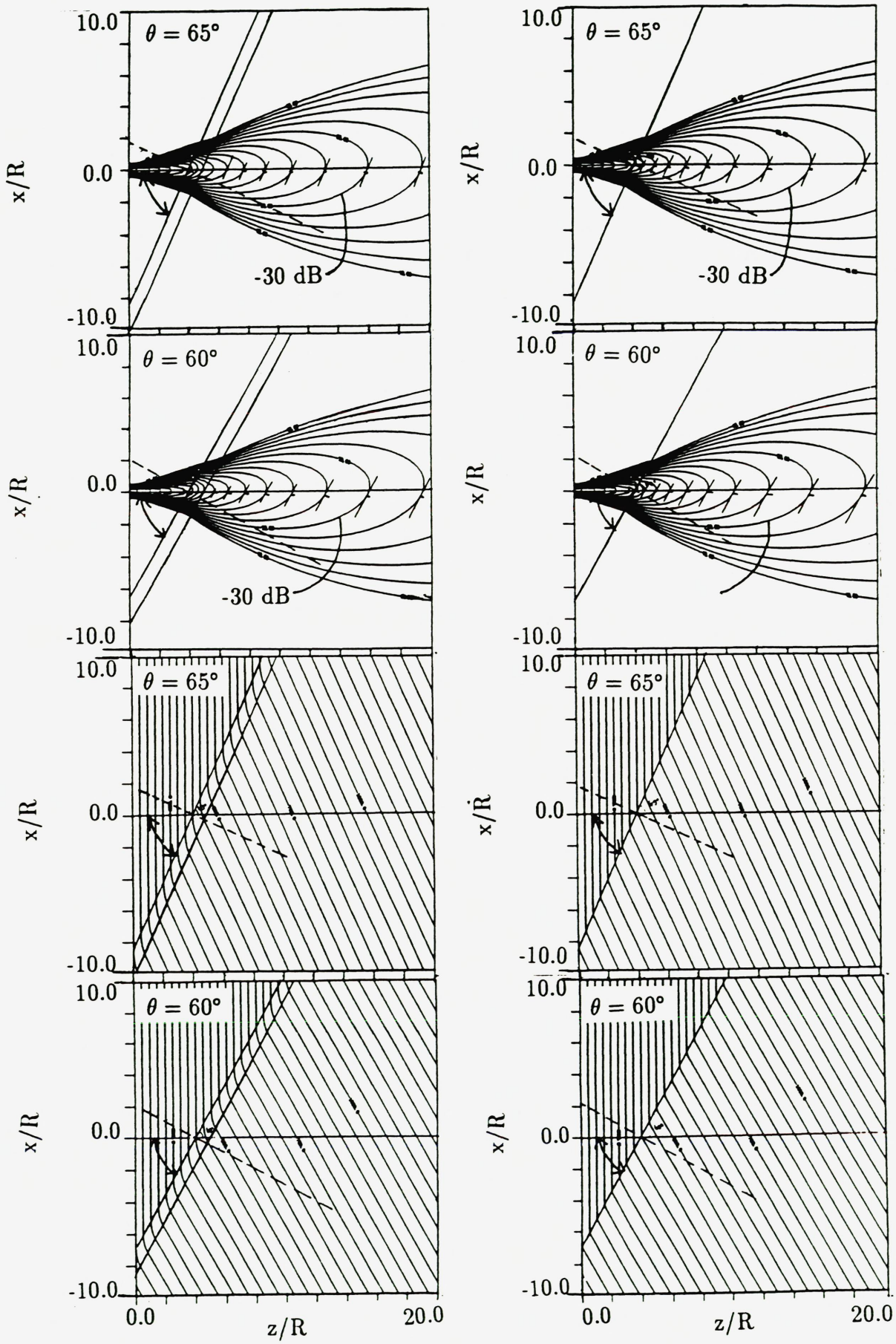

FIG. 4.16. Continuous vs. discontinuous simulation of interface. Amplitude and phase (ϕ). $c_2/c_1 = 2.0$. $\theta = 60°, 65°$. $\Delta dB = 2$, $\Delta\phi = 50$.

appears to be unaffected by the presence of region 2. However, due to propagation through region 2, where c_0 increases linearly, the amplitude in region 3 for case 1 is damped compared to case 2. (2) In region 2, the level curves for ϕ are weakly curved, due to the linearly increasing c_0. Therefore, in region 3, level curves for ϕ in case 1 are slightly delayed relative to the same level curves in case 2, although the curves are parallel for the two cases. (3) The effect of varying θ is the same for both cases: There is hardly any change in acoustic axis, but ϕ is more affected by variations in θ. For decreasing θ, i.e., increasing angle of incidence: $\nabla\phi$ departs more from the normal to the interface. [This is a valid observation even though $\Delta = \sin 65°$ for $\theta = 65°$ and $\Delta = \sin 60°$ for $\theta = 60°$.] This is in accordance with the behavior of a plane wave propagating through an interface into a medium with higher soundspeed: the plane wave attempts to "avoid" the region in space where c_0 increases the most.

To conclude, there is little difference in our simulation of the cases 1 and 2, except for the behavior of ϕ ("the simple wave part of the beam", through $\exp i(t - \phi)$). The reason for this may be that our simplified model cannot handle discontinuities in soundspeed and density consistently. In the following, we will therefore only consider case 1 and the effects on the amplitude due to varying θ and ka respectively, fixing the thickness of region 2 (Δ).

The behavior of ϕ can be discussed analytically for a more general continuous c_0. As before, the beam is studied in a plane spanned by ∇c_0 and $\mathbf{e}_z$ (the z-direction is the start direction of the beam): $c_0 = f(1 + Ax + Bz)$, where $f, f' = O(1)$, $|f''|, \ldots \ll 1$, $|A|, |B| \ll 1$, and x, z are normalized to L. Θ is defined as the angle between $\nabla\phi$ and $\mathbf{e}_z$. It can be shown that

$$\tan\Theta = \frac{A}{B}\left(1 - \frac{f(1 + Ax + Bz)}{f(1 + Ax)}\right). \tag{4.17}$$

From Eq. (4.17), Θ can be discussed for either $f' > 0$ or $f' < 0$, varying the signs of A, B. It follows that $\nabla\phi$ avoids the directions where c_0 increases the most. Hence, in the parabolic approximation for beam propagation in inhomogeneous media, both the simple wave on the short scale and the directivity is deformed so that the total field avoids to propagate in regions of larger sound speed.

Figure 4.17 shows the amplitude in case 1 for fixed $ka = 10$ and varying $\theta = 75°$, 45° and 20°. ($c_2/c_1 = 1.5$, $z_1^{(1)} = 4.0$ and $\Delta = \sin 75°/2$.) For increasing angle of incidence (decreasing θ), there is obviously an increasing bending of the directivity of the transmitted beam towards the interface. The direction of the transmitted acoustic axis differs more from the incident axis (= z-axis) and angle of transmission increases. The explanation within our model is: For increasing angles of incidence, the beam must propagate an increasing distance in z-direction in region 2 where c_0 increases. The transverse variations in c_0 appear stronger since the thickness of region 2 in transverse direction decreases. Accordingly, the beam attempts to avoid region 2 and the acoustic axis is bent. This observation compares well qualitatively with

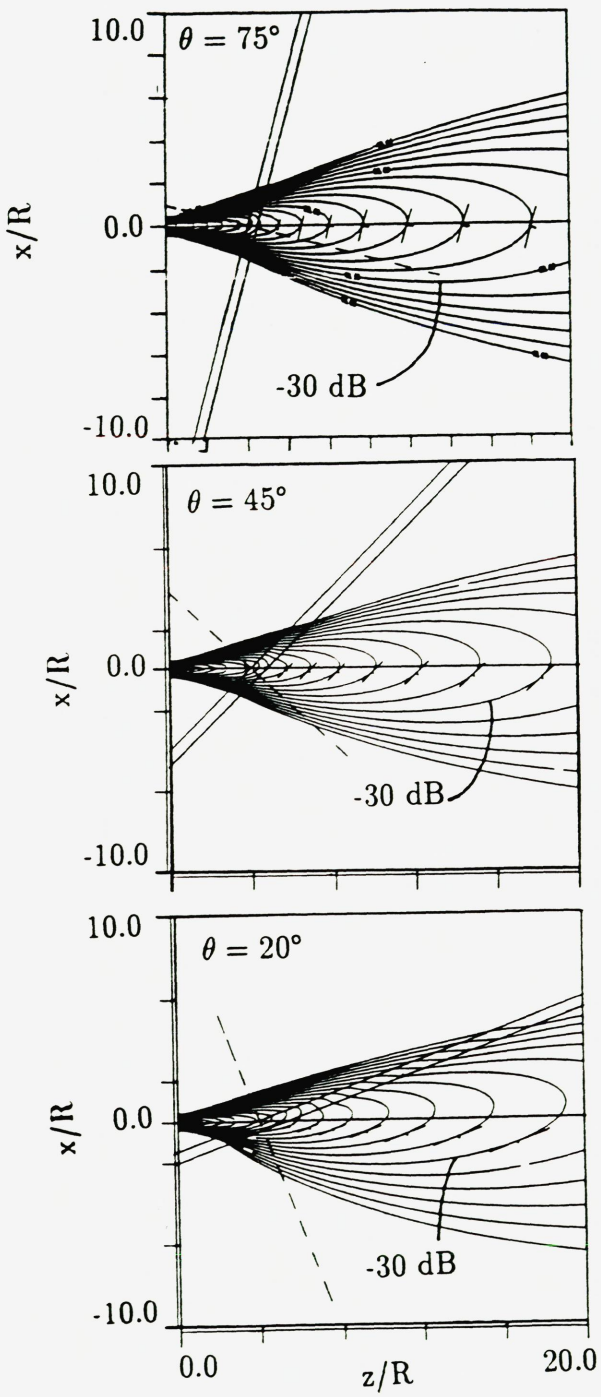

FIG. 4.17. Continuous interface simulation, amplitude: varying θ, fixed ka. $c_2/c_1 = 1.5$. $\theta = 75°, 45°, 20°$. $\Delta dB = 2$.

Fermat's principle (although Snell's law predicts that there should be no transmission above critical incidence, which is 41.8° in this case).

In Fig. 4.18, a is fixed and k varies ($c_2/c_1 = 2.0$, $z_1^{(1)} = 4.0$ and $\Delta = \sin 65°$). Results with $k_1 = 5^{-1/2}k$, $k_2 = 10^{-1/2}k$ are compared, for $\theta = 65°$, 45° and 25°. [I.e., $k_1 a = \sqrt{20}$, $k_2 a = \sqrt{10}$, k corresponds to $ka = 10$. These are low ka-values to be used in the parabolic approximation, but we are only interested in the qualitative effects on the solution due to variations of ka.] It is observed that for decreasing k, the angle of transmission decreases, for the various angles considered. For increasing angle of incidence, (in which case the transverse component of ∇c_0 in region 2 and the horizontal thickness of region 2 increase) the difference in transmitted acoustic axis for the two values of k becomes more obvious. This behavior can be explained within our model by the following: for a fixed θ and increasing ka, the effective longitudinal gradient in region 2 increases. This affects the geometrical spreading of the beam, and the effect on acoustic axis is that angle of transmission increases. (Thus, we may suspect that for even higher k, the tendency will be more pronounced.) Snell's law is not satisfied in any of these cases. The observations are qualitatively in accordance with the results of Refs. (26,27). (There, for directive beams, asymptotic formulas are derived in the farfield of the source and the interface. These formulas can be related to Snell's law for complex angles which must be calculated numerically.)

We will briefly discuss the case of fixed ka, varying k and a individually. In Fig. 4.19 ($\theta = 65°$), $ka = 10$, but the source radius is twice the radius in Fig. 4.16, and the wavenumber is decreased correspondingly. Hence the Rayleigh distance for the beam in Fig. 4.19 is twice the Rayleigh distance for the beams in Fig. 4.16. We observe that there is no difference in the bending of the beam, neither in region 2 nor 3. However, as in Sec. 4.1.4, the value of (almost) coinciding contour lines differ in the two figures, due to different Rayleigh distance and different geometrical damping of the sound pressure.

4.3. Special cases

4.3.1. Phase shading factor.

A natural boundary condition for Eq. (2.54) is $p^{(1)}(\mathbf{x}_\perp, 0, \tau_+) = f(\mathbf{x}_\perp, \tau_+)$, so it is natural to choose $\mathbf{T}$ normal to the source when $z = 0$. [In that case, the linear version of Eq. (2.75) for $P^{(1)}$ can for instance be solved by an integral transform with respect to $\mathbf{x}_\perp$.]

However, in general the source is not plane. A phase shading factor, approximately accounting for weak curvature of the source surface or steering of the beam, can be introduced to avoid complications which would result from boundary conditions given in a plane which is not orthogonal to the longitudinal axis. In the

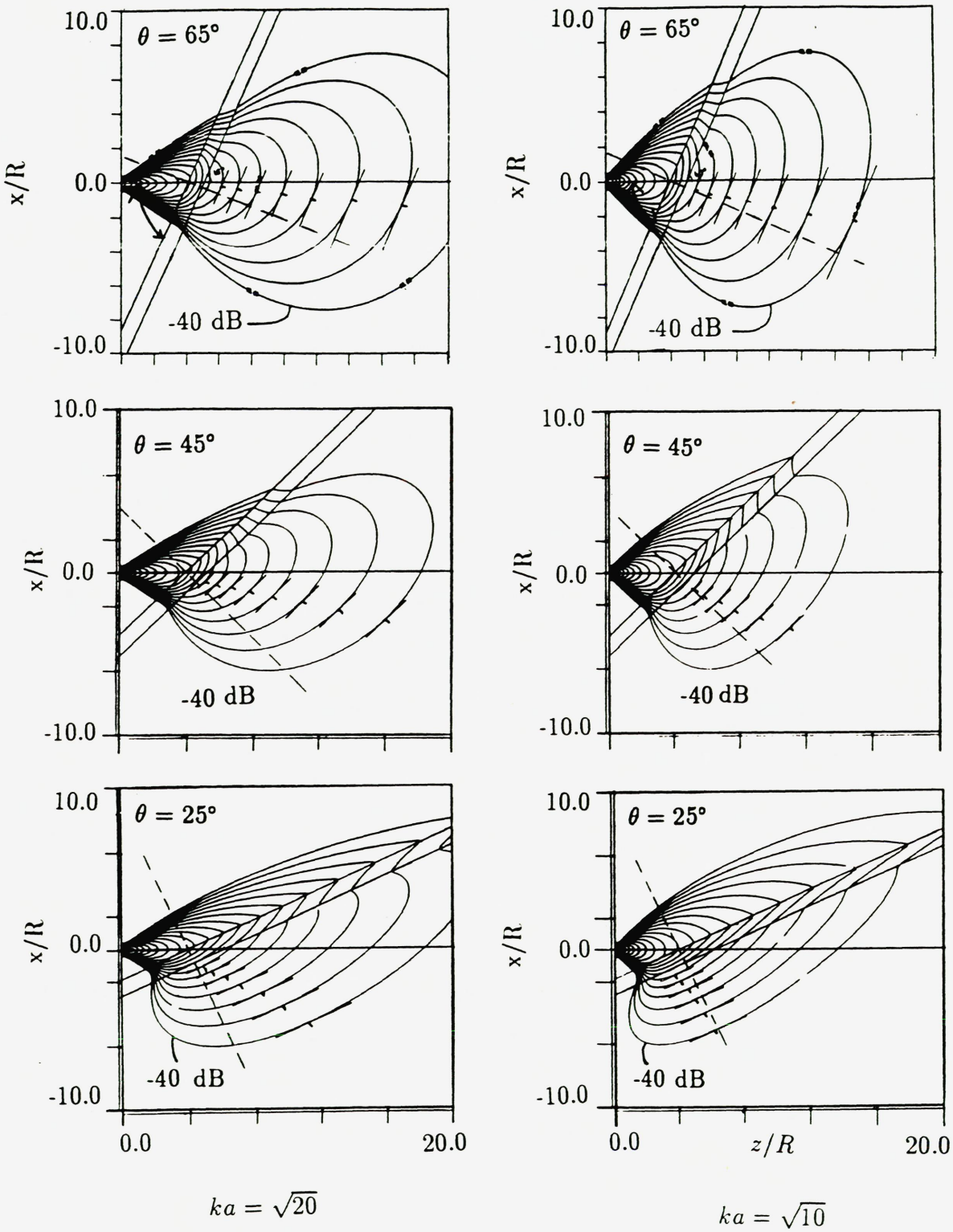

FIG. 4.18. Continuous interface simulation, amplitude: Varying k and fixed source radius. $ka = 20^{1/2}$, $ka = 10^{1/2}$, for $\theta = \theta = 65°, 45°, 20°$. $c_2/c_1 = 2.0$. $\Delta dB = 2$.

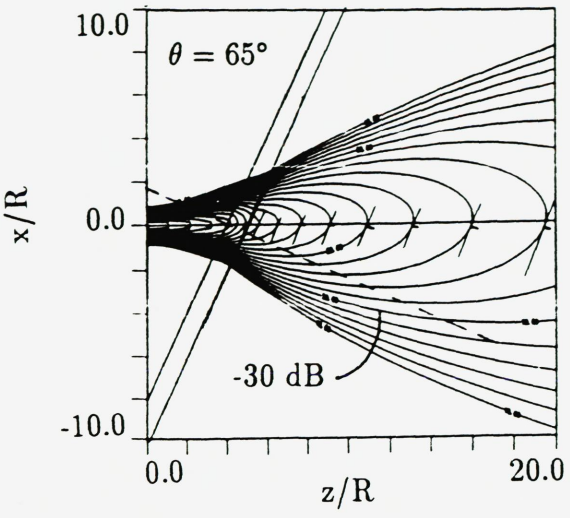

FIG. 4.19. Continuous interface simulation, amplitude: $ka = 10$, $a = 2\bar{a}$, $\theta = 65°$. $c_2/c_1 = 2.0$. $\Delta dB = 2$.

monochromatic case, the boundary condition at the curved source, where $\phi = 0$, is:

$$p_{source} = f(\mathbf{x}_\perp)\exp(it). \tag{4.18}$$

Assume that the surface on which the source is located is $z = z(\mathbf{x}_\perp)$, with z scaled to the short characteristic length L. If $|z(\mathbf{x}_\perp)| << 1$, the source curvature can be ignored on the short scale and a phase shading is not necessary. If $|z(\mathbf{x}_\perp)| \ll H^{-1}$, by Taylor expansion of the pressure amplitude at $z = 0$ with respect to the source surface, equivalent boundary conditions may be specified in the plane $z = 0$:

$$p_{z=0} \simeq f(\mathbf{x}_\perp)\exp(i\tau_+|_{z=0}), \tag{4.19}$$

where

$$\begin{aligned}\tau_+|_{z=0} &= t - \phi(z=0) \\ &\simeq t - \frac{\partial\phi}{\partial z}|_{(z=z(\mathbf{x}_\perp))}(-z(\mathbf{x}_\perp)) + O\left(\frac{\partial^2\phi}{\partial z^2}|z(\mathbf{x}_\perp)|^2\right),\end{aligned} \tag{4.20}$$

i.e., the fast phase ϕ is estimated at $z = 0$ by Taylor expansion around the source surface. Since the reference soundspeed is chosen as the value of c_0 at the source, $\partial\phi/\partial z|_{(z=z(\mathbf{x}_\perp))} = 1$. Also, due to weak inhomogeneity, $\partial^2\phi/\partial z^2 = O(L/L_H) = O(H)$ (since $\nabla^2\phi = O(H)$). If $|z(\mathbf{x}_\perp)|^2 \ll H^{-1}$, it is consistent to neglect the second order terms in the expansion of ϕ.

The term $H|z(\mathbf{x}_\perp)|$ accounts for the difference in calculating σ by integrating from the source surface rather than from the plane $z = 0$:

$$\sigma = \int_{z_1(\mathbf{x}_\perp)}^{z_1} c_0\, dz_1 \qquad \text{instead of} \qquad \sigma = \int_0^{z_1} c_0\, dz_1. \tag{4.21}$$

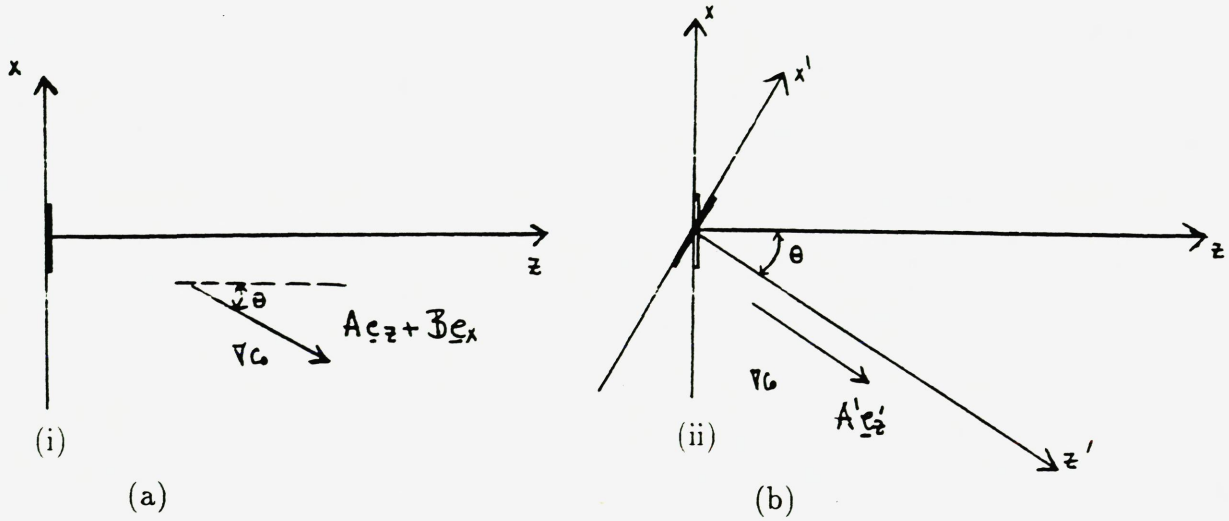

FIG. 4.20. Geometry for comparison of phase shading vs. no phase shading of a plane source. (a) The source location is fixed and the medium rotated. (b) The medium is fixed and the source is rotated.

4.3.2. Tilted plane source, monochromatic case.

The previous linear numerical examples have shown that the beam is more sensitive to longitudinal than to transverse inhomogeneity. It may be interesting to investigate two cases where the source is rotated relative to ∇c_0. Case (i): The medium can be rotated while the source is fixed, i.e., the angle between $\mathbf{T}$ and ∇c_0, θ, is varied. Here σ is calculated by integrating with respect to z in the $\mathbf{T}$-direction; the longitudinal component of ∇c_0 is $|\nabla c_0| \cos\theta$. Case (ii): The source can be rotated, the direction of ∇c_0 being fixed. $\mathbf{T}$ and ∇c_0 are parallel, but the source is phase shaded so that it is tilted an angle θ with respect to a plane orthogonal to ∇c_0 and steered in the z-direction. See Fig. 4.20.

The (x', z') coordinates in case (ii) are rotated an angle $-\theta$ compared to the (x, z) coordinates in case (i):

$$z' = z\cos\theta - x\sin\theta, \qquad x' = z\sin\theta + x\cos\theta. \tag{4.22}$$

σ' is calculated by integration with respect to z' in the $\mathbf{T}$-direction, the longitudinal sound speed gradient is $|\nabla c_0|$.

According to Eqs. (2.67), (3.14), (3.15), the nondimensional, scaled pressure satisfies:

(i)

$$P^{(1)} = \exp(it)F(\mathbf{x}_{\perp 1/2}), \qquad z = 0, \tag{4.23}$$

$$P^{(1)} \simeq \frac{2}{i\sigma}\exp(i(t-\phi) + \frac{i|\mathbf{x}_{\perp 1/2}|^{1/2}}{\sigma})\hat{F}\left(\frac{2\mathbf{x}_{\perp 1/2}}{\sigma}\right), \quad \sigma \gg 1, \tag{4.24}$$

(ii)

$$P^{(1)} = \exp(i(t - ix\sin\theta))F(\mathbf{x}_{\perp 1/2}), \qquad z = 0, \tag{4.25}$$

$$P^{(1)} \simeq \frac{2}{i\sigma'}\exp(i(t-\phi') + \frac{i|\mathbf{x}_\perp{}'_{1/2}|^{1/2}}{\sigma'})\hat{F}\left(\frac{2\mathbf{x}_\perp{}'_{1/2}}{\sigma'} - \mathbf{e}'_x\frac{a}{L}\sin\theta\right), \quad \sigma' \gg 1 \tag{4.26}$$

F is the same in both cases, consistently with the parabolic approximation ($\hat{F}$ = transverse Fourier transform). In the homogeneous case, (i) and (ii) are equivalent for small angles θ.

With $c_0 = \bar{c}f(1 + Az + Bx)$, in case (i):

$$\phi = \int_0^z \frac{dz'}{f(1 + Az' + B\mathbf{x}_\perp)}, \qquad \sigma = \int_0^{z_1} f(1 + A_1 z_1' + B_1\mathbf{x}_{\perp 1})dz_1', \tag{4.27}$$

and in case (ii) ($c_0 = \bar{c}f(1 + A'z')$):

$$\phi' = \int_0^{z'} \frac{dz''}{f(1 + A'z'')}, \qquad \sigma' = \int_0^{z_1'} f(1 + A_1' z_1'')dz_1'', \tag{4.28}$$

$$A_1 = \frac{L}{L_H}A, \qquad B_1 = \frac{L}{L_H}B, \qquad A' = (A^2 + B^2)^{1/2}, \qquad A_1' = \frac{L}{L_H}A'. \tag{4.29}$$

Inserted in the corresponding expressions for $P^{(1)}$, the difference between the formulations (i) and (ii) can be studied. The terms (a) (σ, σ'), (b) $(\mathbf{x}_\perp{}'_{1/2}/\sigma', \mathbf{x}_{\perp 1/2}/\sigma)$ and (c) $(2\mathbf{x}_\perp{}'_{1/2}/\sigma' - \mathbf{e}'_x a/L, 2\mathbf{x}_{\perp 1/2}/\sigma)$ can be compared individually. In the inhomogeneous case, the restriction on θ with respect to the curved coordinates $(\sigma, \mathbf{x}_{\perp 1})$ is the same as the restriction with respect to the coordinates $(z_1, \mathbf{x}_{\perp 1})$ in the homogeneous case ($\theta < 20°$, due to parabolic approximation[28]). In the inhomogeneous case, the angular region of validity in $(z_1, \mathbf{x}_{\perp 1})$-coordinates depends on $|\nabla c_0|$.

An example: For $f = 1 + A_1 z_1 + B_1 x_1$, in case (i):

$$\sigma = \frac{A_1}{2}z_1^2 + (1 + B_1 x_1)z_1, \tag{4.30}$$

and in case (ii):

$$\sigma' = \frac{A_1'\cos^2\theta}{2}z_1^2 + \cos\theta(1 - A'\sin\theta x_1)z_1 + [\frac{A_1'\sin^2\theta}{2}x_1^2 - x_1\sin\theta]. \tag{4.31}$$

The two cases are comparable for $\cos\theta \approx 1$ and $|x_1\sin\theta| \ll z_1$, i.e., for small tilting angle of the source and for a narrow beam. The validity of phase shading combined with weak inhomogeneity in our parabolic approximation can be illustrated by a comparison of $P^{(1)}$ (cf. Eqs. (2.67, 2.75)) and the solution of Eqs. (2.32, 2.33) (for $q = p'/\rho_0{}^{1/2}$) with phase shaded boundary conditions.

4.3.3. Focusing source.

For the special case of a monochromatic, weakly focusing source, we have

$$z(\mathbf{x}_\perp) = d - (d^2 - |\mathbf{x}_\perp|^2)^{1/2} \approx \frac{|\mathbf{x}_\perp|^2}{2d}, \qquad \tau_+|_{z=0} \approx t + \frac{|\mathbf{x}_\perp|^2}{2d}, \tag{4.32}$$

if $a/d << 1$, $|z(\mathbf{x}_\perp)| \approx a^2/2d$ (a = source radius). Here $d = O(L_H)$ is the curvature radius of the source (focal distance). Following the discussion above, $\sigma = 0$ at the plane $z = 0$, thus the focusing boundary conditions are identically formulated in the homogeneous and in the inhomogeneous case. For the linear case: in the formalism for the homogeneous case, z and $p^{(1)}$ can be replaced by σ and $P^{(1)}$. Then the focal plane in the homogeneous case becomes a "focal surface" in the inhomogeneous case, given by $\sigma(z_1, \mathbf{x}_{\perp 1}) = d/L_H$, i.e., $z_d = z_1(\sigma = d/L_H, \mathbf{x}_{\perp 1})$. Depending on ∇c_0, the "inhomogeneous focal surface" may be distorted compared to the geometrical focal plane of the source.

The numerical approach in Ref. (15) can be applied:

$$\sigma_1 = \frac{L_H \sigma - d}{d} \tag{4.33}$$

can be inserted in the generalized KZK–equation in curved coordinates, Eq. (2.75), and a coordinate transform which improves the numerical calculations in the focal region can be introduced (the grid is more dense in the focal region):

$$\tau_p = \tau_+ - \frac{L_H}{d} \frac{|\mathbf{x}_{\perp 1/2}|^2}{\sigma_1 \pm \delta}, \qquad \mathbf{u} = \frac{\mathbf{x}_{\perp 1/2}}{\sigma_1 \pm \delta}. \tag{4.34}$$

Pulsed signals can also be described. In dimensional coordinates, the linearized inhomogeneous, nondissipative equation and boundary conditions are (cf. Eq. (2.77)):

$$\frac{2}{\bar{c}} \frac{\partial^2 \bar{p}^{(1)}}{\partial \tau_+ \partial \sigma_0} - \nabla_\perp^2 \bar{p}^{(1)} = 0, \tag{4.35}$$

$$\bar{p}^{(1)}_{z=0} = \bar{p}^{(1)}_{\sigma_0 = 0} = v(\mathbf{x}_\perp, t + \frac{x^2}{2d\bar{c}}). \tag{4.36}$$

Let p_u denote the corresponding solution for the case of an unfocused source, i.e., for which $d = 0$. It can be shown that[18,19,20]

$$\frac{1}{\sigma_0} p_u(\mathbf{x}_{\perp d}, \sigma_d, \tau_{+d}) = \frac{1}{\sigma_d} \bar{p}^{(1)}(\mathbf{x}_\perp, \sigma_0, \tau_+), \tag{4.37}$$

where

$$\tau_{+d} - \frac{\mathbf{x}_{\perp d}^2}{2\sigma_d \bar{c}} = \tau_+ - \frac{\mathbf{x}_\perp{}^2}{2\sigma_0 \bar{c}}, \qquad \frac{\mathbf{x}_{\perp d}}{\sigma_d} = \frac{\mathbf{x}_\perp}{\sigma_0}, \qquad \frac{1}{\sigma_d} = \frac{1}{\sigma_0} - \frac{1}{d}. \tag{4.38}$$

In the notation of geometrical optics, if σ_d is the position of the object, σ_0 is the position of the image through a lens with focal distance d. For $\sigma_0 = d$, $\sigma_d \to \infty$, i.e., the farfield is transformed into the focal surface.

Chapter 5

Nonlinear propagation

In this chapter we present results from a numerical solution of the truncated system Eqs. (3.9, 3.10). The sound source is either a circular uniform piston of radius a, or a Gaussian source with Gaussian radius a. We assume that the excitation is monochromatic with wave number k. The values of k, a are the same for all cases, with $ka = 10$, as well as the characteristic length for inhomogeneity: $AL_H = AR = 1$, where R is the reference Rayleigh distance and $A = |\nabla c_0|/c_0$. We will study the fundamental and second harmonic components for the sound pressure field from a uniform piston source in the quasilinear approximation, and the fundamental, second, third and fourth harmonic components from a Gaussian source, using the fully nonlinear equation.

In the quasilinear, nondissipative case, the pressure amplitude is presented in the plane spanned by the z–axis and one transverse axis, in a square region with sides $2R$. The sound pressure level at the source gives $R/l_d = 0.05$ (l_d is the reference shock formation distance corresponding to the wavenumber k, cf. Sec. 2.3). Figures 5.1, 5.2, 5.3, 5.4 show the amplitudes of the fundamental (i.e., linear solution) and the second harmonic components for sound speed profiles 1, 11, 2, 22 (cf. Eqs.(4.1)–(4.4)) with $\theta = 90°$ and $x_c = 0$. On Fig. 5.1, the second harmonic is shown both in the xz-plane and the yz-plane, while on the other figures, only the amplitude in the xz-plane is shown.

Comparing the quasilinear solutions corresponding to four different sound speed profiles for $\theta = 90°$, we see that the effect of transverse inhomogeneity on the second harmonic component is qualitatively the same as for the fundamental. Both harmonic components tend to avoid the regions in space of larger c_0. However, the bending of the second harmonic is weaker than for the fundamental, and most pronounced for the side lobes. This may be explained by: (1) Due to inhomogeneity, the nonlinearity coefficient $\mathcal{P}^*_{nonl}$ defined in Eq. (2.76) is a decreasing function of c_0, i.e., the value is largest in regions in space where c_0 is most decreasing. The effective shock formation distance is $c_0 T/\beta\epsilon$ and proportional to c_0. (2) The second harmonic

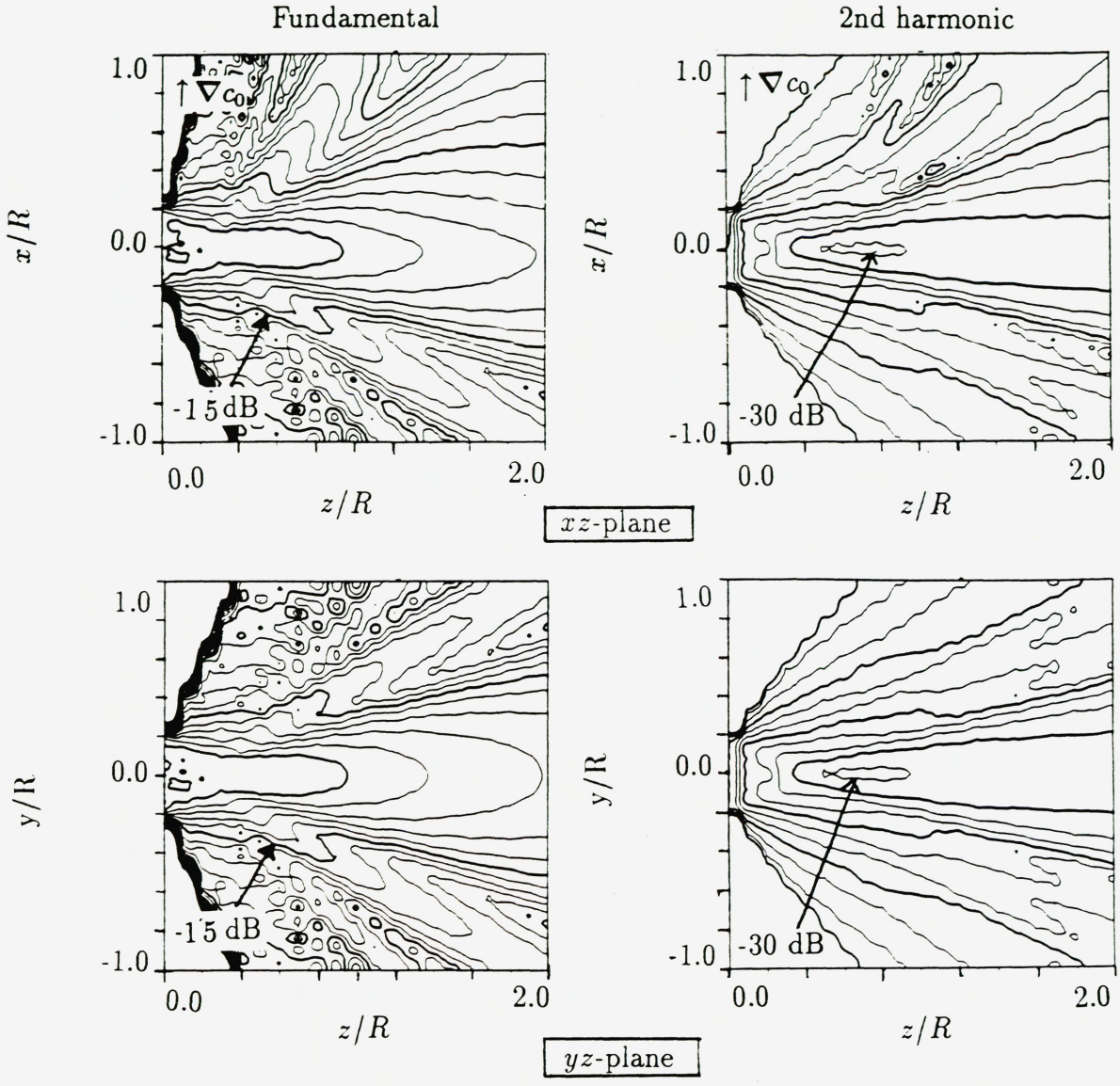

FIG. 5.1. Uniform source, quasilinear case, $R/l_d = 0.05$, $R\bar{\alpha} = 0$. c_0 = Profile 1, $\theta = 90°$, $x_c = 0$. Fundamental: $\Delta dB = 3$, second harmonic: $\Delta dB = 6$.

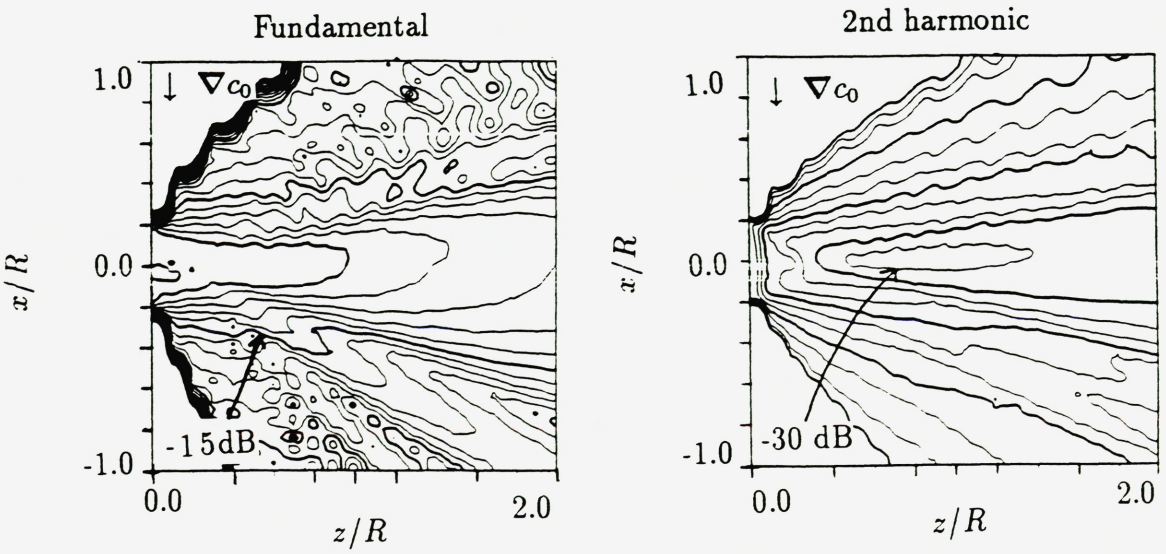

FIG. 5.2. Uniform source, quasilinear case, $R/l_d = 0.05$, $R\bar{\alpha} = 0$. c_0 = Profile 11, $\theta = 90°$, $x_c = 0$. Fundamental: $\Delta dB = 3$, second harmonic: $\Delta dB = 6$.

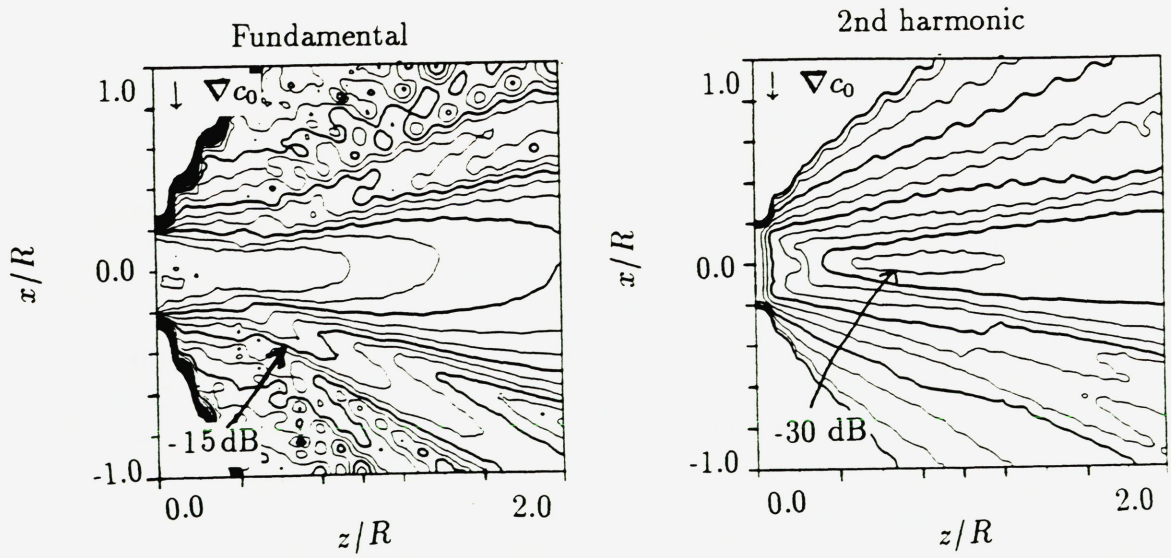

FIG. 5.3. Uniform source, quasilinear case, $R/l_d = 0.05$, $R\bar{\alpha} = 0$. c_0 = Profile 2, $\theta = 90°$, $x_c = 0$. Fundamental: $\Delta dB = 3$, second harmonic: $\Delta dB = 6$.

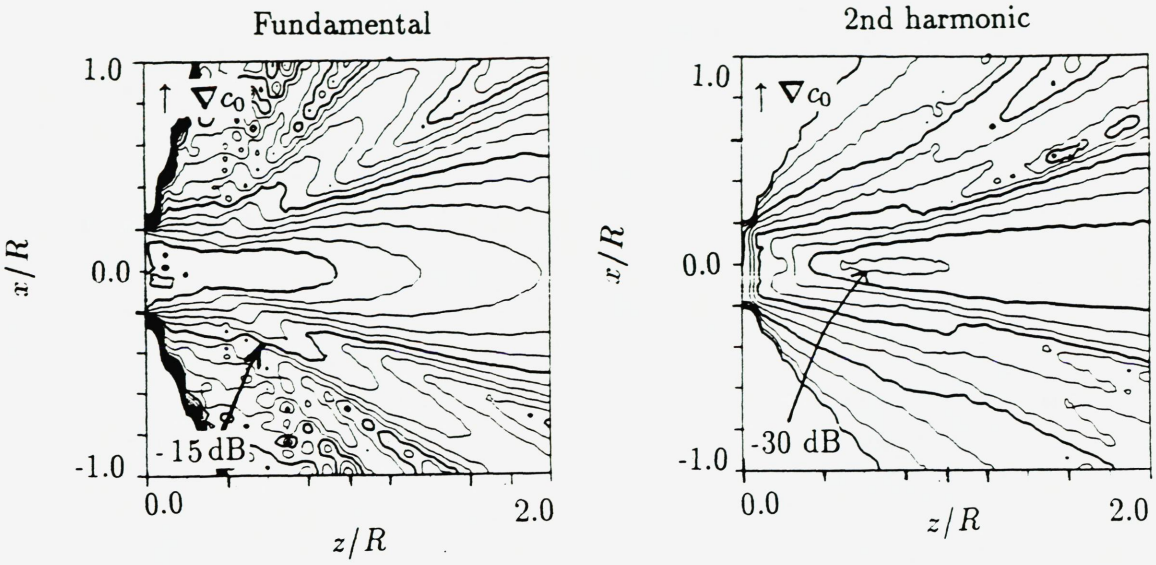

FIG. 5.4. Uniform source, quasilinear case, $R/l_d = 0.05$, $R\bar{\alpha} = 0$. c_0 = Profile 22, $\theta = 90°$, $x_c = 0$. Fundamental: $\Delta dB = 3$, second harmonic: $\Delta dB = 6$.

receives contributions from all the virtual sources with density $(p^{(1)})^2$ in planes behind the observation point. In each of these planes, $p^{(1)}$ is asymmetric in x due to inhomogeneity. Therefore the amplitude of the virtual sources is relatively larger in regions in space where c_0 decreases.

A comparison of Figs. 5.1 and 5.4, and of Figs. 5.2 and 5.3, shows how the bending of the second harmonic is more pronounced for larger $|Af'|$, i.e., shorter effective inhomogeneity length, as expected. However, in all examples shown here the bending due to inhomogeneity is very weak. The reason may be that the pressure is only calculated up to $z = 2R$, while the inhomogeneity effects will accumulate over several units of $R = L_H$, depending on the choice of f.

In the fully nonlinear, nondissipative case, $R/l_d = 0.25$ and 8 harmonics are kept in the computations. The four first harmonic components are studied in the xz- and yz-planes. All results are presented in a coordinate frame of $10R$ in both longitudinal and transverse directions. The homogeneous reference case for comparisons is shown in Fig. 5.5.

In Figs. 5.6, 5.7, 5.8 the harmonic components are presented in the xz-plane, for c_0 = Profiles 1, 2, 11 with $x_c = 0$ and $\theta = 90°$. Due to the transverse ∇c_0, all the harmonic components are bent similarly as in the linear case, cf. Figs. 4.5, 4.6. However, the fundamental is most influenced by ∇c_0; for increasing harmonic number, the amplitudes are less bent. When ∇c_0 has a longitudinal component, for instance $\theta = 75°$, as in Figs. 5.9, the behavior is quite different. For increasing harmonic number, the harmonic components are more influenced by the longitudinal

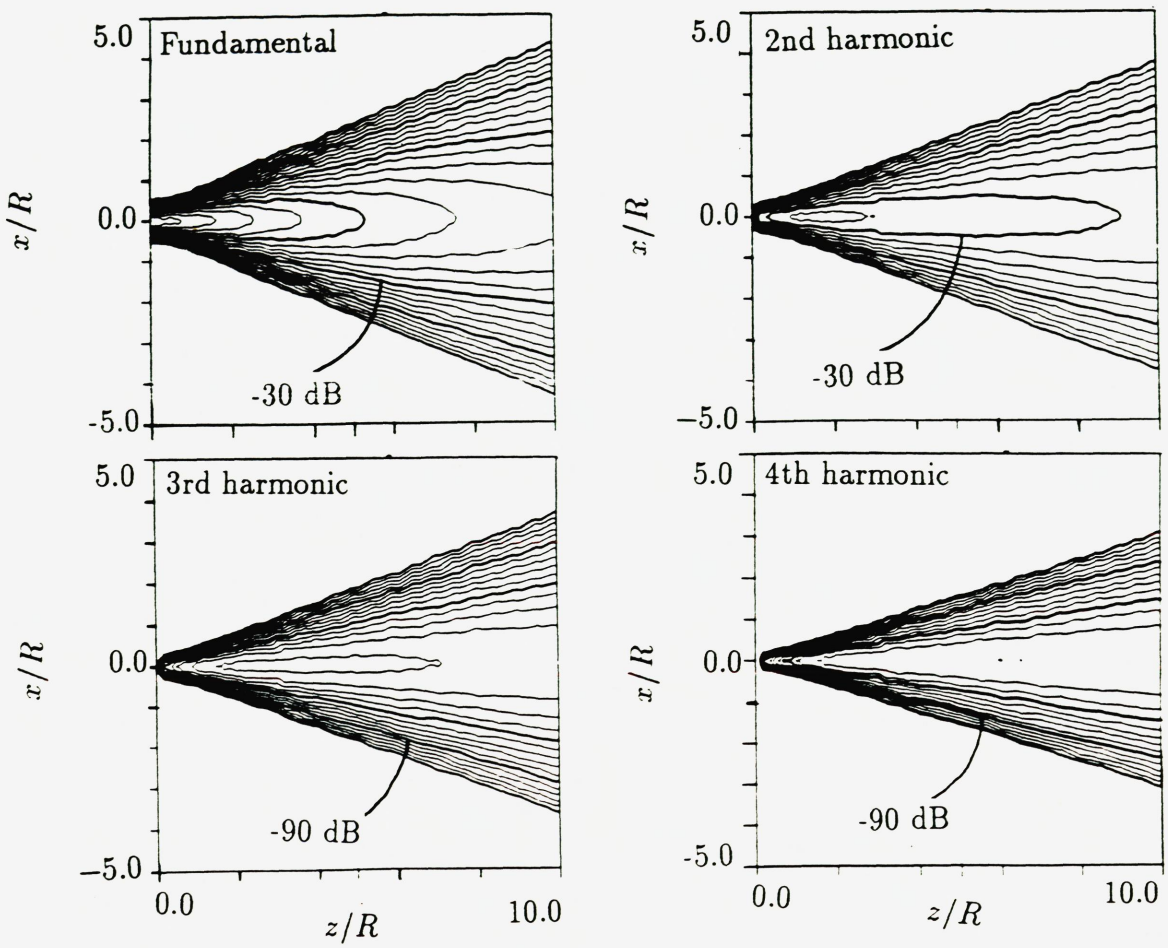

FIG. 5.5. Gaussian source, fully nonlinear case, $R/l_d = 0.25$, $R\bar{\alpha} = 0$. Homogeneous, nondissipative medium. Fundamental: $\Delta dB = 3$, higher harmonics: $\Delta dB = 6$.

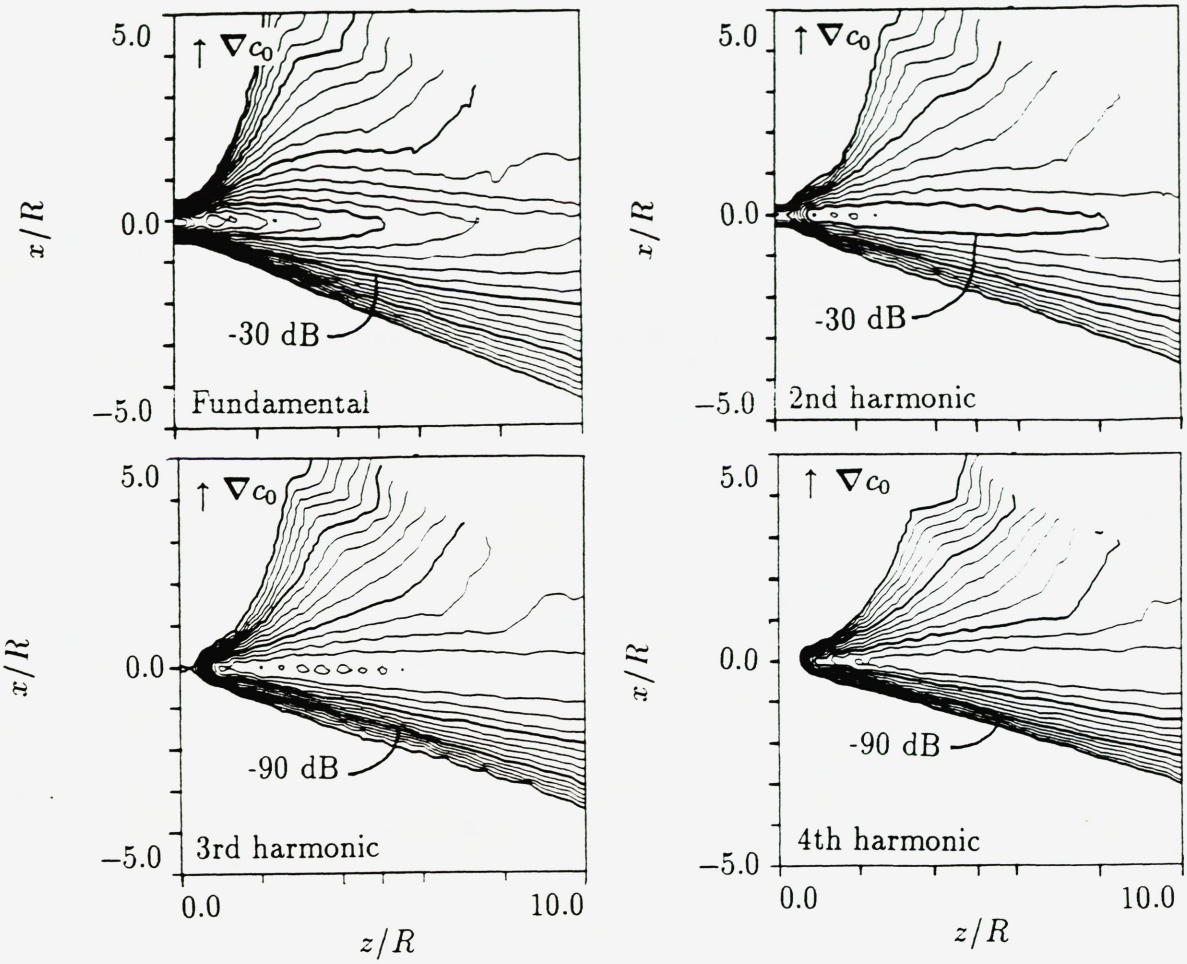

FIG. 5.6. Gaussian source, fully nonlinear case, $R/l_d = 0.25$, $R\bar{\alpha} = 0$. c_0 = Profile 1. $\theta = 90°$, $x_c = 0$. Fundamental: $\Delta dB = 3$, higher harmonics: $\Delta dB = 6$.

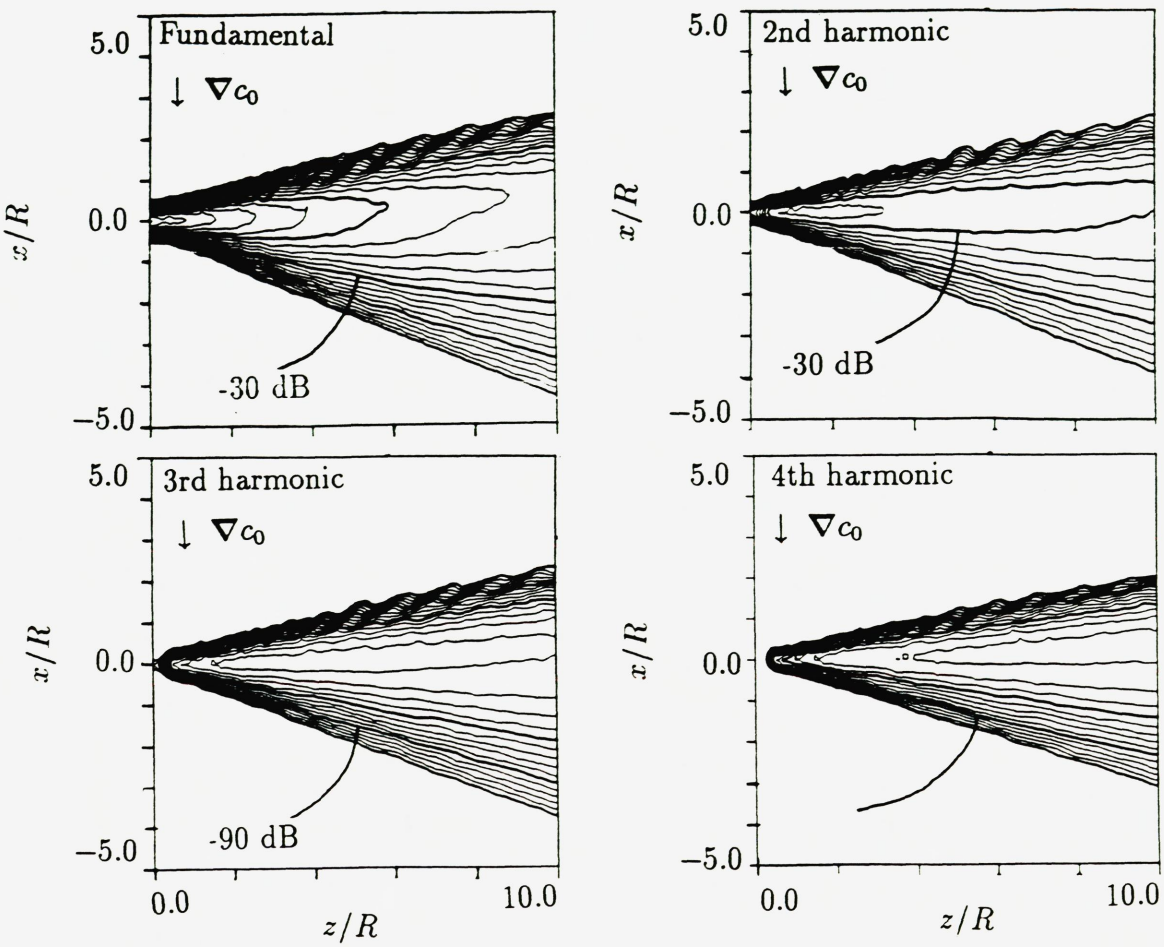

FIG. 5.7. Gaussian source, fully nonlinear case, $R/l_d = 0.25$, $R\bar{\alpha} = 0$. c_0 = Profile 2, $\theta = 90°$, $x_c = 0$. Fundamental: $\Delta dB = 3$, higher harmonics: $\Delta dB = 6$.

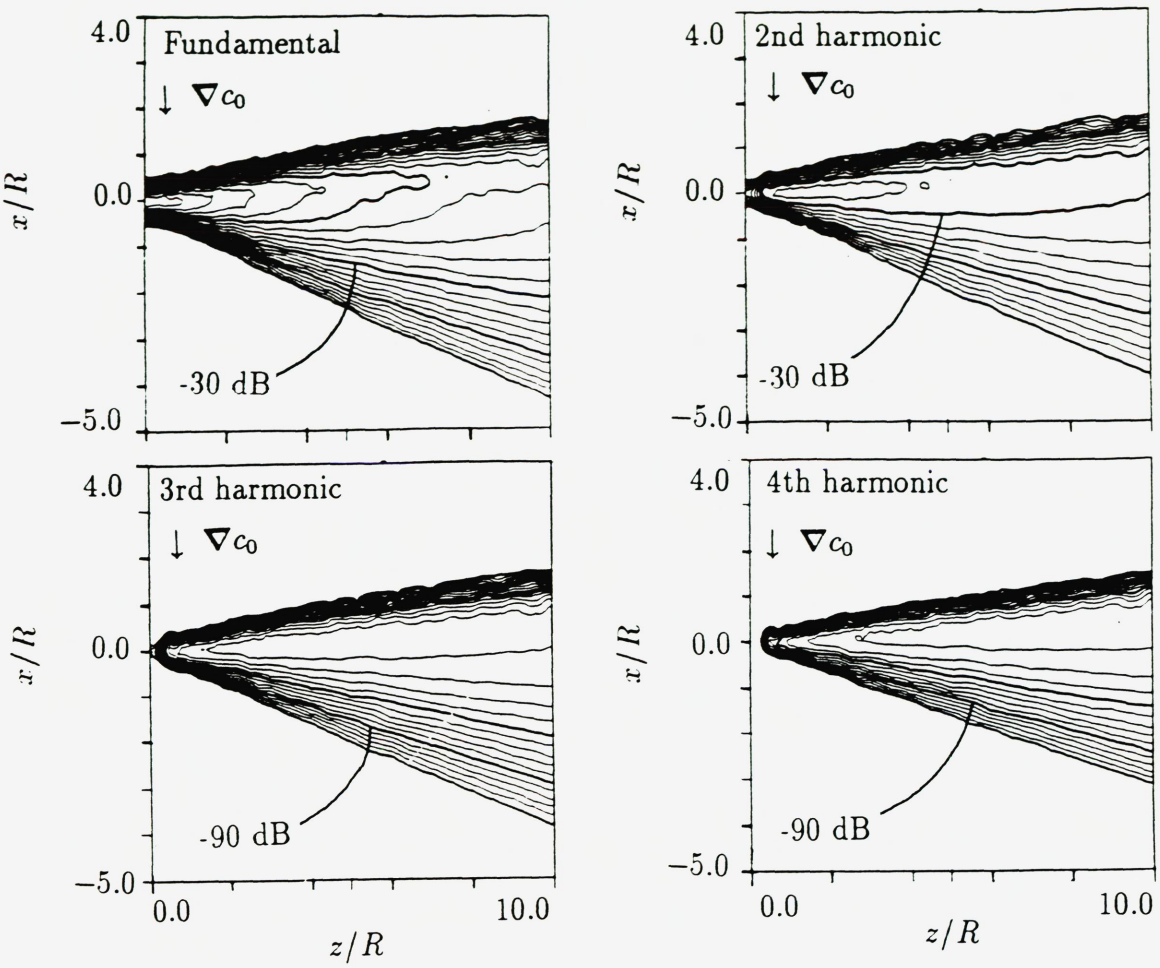

FIG. 5.8. Gaussian source, fully nonlinear case, $R/l_d = 0.25$, $R\bar{\alpha} = 0$. c_0 = Profile 11, $\theta = 90°$, $x_c = 0$. Fundamental: $\Delta dB = 3$, higher harmonics: $\Delta dB = 6$.

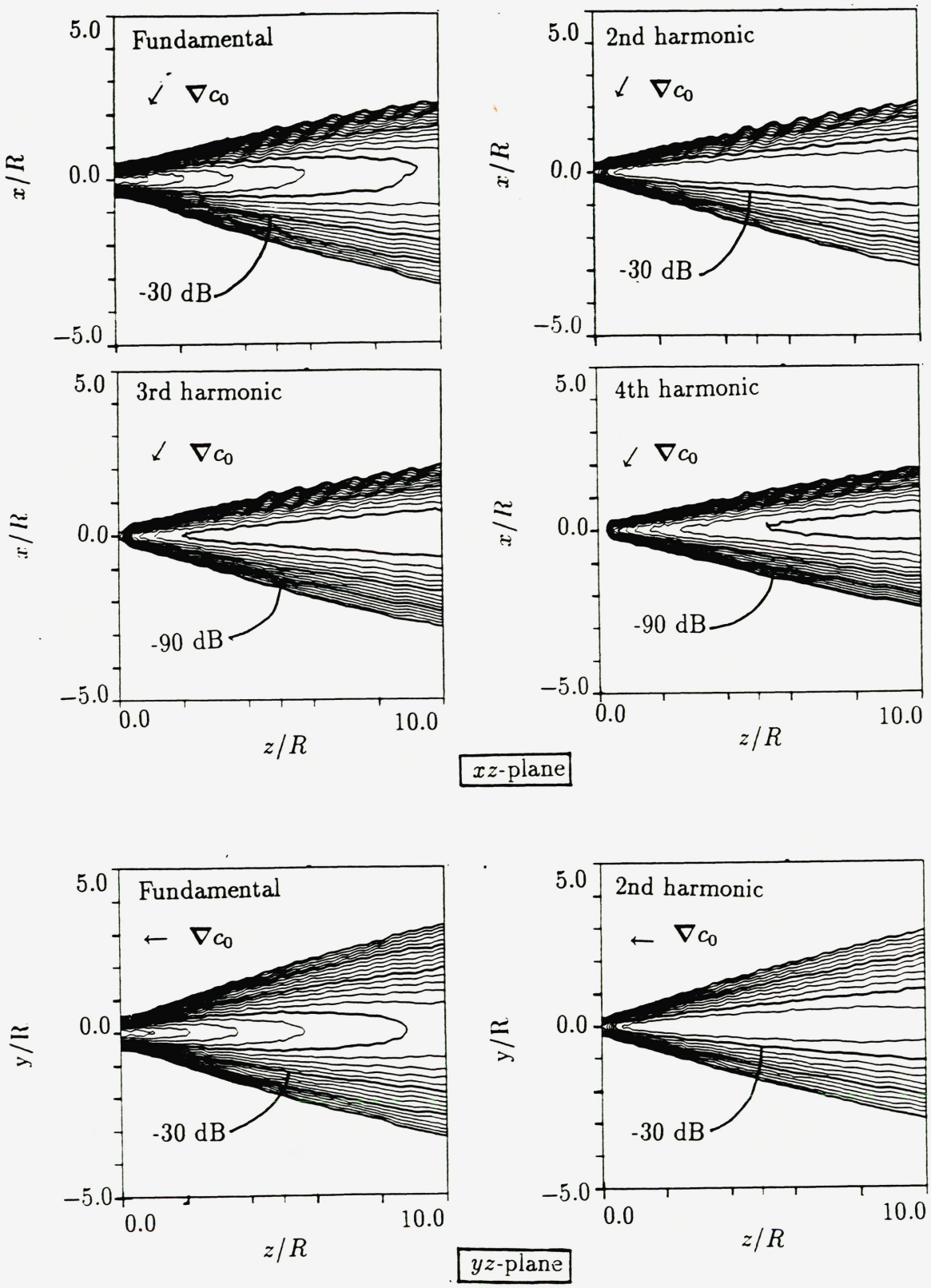

FIG. 5.9. Gaussian source, fully nonlinear case, $R/l_d = 0.25$, $R\bar{\alpha} = 0$. c_0 = Profile 2. $\theta = 75°$, $x_c = 0$. Fundamental: $\Delta dB = 3$, higher harmonics: $\Delta dB = 6$.

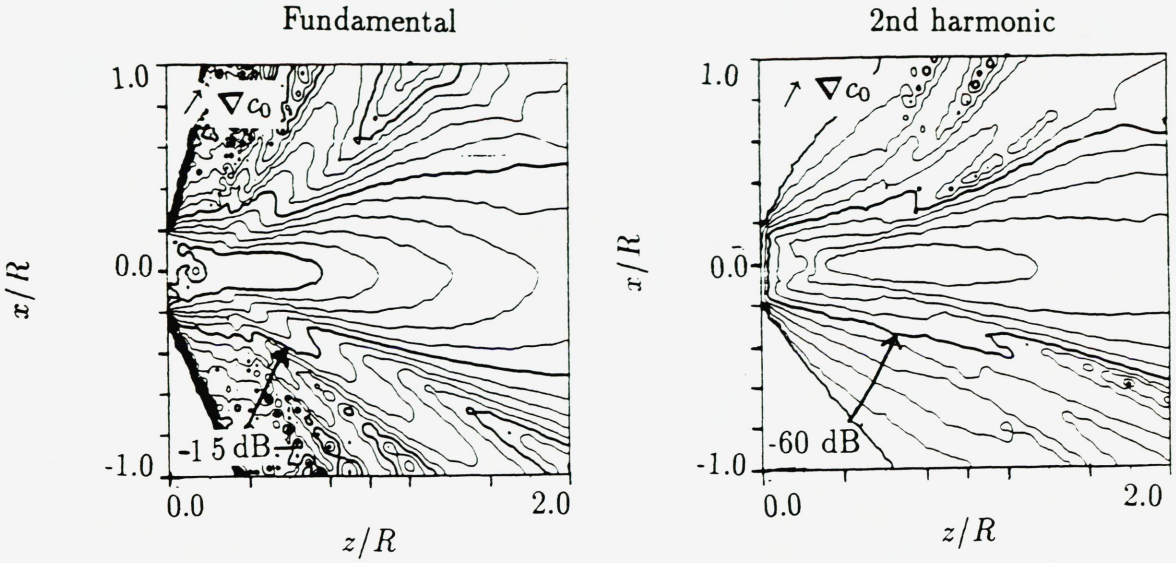

FIG. 5.10. Uniform source, quasilinear case, $R/l_d = 0.05$, $R\bar{\alpha} = 0$. c_0 = Profile 1, $\theta = 75°$, $x_c = 0$. Fundamental: $\Delta dB = 3$, second harmonic: $\Delta dB = 6$.

inhomogeneity. This may be explained by considering each harmonic component individually as a beam with increasing frequency and fixed source radius. In the linear case, it was shown that for increasing ka with a fixed source radius, the beam was more affected by longitudinal inhomogeneity, and less affected by transverse inhomogeneity. This trend is also followed by the second harmonic component, as illustrated by comparison of Figs. 5.1 and 5.10.

In the yz-plane, c_0 is independent of transverse variable, but still the various harmonic components are influenced by inhomogeneity. The amplitudes of the second harmonics along the z-axis differ in the xz- and yz-planes in Fig. 5.1, even though c_0 is independent of longitudinal variable. This behavior is a result of the asymmetry of $(p^{(1)})^2$, due to inhomogeneity. [In the linear case: If ∇c_0 only has a transverse component in the xz-plane and $x_c = 0$, the behavior of the beam in the yz-plane is independent of c_0.]

In Fig. 5.11 the fundamental and the second harmonic components obtained from fully nonlinear computations are compared in the yz-plane, for Profiles 1, 2, 11 ($\theta = 90°$). These curves can be compared with the homogeneous case, Fig. 5.5. The fundamental appears to be practically unaffected by inhomogeneity, while for increasing harmonic number, the amplitudes depart more and more from the homogeneous amplitudes; this occurs around the z-axis. For the profiles 2 and 11 (c_0 decreases in transverse direction), the amplitude values of the higher harmonics are higher than in the homogeneous case, while for profile 1 (c_0 increases in transverse direction), the amplitude values of the higher harmonics are lower than in the homogeneous

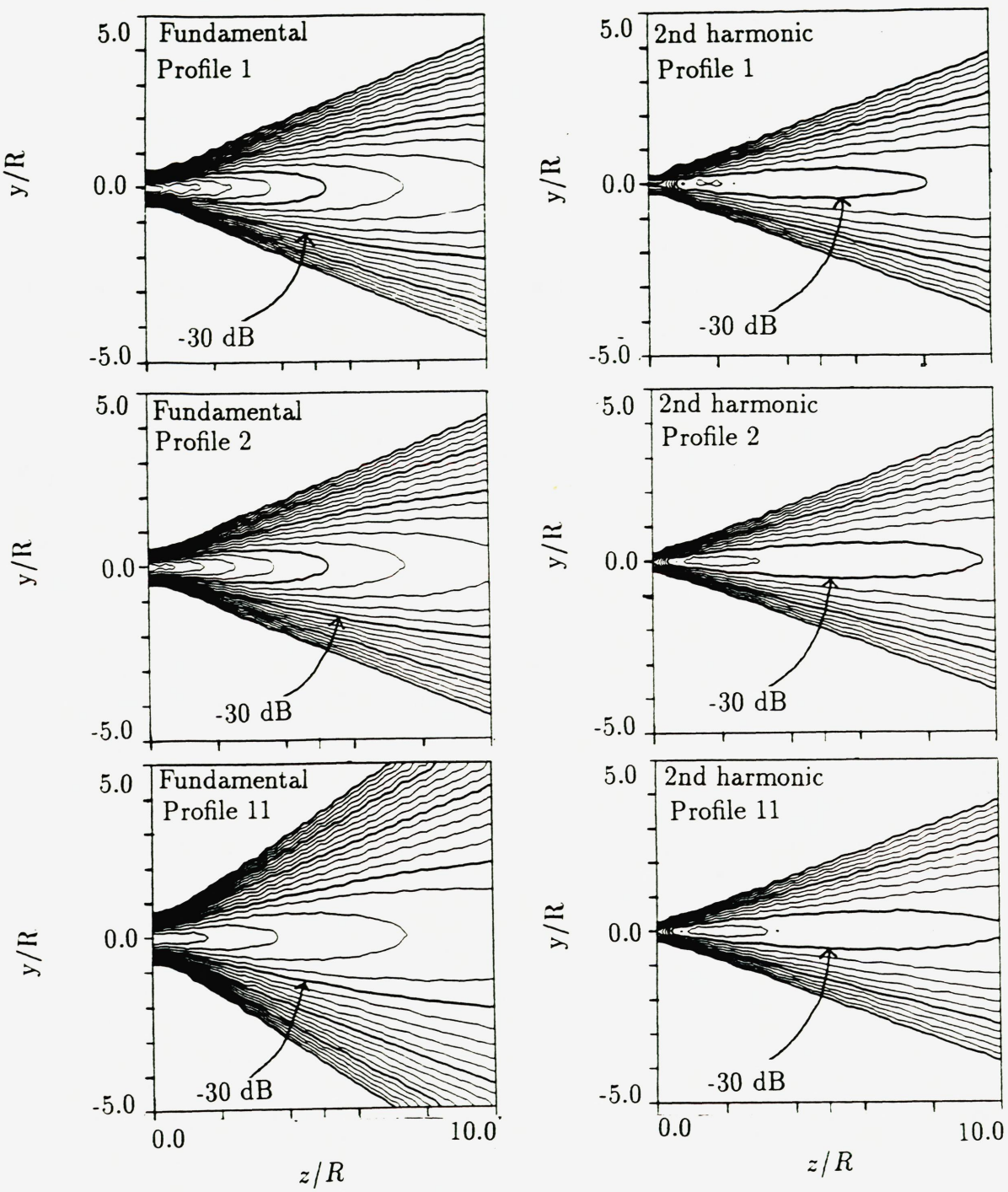

FIG. 5.11. Gaussian source, fully nonlinear case, $R/l_d = 0.25$, $R\bar{\alpha} = 0$. Amplitude in the yz-plane, where there is no transverse component of ∇c_0. $\theta = 90°$, $x_c = 0$. Fundamental: $\Delta dB = 3$, higher harmonics: $\Delta dB = 6$.

case. However: c_0 is independent of longitudinal variable! This behaviour may be explained by considering the truncated Eqs. (3.9) ($n_{max} = 8$): The nonlinear terms in the equations for a_n and b_n depend on all other harmonics except harmonic number n. Hence the source term for the fundamental depends on the higher harmonics, while the nonlinear source term for the higher harmonics contains the fundamental. We have seen that in the xz–plane, the higher harmonic components are less influenced by a transverse ∇c_0 than the fundamental component is. Hence the nonlinear source term for the fundamental is less asymmetric than the nonlinear source term for the higher harmonics, due to less influence of inohomogeneity. Accordingly, for increasing harmonic number, the inhomogeneity effects will be more pronounced in the yz-plane. [Accounting for more than 8 harmonics in the computations could modify these conclusions. However, we believe that computations with higher number of harmonics would not change significantly the first four harmonics.]

The comparison of the harmonic components in the xz- and yz-planes gives an indication of the relative influence of inhomogeneity on nonlinearity due to: (1) the curved coordinates, and (2) the varying $\mathcal{P}_{nonl}$. [In the plane along the z–axis and orthogonal to $\nabla_\perp c_0$, σ is independent of transverse variable. Hence, in this plane, the effect of the transform $\sigma(z, \mathbf{x}_\perp) = \sigma(z, 0)$ is a stretching/compression of the longitudinal axis.] Apparently, the bending of the harmonics and the variation of $\mathcal{P}^*_{nonl}$ in the xz-plane have strongest effect on the individual harmonics around the z-axis in the yz-plane. From this observation one may draw the conclusions: (1) Bending in the xz-plane is mainly caused by the coordinate transform. (2) The varying nonlinearity parameter has most effect close to the σ-axis, both in the xz-plane and in the yz-plane, and the effect is more pronounced for increasing harmonic number.

In the quasilinear model, the fundamental is identical to the fundamental in the linear model. This is not the case in the fully nonlinear model. There will be nonlinear attenuation of the fundamental due to build up of higher harmonic components. This effect is strongest in the regions of decreasing c_0. Thus the fundamental component will be less bent than the linear sound beam. This is confirmed by a comparison of Figs. 4.4 and 5.9. Investigating the contour lines for $-30dB$ at $z/R = 10.0$, we find that the corresponding value of x/R is 1.74 in the linear case and 1.58 in the nonlinear case, even though $AL_H = 0.5$ in the linear case and 1.0 in the nonlinear case. Hence the linear beam is more bent towards the direction of decreasing c_0 ($\theta = 75°$) than the fundamental component is.

In the dissipative case, results obtained by fully nonlinear calculations are presented in Fig. 5.12. The fixed reference absorption length is $10R$ for the fundamental, and sound speed profile 2 is considered with $x_c = 0$ and $\theta = 90°$. The bending of the various harmonic components has a different character. The bending of the harmonic components in the direction of decreasing c_0 (i.e., increasing x) is less pronounced than in the nondissipative case on Fig. 5.7. The asymmetric deformation

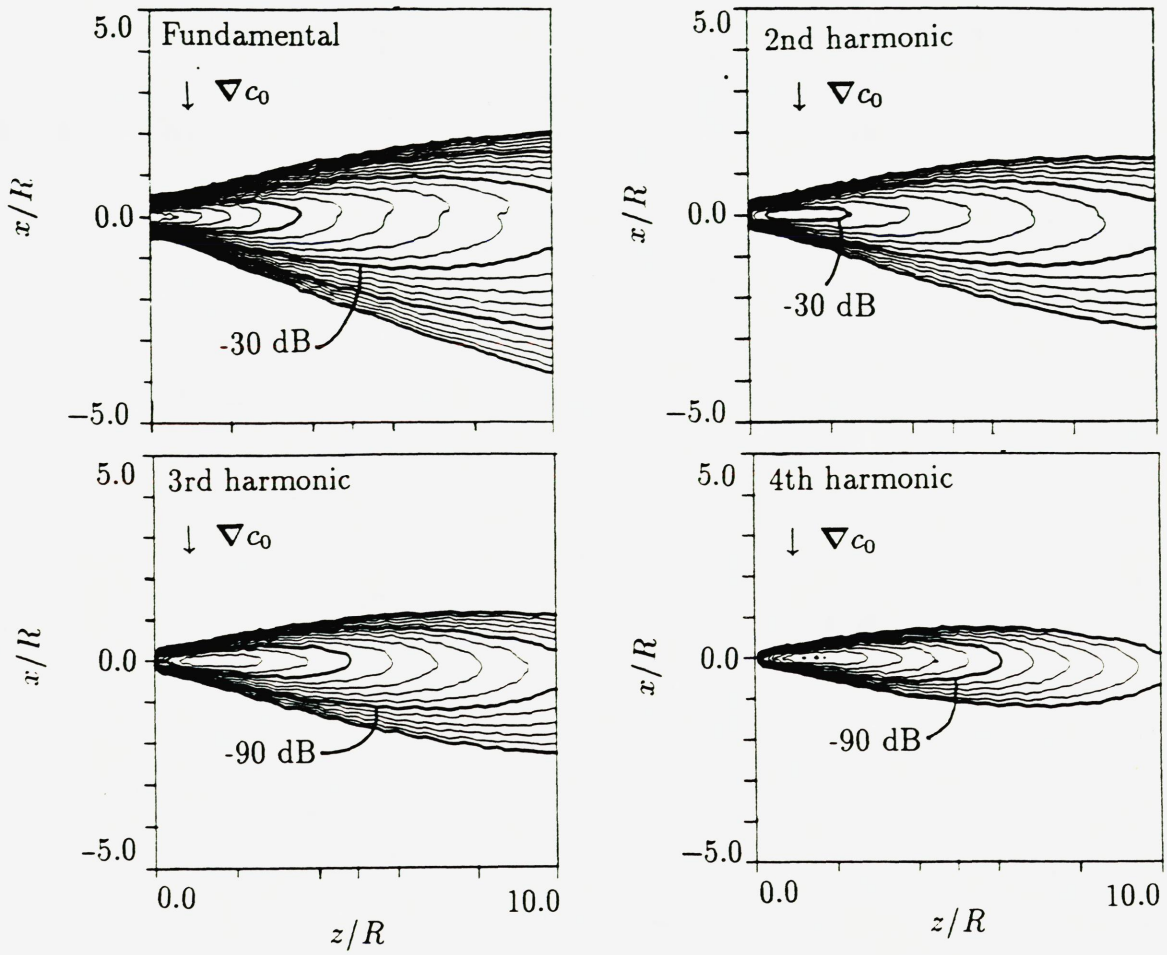

FIG. 5.12. Gaussian source, fully nonlinear case, $R/l_d = 0.25$, $R\bar{\alpha} = 0.1$. c_0 = Profile 2, $\theta = 90°$, $x_c = 0$. Fundamental: $\Delta dB = 3$, higher harmonics: $\Delta dB = 6$.

of the beam is most expressed for the fundamental. For the higher harmonic components, the bending decreases as the harmonic number increases. Comparison with Fig. 5.7 shows that the bending is also much weaker than for the case of the nondissipative medium. To explain this result, it is important to note the following: (1) Since higher harmonic components have a larger effective absorption coefficient and a smaller wavelength, the effect of a transverse gradient is relatively less important and the absorption is mainly felt in the z direction. (2) In a thermoviscous fluid the absorption coefficient is a decreasing function of c_0. Thus the damping is least in regions where c_0 is larger.

Generally, the sound beam tends to avoid the regions of space where the sound speed and absorption are larger. A similar behavior (for the linear case) was found in Ref. (27) for the case of a sound beam propagating through the interface between two homogeneous fluid layers. Thus, it is in qualitative agreement with a generalized form of Fermat's principle that accounts for the effects of absorption.

When $\mathcal{P}^*_{nonl}$ varies in space, the effective shock formation distance varies, and it is difficult to predict where the main contributions to the density of the virtual sources would come from. Also, for varying $\mathcal{P}^*_{abs}$, the effective absorption distance will vary in space. Asymptotic results derived within a quasilinear model valid in a homogeneous medium depend on an analytical solution for the linear case and on the fact that $\mathcal{P}^*_{nonl}$ and $\mathcal{P}^*_{abs}$ are constants[23,24,25]. The error function E_1 appears in an integral for the second harmonic; this integral can be evaluated asymptotically for special cases. In the case of an inhomogeneous medium, the corresponding integral (derived as in Refs. 23,24) for the second harmonic will not be of this specific form, hence asymptotic results for the homogeneous case cannot easily be applied. However, we will not proceed this discussion.

Chapter 6

Discussion of other models

In this chapter, various models to describe acoustic propagation in inhomogeneous media will be reviewed in relation to our own model. Existing models can be classified in two groups: (1) models related to ray theory, and (2) models related to parabolic approximation. Since our own model contains both of these elements, examples from both groups are considered. The assumptions in the various models are discussed.

6.1. Models related to ray theory

In classical ray theory, wavefronts ar defined, along which the field is approximately constant:

$$p - p_0 = p' \exp(-i\tau), \qquad \tau = t - \phi(\mathrm{x}), \tag{6.1}$$

where p' = acoustic amplitude and $\phi(\mathrm{x})$ = const. is the wavefront (t = time variable). A basic assumption is that locally the wavefront can be approximated by a plane which in a coordinate system moving along with the medium, propagates with the local value of the speed of sound. Thus, diffraction and dissipation effects are neglected.

The governing equations in linear ray theory[29,30] are the eikonal equation for variations in phase and the transport equation for variation in amplitude along a ray:

$$|\nabla\phi|^2 = \frac{1}{c_0^2}, \qquad \frac{\partial p'}{\partial l} + \frac{\rho_0 c_0}{2A}\frac{\partial}{\partial l}\left(\frac{A}{\rho_0 c_0}\right) p' = 0. \tag{6.2}$$

Equations (6.2) can be derived by WKB-approximation of the linear wave equation. Here, A is the area of the cross section of a ray tube and l is the curve length parameter along a ray, c_0 is unperturbed soundspeed. The transport equation can be integrated to give energy conservation in a ray tube. Since variations transverse to each ray are neglected, the solution breaks down in regions where $A = 0$, i.e., rays intersect and caustics occur.

Nonlinear ray theory[32,33] is derived from the nonlinear wave equation which results from the hydrodynamic equations, discarding dissipation and vorticity, and neglecting diffraction. There are two scales along the ray: the fast variable is $\tau = t - \phi$, where ϕ is the eikonal and the slow variable is the curvelength of a ray, l. The eikonal equation is solved exactly, by integrating along a ray. Hence:

$$\phi = \int_0^l \frac{dl}{c_0(l)}, \qquad \frac{\partial p'}{\partial l} + \frac{\rho_0 c_0}{2A}\frac{\partial}{\partial l}\left(\frac{A}{\rho_0 c_0}\right)p' - \frac{\beta}{\rho_0 c_0^3}p'\frac{\partial p'}{\partial \tau} = 0, \tag{6.3}$$

where β is the the nonlinearity parameter in the medium. By transforming dependent and independent variables, Burgers equation results, as in Refs. (32,33). The implicit solution is obtained as:

$$P' = P_m F\left(w\tau + \frac{zP'}{R_* P_m}\right), \tag{6.4}$$

where R_* is the shock formation distance for a plane wave with amplitude P_m. Since diffraction is neglected, this solution becomes multivalued for $z \geq R_*$. Also, caustics appear for the same reason as in linear ray theory. Nonlinearity is sometimes included already in the eikonal equation, by integrating the local soundspeed instead of the unperturbed value[34,35,36,37]. However, the caustics are a mathematical singularity that occur as long as diffraction is neglected in the problem formulation and are thus not avoided by including the pressure amplitude in the eikonal equation. [Also, cf. the discussion in Sec. 2.4, where we derive a generalized Burgers equation by choosing the order of the diffraction number as $N = O(\epsilon)$.]

Following are some models that are based on ray theory, but including diffraction more or less heuristically. They all have in common that the caustics problem is avoided.

In Ref. (38) a nonlinear equation accounting for diffraction is derived for the longitudinal velocity perturbation w in an inhomogeneous, nondissipative medium. Third and higher order terms in the Mach number ϵ are neglected. Stretched coordinates along a specific ray are introduced: ρ', p', $w = f(\epsilon l, \epsilon^{1/2} n, \tau)$, where n is the variable transverse to this ray and l is the longitudinal variable. The transverse velocity is said to be of $O(\epsilon^{3/2})$, consistent with scaling of transverse independent variable. A parabolic equation is obtained:

$$\frac{\partial}{\partial \tau}\left(\frac{\partial w}{\partial l} - \frac{w}{c_0^2}\frac{\partial w}{\partial \tau} + \frac{w}{2c_0}\frac{\partial c_0}{\partial l}\right) = \frac{1}{2}\frac{\partial^2 (c_0 w)}{\partial n^2}. \tag{6.5}$$

The right hand side of Eq. (6.5) is:

$$\frac{w}{2}\frac{\partial^2 c_0}{\partial n^2} + \frac{\partial c_0}{\partial n}\frac{\partial w}{\partial n} + \frac{c_0}{2}\frac{\partial^2 w}{\partial n^2}, \tag{6.6}$$

and the left hand side:

$$\frac{\partial^2 w}{\partial \tau \partial l} - \frac{\partial}{\partial \tau}\left(w\frac{\partial w}{\partial \tau}\right)\frac{1}{c_0^2} - w\frac{\partial w}{\partial \tau}\frac{\partial}{\partial \tau}\left(\frac{1}{c_0^2}\right) + \left(\frac{\partial w}{\partial \tau}\right)\frac{1}{2c_0}\frac{\partial c_0}{\partial l} + \frac{w}{2}\frac{\partial}{\partial \tau}\left(\frac{1}{c_0}\frac{\partial c_0}{\partial l}\right). \tag{6.7}$$

Equation (6.5) can be compared to Eq. (2.54), for a nondissipative fluid. Equation (6.5) contains derivatives of c_0 with respect to τ, n and l, i.e., over all the different scales, while Eq. (2.54) only contains derivatives of c_0 with respect to the slow longitudinal variable ϕ_1. Equation (2.54) contains terms resulting from presence of external force and variations of ρ_0; there are no such terms in Eq. (6.5). However, for a homogeneous fluid, both equations reduce to the KZ equation.

For consistence, all terms in Eq. (6.5) should be of the same order, i.e., $O(\epsilon^2)$ (since $w = O(\epsilon)$). Thus: $\partial c_0/\partial \tau = O(1)$, $\partial c_0/\partial n = O(\epsilon^{1/2})$ while $\partial c_0/\partial l = O(\epsilon)$. In the derivation of Eq. (2.54), the ordering of inhomogeneity implied that to leading order, $\nabla \times \mathbf{v}$ could be neglected and the linear impedance relation applied. In the derivation of Eq. (6.5), scaling of transverse velocity indicates that $\nabla \times \mathbf{v}$ has been neglected to $O(\epsilon)$. However, according to the vorticity equation, Eq. (2.12), the scaling of inhomogeneity in this model implies that $\nabla \times \mathbf{v}$ is generated. Hence, Eq. (6.5) may not be consistent. Finally, as in classical ray theory, the eikonal equation is solved exactly. But the beam axis is defined to be a ray, whose behavior depends on how the medium varies. Assuming a specific inhomogeneity with respect to the ray coordinates before the eikonal equation is solved represents a circle argument.

Equation (6.5) for w is solved by transforming it over to a Burgers type equation with diffraction and seeking an implicit solution on the form

$$P = P(\Theta), \qquad \Theta = \Theta(n, \tau, P), \tag{6.8}$$

which can be interpreted as a "simple wave" with diffraction included. The solution is found as in Ref. (4) for confined beams in homogeneous media.

Gaussian beam approximation (GBA) is another method to describe acoustics in inhomogeneous media. This approach is also based on ray theory, but the eikonal equation is treated differently. Orthogonal curvilinear coordinates are defined along one specific ray with a given starting point and direction from the source. Here l is the curvelength along the ray, and n is the transverse variable. The eikonal equation is only satisfied on the l–axis, and Taylor expanded in n.

In linear GBA[40,41,42,43], the acoustic field and boundary conditions are superpositions of Gaussian beams. In nonlinear GBA[44], only one Gaussian beam is considered, i.e., central ray theory. However, in both cases some discrepancy exists about which equation of state to use for an inhomogeneous medium: for some models ρ_0 is constant and c_0 varies, while in others both vary. If thermodynamic relations are to be used consistently, the last version must be chosen [cf. the discussion in Sect. 2.1].

In the linear model, the solution for p' is assumed to be:

$$p'(l, n, t) = exp(-i\omega\tau)U(l, n, \omega) \tag{6.9}$$

where $\tau = t - \int_{l_0}^{l} c_0^{-1}(l', 0)\, dl'$. Nondimensional, stretched coordinates are introduced by defining $\nu = \omega^{1/2} n$, so that three different scales are present: fast variable $\omega\tau$,

slow longitudinal variable l and transverse variable $\omega^{1/2}n$. ω can be interpreted as a nondimensional frequency proportional to a nondimensional wavenumber. Characteristic lengths for variation of ρ_0, c_0 can be related to ω^{-1}. Asymptotic expansions are made for the limit $\omega \to \infty$ (as for classical ray theory), terms of $O(\omega^r), r \geq 1$ are kept in the final equation. Accordingly:

$$\frac{2i}{c_0(l,0)}\frac{\partial U}{\partial l} + \frac{\partial^2 U}{\partial \nu^2} - \left(\frac{i}{c_0^2(l,0)}\frac{\partial c_0}{\partial l} + \frac{i}{\rho_0 c_0}\frac{\partial \rho_0}{\partial l} + \frac{c_{0,nn}\nu^2}{c_0^3}\right) U = 0. \tag{6.10}$$

All the coefficients are evaluated on the central ray, and the last term in paranthesis follows from an expansion of the eikonal equation around the central ray:

$$\omega^2\left(\frac{1}{c_0^2(l,n)} - \frac{1}{h^2 c_0^2(l,0)}\right) h \simeq -\frac{1}{c_0^3(l,0)}\frac{\partial^2 c_0}{\partial n^2}(l,0)\omega\nu^2, \quad h = 1 + \frac{\partial c_0(l,0)}{\partial n}\frac{n}{c_0(l,0)}. \tag{6.11}$$

A scaling factor $(\rho_0(l,0), c_0(l,0))^{-1/2}$ can be introduced to get the equation in a more familiar form of the parabolic equation.

Solution is sought as

$$W(l,\nu) = (\rho_0(l,0), c_0(l,0))^{-1/2} U(l,\nu) = A(l) exp\left[\frac{i}{2}\nu^2\Gamma(l)\right] \tag{6.12}$$

Equation (6.12) inserted in Eq. (6.10) yields a Riccati equation for $\Gamma(l)$ and an equation for $A(l)$. A first order linear system[43] is constructed, its solution is easily computed numerically. Γ is interpreted as a sum of beamwidth of the specific Gaussian beam and curvature of the wavefront.

Reference (42) gives an example of application of the model to an underwater acoustics problem with a point source in water, and with boundary conditions in the pressure perturbation given at the ocean surface and bottom, i.e., an ocean waveguide. (Usually the ocean waveguide is defined through pressure release surface and rigid bottom, although this is not specified in Ref. (42)). The results are compared with the solution of the same problem formulated in classical ray theory. In the ray model, caustics are created due to intersection of rays reflected from the water surface (the rays emitted from a point source have different launching angles). The caustics picture depends on the functional expression for the sound speed profile. In the GBA the caustics are avoided due to the selection of central rays, the spacing between them and the amplitude shading across each ray. When comparing with a normal mode solution for the same problem, the results of GBA are excellent. Apparently the GBA is an improvement of classical ray theory for describing the field excited from a point source in an ocean waveguide with varying soundspeed: The mathematical singularities in the solution of the eikonal equation are removed, and the method compares better with normal mode theory than ray theory does. The method is applicable to studying long range propagation of acoustic signals emmited

from a relatively small omnidirectional source. Due to the construction of GBA, one can also expect that caustics will neither occur in the solution in an unbounded environment, where certain soundspeed profiles (for instance, profiles that create sound channels) otherwise guarantee caustics in the solution of the ray tracing equations. A beam in an unbounded medium could be simulated by choosing a Gaussian amplitude shading and only consider one central ray from a given point. However, it is questionable whether the inhomogeneity transverse to the ray is treated consistently, as will be illustrated in the discussion of nonlinear GBA. So far, there do not appear to be any numerical simulations of a beam emitted from a real source, according to GBA.

In the nonlinear model, stretched coordinates are introduced along a central ray:

$$\frac{\partial}{\partial s}\left[\frac{\partial p'}{\partial l}+\frac{\beta}{\rho_0 c_0^3}p'\frac{\partial p'}{\partial s}\right]+\frac{c_0}{2}\nabla_\perp^2 p'+\frac{1}{2c_0^2}\frac{\partial^2 c_0(l,0)}{\partial n^2}n^2\frac{\partial^2 p'}{\partial s^2}=0. \tag{6.13}$$

For Eq. (6.13) to be consistent, all the terms must be of $O(\epsilon^2)$. This implies that there must exist a relation between the Mach number ϵ and the different characteristic lengths determined by the nondimensional frequency ω:

$$\frac{\partial p'}{\partial l}=O(\epsilon\omega^{-1}),\quad p'\frac{\partial p'}{\partial s}=O(\epsilon^2),\quad \nabla_\perp^2 p'=O(\epsilon\omega^{-1}),\quad \frac{\partial^2 c_0}{\partial n^2}n^2\frac{\partial^2 p'}{\partial s^2}=O(\epsilon^2). \tag{6.14}$$

The scale for longitudinal, slow variation in p' is ϵ, while the transverse scale for p' is $\epsilon^{1/2}$. Accordingly, scale for transverse variation of c_0 must be $\epsilon^{1/2}$. Variations in c_0 with respect to l is not accounted for, so the first order derivatives of c_0 must be of higher order than $O(\epsilon)$. However, in linear GBA longitudinal inhomogeneity is included through a factor $(\rho_0(l,0),c_0(l,0))^{-1/2}$. If this also can be applied to the nonlinear theory, it is another indication that the scale for l-variations in c_0,ρ_0 is of $O(\epsilon)$ or higher. The ordering of transverse variations in c_0 (hence ρ_0) implies that it is not correct to neglect $\nabla\times\mathrm{v}$ and apply the acoustic impedance relation along the central ray. [Apparently, this has been done here, since the second order nonlinear PDE Eq. (6.13) only contains one dependent acoustic variable.]

When curvature of the wavefronts happens on a shorter scale than the wavelength scale, caustics result from the solution of the eikonal equation and the rays intersect. In that case, the field can be described through boundary layer approaches inspired by Ludwig's method[47,48] and the solution is matched to the solution valid outside the caustics region. This can also be used in inhomogeneous media[49].

In caustics areas the eikonal ϕ decomposes into

$$\phi(\mathrm{x},\beta)=\theta+\rho\xi-\frac{\xi^3}{3}, \tag{6.15}$$

where ξ is some parameter, $\partial\xi/\partial\beta\neq 0$. From the eikonal equation:

$$\begin{aligned}|\nabla\theta|^2+\rho|\nabla\rho|^2-1&=0,\\ 2\nabla\theta\cdot\nabla\rho&=0.\end{aligned} \tag{6.16}$$

The eikonal yields a progressive and a regressive phase, $\phi^{\pm} = \theta \pm \frac{2}{3}\rho^{3/2}$. The field can no longer be decomposed into progressive and regressive simple waves. θ is interpreted as a variable along the caustics, and ρ a variable transverse to the caustics. In 2 dimensions, this method implies having an orthogonal curvilinear coordinate system along a caustics surface using the "thickness" of the caustics zone as a characteristic length. Hence, an inner solution to the Helmholtz equation is obtained and it is matched asymptotically with the "ordinary" outer solution, where characteristic length on the fast scale is the wavelength.

Accordingly, in Ref. (49) a method for solving a first order hyperbolic system of nonlinear equations that describe physical conservation laws, is constructed. Expansion parameters are: nondimensional amplitudes of the signal far from and near caustics, and ratio between the signal's wavelength and distance the signal has to propagate from the source untill caustics occur. However: scaling of diffraction effects and of inhomogeneity effects is not specified explicitly.

The system of equations is solved by the method of asymptotic matching. Away from caustics, to leading order the eikonal equation is the characteristic equation for the system. The amplitude satisfies a transport equation with diffraction included, both for the linear and the nonlinear case. In the caustics zone the Tricomi equation is derived:

$$\Psi_{\rho\rho} + (M_0\Psi_\theta - \rho)\Psi_{\theta\theta} = 0 \tag{6.17}$$

where Ψ is a functional expression for the amplitude of the signal, θ is a variable along the caustics, ρ is a variable transverse to the caustics and M_0 is a fuction that treats the nonlinearity of the system. Equation (6.17) is hyperbolic for $\rho > M_0\Psi_\theta$ (illuminated zone) and elliptic for $\rho < M_0\Psi_\theta$ (shadow zone). In Ref.(50) it is shown that the KZK equation for the pressure amplitude can be derived by a similar method.

The main reason that ray theory breaks down, is that diffraction is neglected, hence the amplitude is not described correctly. Also, the eikonal equation is solved exactly. Caustics are unphysical and a result of inconsistent modeling. The previous models illustrate how ray theory can be "fixed" to avoid the caustics problem, but still the model can be inconsistent. Accounting for diffraction and inhomogeneity on suitable scales and accordingly simplifying the solution of the eikonal equation, the caustics singularity can be avoided in the problem formulation.

6.2. Parabolic approximation in underwater acoustics.

It is natural to consider the ocean to be an inhomogeneous medium. The usual physical situations studied in underwater acoustic are characterized by long range propagation compared to the ocean depth. The distances the signal propagates over are so large that the source dimension is approximately zero. Often the source is omnidirectional (line or point source). The ocean is modeled as a wave guide with

boundary conditions in the acoustic variables at the water surface and at the bottom: for instance pressure release surface and rigid or penetrable bottom.

6.2.1. Tappert's parabolic equation.

F. Tappert[51] derived a now classical parabolic model for linear underwater acoustics, postulating that, to leading order, all significant low frequencies acoustic waves in the ocean propagate primarily in the horizontal direction, away from the source. He starts from the Helmholtz equation with varying wavenumber, r is horizontal variable, z is vertical variable, ϕ is asimuthal angle and p is pressure perturbation, and defines:

$$p(z,r,\phi) = \psi(z,r,\phi)H_0^{(1)}(k_0 r), \tag{6.18}$$

where $k_0 = \omega/C_0$ and C_0 a constant reference sound speed. $|k_0 r| \gg 1$ and $\partial^2\psi/\partial r^2 \ll 2ik_0\partial\psi/\partial r$ gives:

$$\frac{\partial^2\psi}{\partial z^2} + \frac{1}{r^2}\frac{\partial^2\psi}{\partial\phi^2} + 2ik_0\frac{\partial\psi}{\partial r}(1 + O((k_0 r)^{-2})) + K_0^2\psi = 0, \tag{6.19}$$

where

$$K_0^2 = k_0^2[n^2(z,r,\phi) - 1 + i\nu(z,r,\phi)]. \tag{6.20}$$

$n(z,r,\phi) = C_0/c_0$ is index of refraction, c_0 a varying soundspeed and ν is the imaginary part of the wavenumber, accounting for dissipation. r_0 is characteristic length for horizontal variations while a is characteristic length for vertical variations (for instance defined by the depth of a sound channel).

The term $H_0^{(1)}(k_0 r)$ follows from assuming axisymmetry on the characteristic length k_0^{-1} with respect to a vertical line, and outgoing waves from the source. Directionality is accounted for by variations in the asimuthal angle ϕ. The assumption $|k_0 r| \gg 1$ implies that the field is studied in the farfield of the source. For all the terms in Eq. (6.19) to be of same order, $r_0 \sim k_0 a^2$ and $a^{-2} \sim k_0^2(n^2 - 1)$. The sound propagates close to the horizontal plane containing the source, according to the physical situations studied in underwater acoustics. Hence horizontal characteristic length $r_0 \gg$ vertical characteristic length a. The boundary conditions for p at the ocean surface and bottom provide boundary conditions for ψ. Equation (6.18) is best suited for the case of a vertical line source. Thus: this model cannot easily be generalized to other geometries and source configurations.

Even though the index of refraction is varying, the medium is assumed to be locally homogeneous. For an inhomogeneous medium Tappert starts from

$$\rho_0\nabla\cdot\left(\rho_0^{-1}\nabla p\right) + \frac{\omega^2}{c_0^2}p = 0, \tag{6.21}$$

with ρ_0 varying. By defining $q = \sqrt{p/\rho_0}$:

$$\nabla^2 q + k_0^2 n^2 q = 0, \qquad n^2 = \frac{C_0^2}{c_0^2} + \frac{1}{2k_0^2}\left[\frac{\nabla^2\rho_0}{\rho_0} - \frac{3}{2}(\frac{\nabla\rho_0}{\rho_0})^2\right]. \tag{6.22}$$

This is just a special case of the Helmholtz equation with varying index of refraction. However, variations in the speed of sound imply variations in the ambient density, as a consequence of the nondissipative equation of state. Thus the last version of the model should be prefered, according to the thermodynamics.

Transverse inhomogeneity scale is not explicitely specified. However, by considering the order of each of the terms in Eq. (6.19), one can see that the only possibility is $|\nabla c_0|/c_0 = O((k_0 r_0)^{-1})$ at most. Thus characteristic length for inhomogeneity must be of the order of characteristic length for slow variation in horizontal direction, r_0. Then no vorticity is generated linearly. This implies that $\nabla \times \mathrm{v}$ can be neglected within consistency, and the linear impedance relation can be applied horizontally. Hence transverse velocity is of higher order than pressure amplitude and longitudinal velocity. The boundary condition at the ocean bottom is given in terms of $\nabla p \cdot \mathbf{n}$, $\mathbf{n}$ is a unit vector normal to the bottom. This condition is related to the vertical velocity component through the linearized equation of motion, and should be satisfied to leading order. However, the question whether the imposed boundary conditions at the ocean bottom are consistent with the parabolic approximation, is little discussed in underwater acoustics.

Tappert's parabolic approximation is motivated by the use of the method of normal mode decomposition. To avoid coupling of modes, he assumes that inhomogeneity is strongest in vertical direction. The leading order wavefront behavior of the monochromatic field is described through the fast variables $t - r$ and $t + r$ in order to reduce the $\partial^2/\partial t^2$ operator in the linear wave equation, and not explicitly connected to the eikonal. The parabolic approximation is thus not along a beam axis determined from the structure in the medium (as in our model), but is postulated in a specific direction. This implies that a Sommerfeld radiation condition cannot be formulated in the horizontal direction – backscattering and reverberation has to be accounted for, through the term $K_0^2\psi$ in Eq. (6.19). How much this term varies with horizontal and vertical variables is crucial for whether the progressive and regressive components of the field can be separated. It takes into account the real curvature of a beam axis induced by inhomogeneity in transverse direction.

There exist normal mode models for sound propagation in waveguides with constant water depth, where the soundspeed varies only with respect to vertical variable. The governing equation is then Eq. (6.22) combined with Eq. (6.18) for each of the wavenumber components[52]. This is a separable situation. For the case of a point source and in the farfield for each of the excited modes, analytical solutions can be achieved, and these can be compared to the parabolic approximation of the same problem definition. (For a real source in a homogeneous fluid, for instance located in

a vertical plane, the normal mode approach may be cumbersome, since the continuous spectrum cannot be neglected[53]. The vertically axisymmetric fundamental solution cannot be applied for this geometry.) Wide–angle versions[54] of the parabolic approximation are shown to compare quite well with the normal mode model for the point source case. These versions consist of different expansions of the operator $(1+L)^{1/2}$, where $L = n^2 - 1 + k_0^2\partial^2/\partial z^2$.

The parabolic approximation models in respectively underwater acoustics and for a beam generated by a real source in a semi–infinite medium, are thus fundamentally different. In the beam model the source configuration is a basis for the transverse scale, and the ratio of wavelength of the signal and source radius is the parameter that decides how good the approximation is compared to an elliptic or hyperbolic formulation. One–way propagation is studied, and vorticity is neglected – which implies that the beam axis is far away from parallel boundaries. Thus waveguide problems cannot immediately be formulated. As mentioned, in underwater acoustics, the model is valid for symmetry with respect to a vertical axis, at ranges $\gg$ the wavelength of the signal, and the expansion parameter accounting for validity compared to the Helmholtz equation, is the angle of propagation relative to the horizontal plane from the source. The transverse characteristic length is the depth of the channel.

To compare a beam model with a waveguide model, the boundary conditions must be comparable – which is not the case for a real, directive source in the beam model contra an omnidirectional (line or point) source in the underwater acoustics model. The beam model would have to be rederived to account for a waveguide problem, for instance by defining 2 transverse characteristic lengths: one defined through the source radius and one through the width of the waveguide. One may then expect that vorticity can no longer be neglected, due to the presence of boundaries parallel to the beam's start direction. Also, the source radius must approach zero, to simulate a point source. For the comparison of two models to be successful, it is important that they can be applied to the same physical situations.

It might be interesting to investigate the difference between Tappert's and our parabolic equations (for the linear, nondissipative case). Our equation expressed in the curvilinear coordinates (cf. Eq. (2.77)) has constant coefficients and no term similar to the term $K_0^2\psi$ in Eq. (6.19) (as a consequence of the weakly curved beam axis). Therefore Eq. (2.77) can be solved by for instance Fourier transform in the transverse variables. For comparison, a 2–dimensional problem must be considered in both models ($r \rightarrow$ horizontal cartesian variable). The $H_0^{(1)}(k_0 r)$–factor due to axisymmetry in Tapperts model must be replaced by a term that accounts for plane wave propagation in the positive horizontal direction. Boundary conditions must be specified on the source located at zero value of the horizontal coordinate. The resulting equation based on Tapperts model has varying coefficients, through the term $K_0^2\psi$, therefore integral transforms cannot easily be applied for arbitrary sound

speed profiles, and it is difficult to obtain analytical solutions.

6.2.2. More recent models.

McDonald and Kuperman, Ref. (55) have derived the Nonlinear Progressive Wave Equation (NPE) in order to describe nonlinear acoustics in inhomogeneous media. They use parabolic approximation in time domain, and describe inhomogeneities in all directions, as well as discontinuities in sound speed. An initial value problem is formulated, with applications to for instance explosion problems. A linear version is derived by Collins, Ref. (57,58,59), the Progressive Wave Equation (PWE). Also, Kriegsmann, Ref. (60) has derived a linear, frequency domain parabolic equation for inhomogeneous media, which is often refered to in underwater acoustics.

McDonald and Kuperman start from

$$\frac{\partial^2 \rho}{\partial t^2} = \nabla^2 p + \nabla\nabla : (\rho \mathrm{vv}). \tag{6.23}$$

The medium is assumed non-dissipative, and the equation of state chosen as $p = p(\rho)$. The correct is to assume p depending on 2 state variables, for instance $p = p(\rho, s)$. For non–dissipative media, $s = s_0(\mathrm{x})$ is the ambient value of the entropy, accounting for the inhomogeneous structure in the medium. Other possibilities are for instance $p = p(\rho, T)$, $p = p(s, T)$. The dependent variables are perturbed relative to a static state of equilibrium:

$$p = p_0 + p', \qquad \rho = \rho_0 + \rho', \qquad \mathrm{v} = 0 + \mathrm{v}, \tag{6.24}$$

where p_0, ρ_0 are constants, i.e., the medium appears to be homogeneous. The equation of state chosen here implies a contradiction: It is assumed that ambient density, ρ_0, is constant; but at the same time the soundspeed is varying as a consequence of inhomogeneity. This is impossible if the soundspeed is only a function of one variable of state, ρ.

A coordinate system moving with constant velocity c_0 is introduced, and stretched variables are defined:

$$\tau = x - c_0 t, \quad y_1 = \epsilon^{1/2} y, \quad z_1 = \epsilon^{1/2} z, \tag{6.25}$$

$$t_1 = \epsilon t, \quad c = c_0 + \epsilon c_1. \tag{6.26}$$

ϵ is here a "small" parameter. [Apparently, ϵ is of the order of the Mach number, although this is not specified in the paper. However, in the appendix, the authors argue that ϵ is also $O(\theta^2)$, where θ is the propagation angle of the signal.] It is unclear whether the authors consider inhomogeneity an effect connected to nonlinearity or a condition of the medium, since ρ_0 is constant. Neither is it clear why they choose this specific scaling of transverse variations and slow time – is the choice

for instance related to a characteristic source radius or to the width of a waveguide? The progressive retarded time indicates that the Sommerfeld radiation condition has been applied. The fast variation through the retarded time is postulated to be as a plane wave in the x-direction, independent of the sound speed gradient; this is not justified mathematically. Also, it is unclear why it is correct to introduce parabolic approximation in time domain when the medium is inhomogeneous. The equation of state is expanded to second order in $(\rho - \rho_0)$. c^2 is defined as $(\partial p/\partial \rho)$, without specifying whether this is evaluated at ambient or perturbed state.

The acoustic variables are expanded in asymptotic series with expansion parameter ϵ (ϵ must now be interpreted as the Mach number). These are inserted in the equations of continuity, momentum and state, and terms of equal order in ϵ are collected. The linear impedance relation is applied, and to $O(\epsilon^2)$ the authors arrive at:

$$\frac{\partial R}{\partial t_1} = -\frac{\partial}{\partial \tau}\left(c_1 R + \frac{\beta c_0}{2} R^2\right) - \frac{c_0}{2}\nabla^2_{\perp,1}\int_{\tau_f}^{\tau} R\, d\tau \tag{6.27}$$

where $R = \rho_1/\rho_0$, β = the nonlinearity parameter. Equation (6.27) is derived by considering ρ_0 to be constant (or $\nabla\rho_0/\rho_0$ of a higher order than ϵ), while c_1 varies on the short scale and is of $O(\epsilon)$ (this is the only possibility for all terms in Eq. (6.27) to be of the same order). This is inconsistent according to the equation of state: $p = p(\rho)$ implies $c = c(\rho_0)$, (with c evaluated with respect to the equilibrium state), but ρ_0 was assumed constant. Hence, Eq. (6.27) does not describe inhomogeneity in a proper way. Although, for homogeneous media, that is, $c_1 \equiv 0$, Eq. (6.27) is nothing else than the KZ equation in time domain integrated with respect to τ, if one makes sure the nonlinearity parameter is evaluated at the unperturbed state. Equation (6.27) has been applied to examples with an omnidirectional source in an ocean waveguide, including discontinuity in c_1[56]. According to the previous discussion, this is inconsistent, especially since discontinuity in c_1 would introduce a term in Eq. (6.27) that is infinitely large.

Collins starts from:

$$\rho\nabla\cdot\left(\frac{1}{\rho}\nabla p\right) = \frac{1}{c^2}\frac{\partial^2 p}{\partial t^2}, \tag{6.28}$$

where c, ρ are ambient values of soundspeed and density which depend on horizontal variable r and vertical variable z. A point source is considered. The expansion parameter is $\epsilon = \tan(\alpha_M)$, where α_M is maximum angle of propagation of the signal relative to a horizontal line. He assumes $|\partial\rho/\partial r| \ll |\partial\rho/\partial z|$ and $c = c_0 + O(\epsilon)$, where c_0 is constant, and $|\nabla c/c_0| = O(\epsilon)$ both horizontally and vertically. But these assumptions are inconsistent, since $c = c(\rho)$ implies ∇c parallel to $\nabla\rho$, which is not satisfied here. Following McDonald and Kuperman, he uses parabolic approximation

in time domain, and obtains:

$$\frac{\partial u}{\partial t} = \frac{c_0}{2}\int_s^\infty \left(\frac{\partial^2 u}{\partial z^2} - \frac{1}{\rho}\frac{\partial \rho}{\partial z}\frac{\partial u}{\partial z}\right) ds' + (c - c_0)\frac{\partial u}{\partial s}, \tag{6.29}$$

where $s = r - c_0 t$, $u(s,z,t) = p(s + c_0 t, z, t)$. Equation (6.29) is a linear version of Eq. (6.27), (except the right hand sides in the two equations have opposite sign, because of different limits of integration). Equation (6.29) is solved for boundary conditions given with respect to transverse variable: pressure release ocean surface and rigid bottom, as in other parabolic models in underwater acoustics.

To account for absorption, Collins defines an ad hoc dissipation term through a complex wavenumber depending linearly on frequency and $1/c$. This adds an integral term to Eq. (6.29). Even though the medium is considered inhomogeneous, thermodynamic relations are not specified when dissipative effects are included.

Kriegsmann derives a parabolic equation in frequency domain by starting from

$$\rho \nabla \cdot \left(\frac{1}{\rho}\nabla p\right) + k'^2 n^2 p = 0, \qquad k' = \frac{\omega}{c_0} \qquad n = \frac{c_0}{c}, \tag{6.30}$$

where ρ is a varying ambient density, c varying sound speed and c_0 a constant reference sound speed. He assumes an axisymmetric vertical line source, hard ocean bottom, pressure release surface, and the Sommerfelds radiation condition. Similarly as in Collins' model, nondimensional coordinates are introduced: $r = \epsilon k' r'$, $z = \epsilon^{1/2} k' z'$. $\epsilon = (H/R)^2$ with x', z' physical variables, where H is ocean depth and R is maximum horizontal range of interest. ϵ small indicates propagation near the horizontal. $|\nabla c/c_0| = O(\epsilon)$, but $\rho = \rho(r,z)$ and varies therefore on different scales horizontally and vertically. Since $c = c(\rho)$, this is an inconsistent description of the medium, for the same reason as in the previous model. Also, since inhomogeneity is stronger in transverse direction, vorticity may be generated, hence the boundary conditions in the waveguide may be complicated. This problem is not considered. The resulting equation is:

$$-2i\frac{\partial u}{\partial r} = \sqrt{\rho}\frac{\partial}{\partial z}\left[\frac{1}{\rho}\frac{\partial}{\partial z}(\sqrt{\rho}u)\right] + fu \tag{6.31}$$

where $n^2(x', y', z') = 1 + \epsilon f(r,z)$, $u = \sqrt{r/\rho}A$, A is the slowly varying amplitude of a progressive signal. The boundary conditions from the elliptic problem are transferred over to the parabolic equation. Kriegsmann claims that this equation can be applied to arbitrary on-source conditions and also to interface problems. However: only axisymmetric sources can be included in this formalism, and it is questionable whether the ordering process used to derive the parabolic equation is valid when the density gradient becomes very large.

To summarize, the weak points in the models reviewed in this section are: (i) c and ρ vary on different space scales, although the equation of state is given as $p = p(\rho)$ which implies $c = c(\rho)$. (ii) On the short scale, the sound pressure is considered as a progressive wave in horizontal direction (through the definition of retarded time in each model), without regard of the orientation of ∇c_0.

The weak points in our own model are: (i) Only weakly inhomogeneous media can be considered, i.e., discontinuities cannot be described consistently. (ii) The on–source boundary condition must have a high characteristic source radius to characteristic wavelength ratio. (iii) Only one–way sound propagation can be described, i.e., the inhomogeneous medium must be unbounded. However, in our model, the direction for parabolic approximation changes weakly due to the varying sound speed; contrary to the models discussed above.

Chapter 7

Summary and conclusion

We have derived a governing parabolic partial differential equation to describe the nonlinear propagation of a sound beam in an inhomogeneous, thermo-viscous fluid, Eq. (2.54). This equation consistently accounts for the effects of diffraction, dissipation, nonlinearity and inhomogeneity; the ordering of inhomogeneity number $H = O(\epsilon)$, Stokes number $S = O(\epsilon)$ and diffraction number $N = O(\epsilon^{1/2})$, where ϵ is the Mach number, result from a singular perturbation method. This ordering implies that vorticity is neglected and that the linear impedance relation is valid to order ϵ. Equation (2.54) is a generalization of the KZK equation, in terms of curved coordinates determined by an approximate solution of the eikonal equation, consistent with the scaling of inhomogeneity relative to diffraction. Hence, Eq. (2.54) can be further simplified to provide Eq. (2.75), i.e., the KZK equation with varying nonlinearity and absorption coefficients and external force term, in terms of a transformed nondimensional pressure, defined in Eq. (2.67).

In the derivation of the parabolic model equation, the inhomogeneity length is of the order of the reference Rayleigh distance of the problem. Therefore: (i) The gradients in the medium cannot be too large; in particular, discontinuities in c_0, $\rho_0, \ldots$ cannot be included consistently. (ii) The diffraction number cannot be of the order of the inhomogeneity number, in that case it is no longer consistent to solve the eikonal equation approximately to find the curved coordinates. Thus it is a singular limit process to let $N \to 0$, or $ka \to \infty$ in our parabolic equation. If $N = O(\epsilon)$, we arrive at a generalized version of Burgers equation, Eq. (2.82), expressed in curved coordinates that now are determined by exact rays; hence the caustics problem is not avoided.

Other models that describe wave propagation in inhomogeneous media were presented and discussed. None of them turned out to be identical to our parabolic model, although some were close. We indicated that some of the models may be inconsistent.

Accordingly, the two extreme situations that can be compared with the parabolic

model to check the aproximations in the derivation of the governing equation are: The Helmholtz equation with varying wavenumber in terms of Cartesian coordinates and the generalized Burgers equation in terms of exact ray coordinates. We did not carry out numerical comparisons.

The model developed was applied to the case of an axisymmetric, monochromatic, plane source with uniform or Gaussian amplitude distribution, radiating in the positive z-direction. Numerical results for both the linear and the nonlinear case were presented and discussed. [Asymmetric and weakly curved sources could also be described, as well as arbitrary time dependence on the source. Also, external forces are included in the model, but were discarded in the numerical calculations.]

We found that the longitudinal component of ∇c_0 has the effect of stretching or compressing the sound field. The transverse component has the effect of deforming the directivity. The total effect of inhomogeneity in a nondissipative fluid is that the beam tends to avoid regions of space where c_0 increases the most.

By varying the direction of ∇c_0 relative to the source, we observed that the beam is more sensitive to longitudinal than to transverse inhomogeneity, depending on an effective inhomogeneity length, which is determined by the functional expression for c_0.

Dissipative effects are present through a varying exponential factor depending on c_0 and the sound diffusivity. Thus, in the dissipative case, the beam is bent in the direction of increasing c_0, so as to minimize the effect of absorption.

When ka is increased, the effect of longitudinal inhomogeneity becomes stronger. For a given variation of ka with either k or a varying, we observed the same amount of bending of the beam. However, the amplitude values differ, due to different variations of Rayleigh distance with respect to a and k, and therefore different effect of longitudinal inhomogeneity.

Fluid–fluid interfaces were simulated in two different approaches: (i) Discontinuity in ∇c_0, and (ii) Two homogeneous media connected by a layer where c_0 varies linearly. Although a discontinuity in c_0 is incompatible with the assumptions in our model, numerical computations show that practically identical results are obtained by using either approach.

In the case of continuous c_0, incident, reflected and transmitted amplitudes could be identified both for (i) and (ii), even though the beam was described as a progressive wave in z-direction. The sound field was found to behave according to Fermat's principle. For increasing ka, the bending of transmitted acoustic axis was more pronounced.

Numerical results were presented both for the quasilinear and the fully nonlinear cases, for nondissipative and dissipative media, and for various sound speed profiles.

Higher harmonic components appeared to be less affected by the transverse inhomogeneity, and more affected by longitudinal inhomogeneity, compared to the fundamental component.

Since the effective shock formation distance is an increasing function of c_0, the effects of nonlinearity are stronger in regions of lesser c_0. All harmonic components are bent in a direction of lesser c_0. However, in the fully nonlinear case, the fundamental is less bent than in the linear case, due to nonlinear attenuation and energy transfer to the higher harmonic components. Inhomogeneity effects are also observed in planes orthogonal to ∇c_0 (in the case of $\theta = 90°$ and $x_c = 0.0$), although this is most pronounced near the z-axis. The effects of inhomogeneity are due to a combination of varying shock formation distance and the curved coordinate transform.

In dissipative media, the harmonic components are bent in an opposite direction than in nondissipative media. The bending is most pronounced for the fundamental. In thermo–viscous fluids, the absorption coefficient is a decreasing function of c_0. Therefore the damping is least in regions of larger c_0. Since higher harmonics have stronger effective absorption coefficient and smaller wavelength, transverse inhomogeneity is less important and the absorption is most effective longitudinally.

Hence a generalized Fermat's principle is satisfied both in the linear and the nonlinear case: The beam tends to avoid regions where absorption and sound speed are larger.

REFERENCES

[1]J. Naze Tjøtta and S. Tjøtta, "Nonlinear equations of acoustics with applications to parametric acoustic arrays," J. Acoust. Soc. Am., **69**, 1644–1652 (1981).

[2]S. Tjøtta, "On some non–linear effects in sound fields, with special emphasis on the generation of vorticity and the formation of streaming patterns," Arch. Math. Naturvidensk. **55**, 1–68 (1959).

[3]V.P. Kuznetsov, "Equations of nonlinear acoustics," Sov. Phys. Acoust. **16**, 467–470(1971).

[4]E. A. Zabolotskaya and R. V. Khokhlov, "Quasiplane waves in the nonlinear acoustics of confined beams," Sov. Phys. Acoust. **15**, 35–40(1969).

[5]J. Kervorkian and J. D. Cole, "Perturbation Methods in Applied Mathematics", Springer-Verlag, New York, 1981.

[6]I. Stakgold, "Green's functions and boundary value problems," Wiley–Interscience, 1979.

[7]Abramowitz and Stegun,"Handbook of mathematical functions," Dover Publications, Inc., New York 1970.

[8]C.Johsson, "Numerical solutions of partial differential equations by the finite element method", Studentlitteratur, Lund, 1987.

[9]S.I. Aanonsen, T. Barkve, J. Naze Tjøtta and S. Tjøtta, "Distortion and harmonic generation in the nearfield of a finite amplitude sound beam," J. Acoust. Soc. Am., **75**, 749–768 (1984).

[10]S.I. Aanonsen, M.F. Hamilton, J. Naze Tjøtta and S. Tjøtta, "Nonlinear effects in sound beams," 10th International Symposium on Nonlinear Acoustics, Proceeding, 1984 .

[11]S.I. Aanonsen, "Numerical computations of the nearfield of a finite amplitude sound beam," Dept. of Math., The Univ. of Bergen, Norway, Report no. 73, (1983).

[12]M. F. Hamilton, J. Naze Tjøtta and S. Tjøtta, "Nonlinear effects in the farfield of a directive sound source," J. Acoust. Soc. Am., **78**, 202–216 (1985).

[13]J. Berntsen, "On the use of Richtmyer procedure to compute a finite amplitude sound beam from a piston source," Dept. of Math., The Univ. of Bergen, Norway, Report no. 82, (1987).

[14]Private communication with J. Berntsen.

[15]E. Vefring, "Nonlinear propagation and interaction of collinear sound beams," Dept. of Math., The Univ. of Bergen, Norway, Report no. 86, (1989).

[16]J. Berntsen, "Numerical calculations of finite amplitude sound beams," Proc. 12th International Symposium on Nonlinear Acoustics, 27.-31. August 1990, Austin, Texas, USA; Elsevier Publishers, 1990

[17]E.H. Vefring, J. Naze Tjøtta, S. Tjøtta, "Nonlinear effects in the sound field of a bifrequency source," Proc. 12th International Symposium on Nonlinear Acoustics, 27.-31. August 1990, Austin, Texas, USA; Elsevier Publishers, 1990

[18]Private communication with K.E. Frøysa.

[19]K.E. Frøysa, J. Naze Tjøtta and S. Tjøtta, "Linear propagation of a pulsed sound beam", To be published in J. Acoust. Soc. Am.

[20]Personal communication with J. Naze Tjøtta and S. Tjøtta.

[21]M.F. Hamilton, Lecture notes in nonlinear acoustics, Dept. of Mech.Eng., The Univ. of Texas at Austin.

[22]A.D. Pierce, "Wave equation for sound in fluids with unsteady inhomogeneous flow," J. Acoust. Soc. Am., **87**, 2292–2299, (1990).

[23]G.S. Garrett, J. Naze Tjøtta and S. Tjøtta, "Nearfield of a large acoustic transducer. Part III: General results," J. Acoust. Soc. Am., **75**, 769–779, (1984).

[24]J. Berntsen, J. Naze Tjøtta and S. Tjøtta, "Nearfield of a large acoustic transducer. Part IV: Second harmonic and sum frequency radiation," J. Acoust. Soc. Am., **75**, 1383–1391 (1984).

[25]C.M. Darvennes, M.F. Hamilton, J. Naze Tjøtta and S. Tjøtta, "Effects of absorption on the interaction of sound beams, with application to scattering of sound by sound," to be published in J. Acoust. Soc. Am.

[26]H. Sagen, Thesis for the Cand.Scient. degree, Dept. of Appl. Maths., The University of Bergen, Norway, 1987.

[27]J. Naze Tjøtta, H. Sagen, S. Tjøtta, "Transmission of a sound beam across a two–fluid interface: Numerical results and asymptotic expressions," J. Acoust. Soc. Am., **85**, 24–38 (1989),.

[28]J. Naze Tjøtta, S. Tjøtta, "An analytical model for the nearfield of a baffled piston transducer", J. Acoust. Soc. Am., **68**, 334–339 (1980).

[29]J. Lighthill, "Waves in fluids", Cambridge University Press, 1978.

[30]A. D. Pierce, "Acoustics: An introduction to its physical principles and applications", McGraw–Hill, 1981.

[31]F. D. Cotaras, "Nonlinear effects in long range underwater acoustic propagation", Applied Research Laboratories, University of Texas at Austin, Technical Report 1985.

[32]L. A. Ostrovskii, E. N. Pelinovskii and V. E. Fridman, "Propagation of finite–amplitude waves in an inhomogeneous medium with caustics," Sov. Phys. Acoust., **22**, 516–520 (1976).

[33]E. N. Pelinovskii and V. E. Fridman, "Equations of nonlinear geometrical acoustics," from "Nonlinear Deformation Waves," 143–148, Symposium, Tallinn, Estonian SSR, USSR Aug. 22–28, 1982. Ed. U. Nigul and J. Engelbrecht, Springer–Verlag (1983).

[34]V.E. Fridman, "Self–refraction of weak shock waves", Sov. Phys. Acoust., **28**, 323–328 (1982).

[35]V.E. Fridman, "Nonlinear refraction of acoustic pulses in an isothermal atmosphere", Sov. Phys. Acoust., **31**, 345–346 (1985).

[36]E.N. Pelinovskii and V.E. Fridman, "Exact solution of the Burgers equation for acoustic waves in inhomogeneous media", Sov. Phys. Acoust., **33**, 215–217 (1987).

[37]J.B. Keller, "Geometrical Acoustics. I. The Theory of Weak Shock Waves", Jour. Appl. Phys., **25**, 938–947 (1954).

[38]L. K. Zarembo and I. P. Chunchuzov, "Sound beam in an inhomogeneous medium with a slightly varying velocity of sound," Sov. Phys. Acoust., **23**, 78–79 (1977).

[39]O. V. Rudenko, S. I. Soluyan and R. V. Khokhlov, "Confinement of a quasiplane beam of periodic perturbations in a nonlinear medium," Sov. Phys. Acoust., **19**, 556–559 (1974).

[40]E. N. Pelinovskii, I. A. Soustova and V. E. Fridman, "Diffraction of sound beams in inhomogeneous media," Sov. Phys. Acoust., **24**, 415–418 (1978).

[41]R. Nowack and K. Aki, "The two–dimensional Gaussian beam synthetic method: testing and application", Jour. Geophys. Res., **89**, 7797–7819 (984).

[42]M.B. Porter and H.P. Bucker, "Gaussian beam tracing for computing ocean acoustic fields", J. Acoust. Soc. Am., **82**, 1349–1359 (1987).

[43]V. Cerveny, M. M. Popov and I. Psencik, "Computation of wave fields in inhomogeneous media — Gaussian beam approach," Geophys. J. R. Astron. Soc., **70**, 109–128 (1982).

[44]E. N. Pelinovskii and I. A. Soustova, "Structure of a nonlinear sound beam in an inhomogeneous medium," Sov. Phys. Acoust., **25**, 359–360 (1979).

[45]F. Obermeier, "Some comments on the focusing of weak shock waves," Max–Planck–Institut für Strömungsforschung (1980).

[46]F. Obermeier, "On the propagation of weak and moderately strong, curved shock waves," Max–Planck–Institut für Strömungsforschung, bericht 116/1981.

[47]D. Ludwig, "Uniform asymptotic expansions at a caustic," Comm. Pur. Appl. Math., **XIX**, 215–250 (1966)

[48]R. N. Buchal and J. B. Keller, "Boundary layer problems in diffraction theory," Comm. Pur. Appl. Math., **XIII**, 85–114 (1960)

[49]J. K. Hunter and J. B. Keller, "Caustics of nonlinear waves," Wave Motion, **9**, 429–443 (1987), North–Holland

[50]J. Hunter, "Transverse diffraction of nonlinear waves and singular rays," SIAM J. Appl. Math., **48**, 1–37 (1988)

[51]F. D. Tappert, "The parabolic approximation", Lecture notes in physics: Wave propagation and underwater acoustics, Ed. by J.B. Keller and J.S. Papadakis, Springer–Verlag 1977

[52]M. Porter and E.L. Reiss, "A numerical method for ocean–acoustic normal modes", J. Acoust. Soc. Am., **76**, 244–252 (1984).

[53]T. Mannseth, "On the theory of acoustic shallow water propagation", Dr.Scient. dissertation, Dept. of Appl. Maths., University of Bergen, January 1986.

[54]E. Vefring and S. Mjølsnes, "A parabolic wave equation based on a rational–cubic approximation", J. Acoust. Soc. Am., **87** (2), 619–623 (1990).

[55]B.E. McDonald and W.A. Kuperman, "Time domain formulation for pulse propagation including nonlinear behavior at a caustic", J. Acoust. Soc. Am., **81**, 1406–1417 (1987).

[56]J.J. Ambrosiano, D.R. Plante, B.E. McDonald and W.A. Kuperman, "Nonlinear propagation in an ocean acoustic waveguide", J. Acoust. Soc. Am., **87**, 1473–1481 (1990).

[57]M.D. Collins, "Low–frequency, bottom–interacting pulse propagation in range–dependent oceans", IEEE Jour. Ocean. Eng., Vol.13, No.4, 222–228 (1988)

[58]M.D. Collins, H.B. Ali, M.J. Authement, A. Nagl, H. Überall, J.F. Miller, J.I. Arvelo, "Low–frequency sound interaction with a sloping, refracting ocean bottom", IEEE Jour. Ocean. Eng., Vol.13, No.4, 235–244(1988)

[59]M.D. Collins, "The time–domain solution of the wide–angle parabolic equation including the effects of sediment dispersion," J. Acoust. Soc. Am., **84**, 2114–2125 (1988).

[60]G.A. Kriegsmann, "A multiscale derivation of a new parabolic equation which includes density variations", Comp. Maths. Appls. Vol.11, no.7/8, 817–821 (1985)